University of Parma

Department of Life Sciences

Ph.D. in Biotechnologies

XXVI Course

Biotechnology of nanoparticle interactions with plants and yeasts

Coordinator:

Prof. NELSON MARMIROLI

Supervisors:

Prof. NELSON MARMIROLI

Dr. MARTA MARMIROLI

Candidate:

LUCA PAGANO

“To define is to limit.”

O. Wilde, 1890.

Summary

Introduction

Nanotechnologies

Nanotechnologies are a rapidly growing industry and it is expected to reach a market size of approximately 26 billion dollars by 2015 (BCC Research, 2011). Engineered nanomaterials (NMs) are on the nanoscale level range ca. 1-100 nm, with high reactivity and surface area. NMs showed peculiar physico-chemical properties (optical, magnetical, dielectrical, of density and mechanical resistance) and for those reasons are currently used in different areas such as electronics, biomedicine, pharmaceuticals, cosmetics, environmental analysis and remediation, catalysis and material sciences. There are also NMs ubiquitously in the environment resulting from natural and anthropic processes. Despite some recently acquired knowledge on the effects of NMs on human toxicology and to a lesser extent of their ecotoxicology, very little is known about mechanisms of biological uptake and interaction with cells of living organisms (US National Research Council, 2012) as well as between environmental and biological compartmentalization and chemical behavior in the environment (Ju-Nam *et al.*, 2008; Rico *et al.*, 2011, Lowry *et al.*, 2012). Since the early nineties there has been a huge interest in NMs, regarding their structure, their physico-chemical properties and their relative toxicity. Only recently the problem of their ecotoxicity (Kahru *et al.*, 2010) has been raised and few studies are moving in this direction. Recent studies on NMs provide an initial basis for evaluating the primary issues in a risk assessment framework of nanomaterials (Tsuji *et al.*, 2006), highlighting points as the identification of the hazard through chemical composition, physico-chemical properties, interactions with tissues, and potential exposure levels. The procedure will be variable, considering the nature of the particle case-by-case, and the legislation in force.

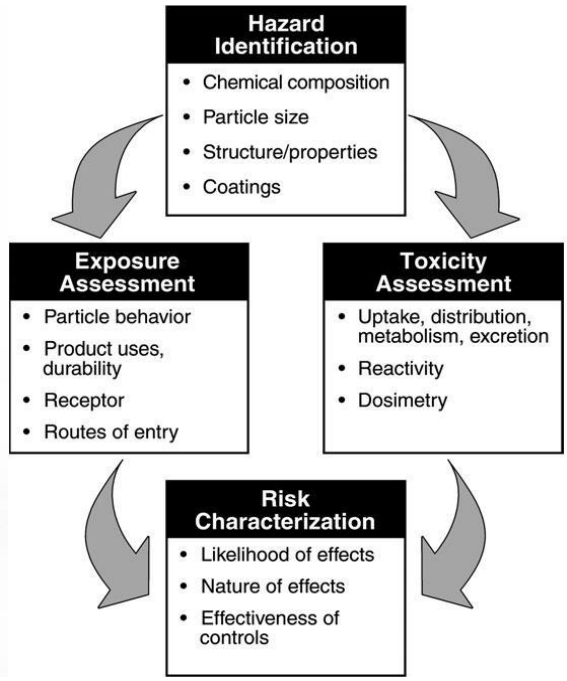

Figure 1. Risk assessment framework for nanomaterials (published on Tsuji *et al.*, 2006).

Current legislation

Legislation concerning NMs is currently under consideration since the variable nature of the molecules investigated. On February 10, 2009, European Food and Safety Authority (EFSA) adopted a scientific opinion on "The potential risks arising from nanoscience and nanotechnologies on food and feed safety" in response to the growing need of regulation of those materials. The first guidance was released from EFSA scientific committee on May 10, 2011 concerning the risk assessment of the application of nanoscience and nanotechnologies in food chain and feed (EFSA, 2011), in which the attention was focused on the evaluation of the methodologies relevant for all the phases of the risk assessment procedure (Tsuji *et al.*, 2006), in six general cases here reported: i) no persistence of NMs in preparations/formulations as marketed, ii) no migration from food contact materials, iii) complete NMs transformation in the food/feed matrix before ingestion, iv) transformation during digestion, v) information on non-nanoform available, vi) no information on non-nanoform available. The guidance underlined how, currently, there are no *in vitro* methods validated to be used for hazard assessment of NMs. However, *in vitro* tests may provide information on hazards, give indication of potential toxicity of an NM and may be used to elucidate possible mode of action, understanding biological responses and mechanisms involved. Absorption, distribution, metabolism and excretion parameters are likely to be influenced by both the chemical

composition of the NM as well as its physico-chemical properties (size, shape, solubility, surface charge and surface reactivity). Conversely, United States Food and Drug Administration (FDA), on April 2012 approved two different draft guidance concerning regulation of nanomaterials in food and cosmetics, allowing de facto the use of ZnO NMs and TiO_2 NMs for sunscreens. On July 26, 2013, the European Commission's (EC) Scientific Committee on Consumer Safety (SCCS) posted two documents available for comments regarding legislation of ZnO and TiO_2 NMs, still under consideration. On December 20, 2013, European Joint Research Center releases online a web platform for the purpose of share and increase the current knowledge concerning nanomaterials both for physico-chemical characterization of the pollutant and also risk assessment procedure (http://ihcp.jrc.ec.europa.eu/our_databases/web-platform-on-nanomaterials).

Current knowledge concerning NMs exposure in plants

Several experiments has led to understand the transport mechanisms and accumulation of Ag NMs in Arabidopsis *thaliana* (L.) Heynh both on the physiological and molecular point of view (Geisler-Lee *et al.*, 2013; Kaveh *et al.*, 2013). Ag NMs mechanisms of response were also investigated in crop species, as *Cucurbita pepo* (L.) (Stampoulis *et al.*, 2009; Musante *et al.*, 2010; Hawthorne *et al.*, 2012). Effects on seed germination and roots growth and uptake of ZnO NMs in *Lolium perenne* (L.) and *Glycine max* (L.) Merr has been partially elucidated (Lin *et al.*, 2007; Lin *et al.*, 2008; Lopez-Moreno *et al.*, 2010; Hernandez-Viezcas *et al.*, 2013). Some studies have shown the ecotoxic effect of TiO_2 NMs (Menard *et al.*, 2011; Servin *et al.*, 2012) and the effect of TiO_2 NMs on human health has been studied because of the widespread use in food and in personal care products (Weir *et al.*, 2012).

In conclusion, as reported in most of the current literature, the mechanisms involved in uptake and translocation of NMs in the plant tissues and their physico-chemical forms inside the plant still remain largely unknown (Rico *et al.*, 2011).

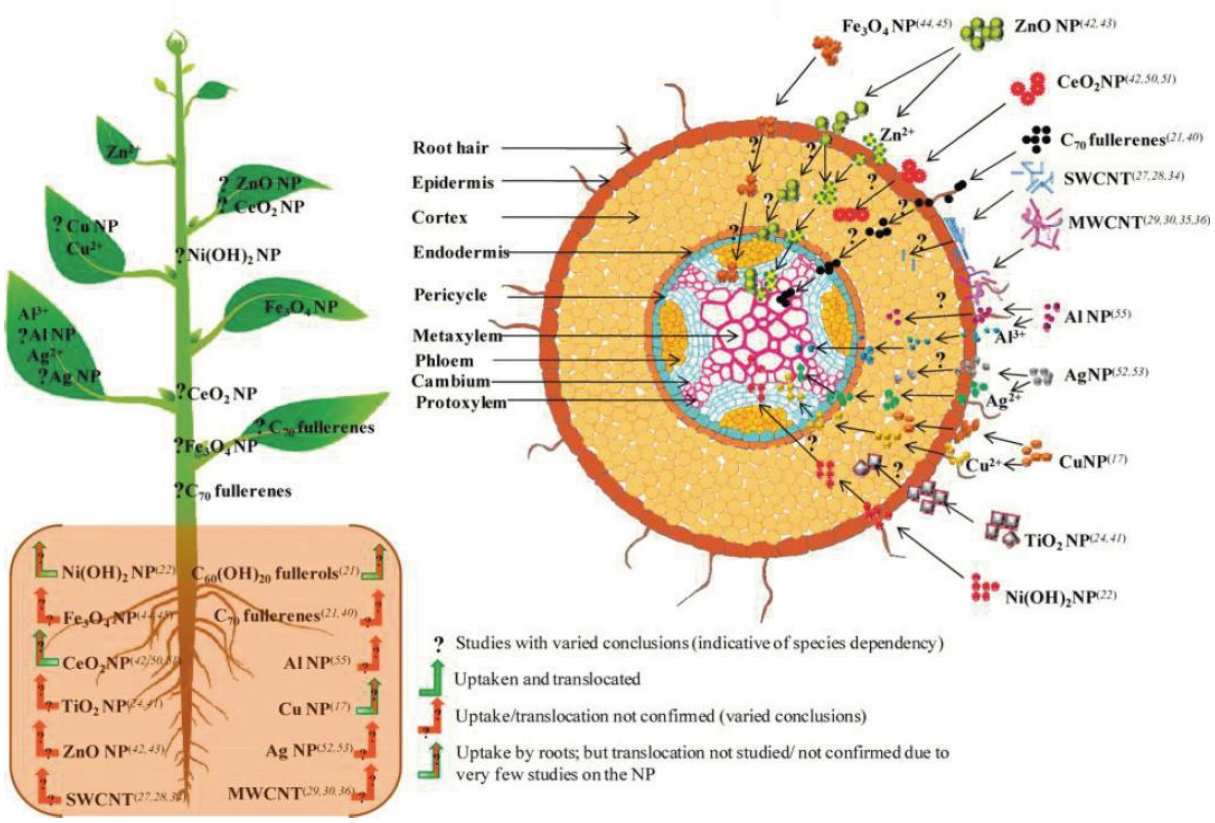

Figure 2. Uptake, translocation, and biotransformation pathway of various nanoparticles in a plant system: plant showing the selective uptake and translocation of nanoparticles (left); transverse cross section of the root absorption zone showing the differential nanoparticle interaction on exposure, published on Rico *et al.*, 2011 (right).

Yeast as model system for the investigation of NMs toxicity

Similarly to plants, the mechanisms involved in NMs toxicity in yeast are still actually unknown. Furthermore, the variability of NMs behavior, along the different types of treatment applicable to yeast strains, led to increase the level of general complexity of the experimental approach used. Several studies performed on yeast revealed the extreme variability of effects ascribable to different categories of NMs (Kasemets *et al.*, 2009), focusing the attention to several properties implicated in toxicity. Differences observed in the NMs responses may caused by stability of the single NM tested: CuO NM, for instance, showed an intrinsic instability of the particle, highlighting how the toxic effect consist in the Cu^{2+} release. In this context it was also analyzed the effect of CuO NM on some yeast strains deleted in genes involved in the detoxification pathway of Cu^{2+} (Kasemets *et al.*, 2012). Conversely, the behavior of ZnO NM, characterized by a considerable size, becomes much similar to the bulk material for itself.

Other types of NMs, as TiO_2, did not shown toxic effect below 20 g L^{-1}. There is not only to consider the effect of the NM properly said since also the coat of the particle can have a major role in the toxic response. The functionalization of Au NMs, that until now were considered as completely non toxic, showed a response implicated in the respiratory metabolism (Smith *et al.*, 2013). In this already complex scenario it is necessary to consider also the primary role of the yeast cell wall in the NMs translocation inside the cytoplasm.

Cadmium Sulphide Quantum Dots (CdS QDs)

Among the many categories of NMs more diffuse on the market are the Cadmium sulfide based quantum dots (CdS QDs) (Fig.3). Their sizes are among the smaller (less than 10 nm). In addition to their size/volume ratio, the distribution of charge over the surface was found to be a key issue in the application of QDs as components of semiconductor electrodes (Favero *et al.*, 2006; Martínez-Castañón *et al.*, 2005; Zhai *et al.*, 2010). They find application in electronic components as cell phones, stereo Hi-Fi, general hardware for informatics. Functionalized CdS QDs (with L-cysteine, or glutathione) are used as water-soluble and biocompatible fluorescent probes both for chemicals (silver ion labeling), as reported in Chen *et al.*, 2005, and protein labeling (Huang *et al.*, 2011). Since their physico-chemical properties, CdS QDs are also used in the synthesis of monolithic aerogels comprising cadmium sulfide nanoparticles partially coated with metallic silver (Gill *et al.*, 2009), which are the basis of the next-gen photovoltaic panels. The uncertainty on the effects of NMs is of concern for the citizens health and Regulatory Institutions increasing the need of environmental health and safety (EHS) research dedicated to understand the potential toxicity of NMs for humans and environment.

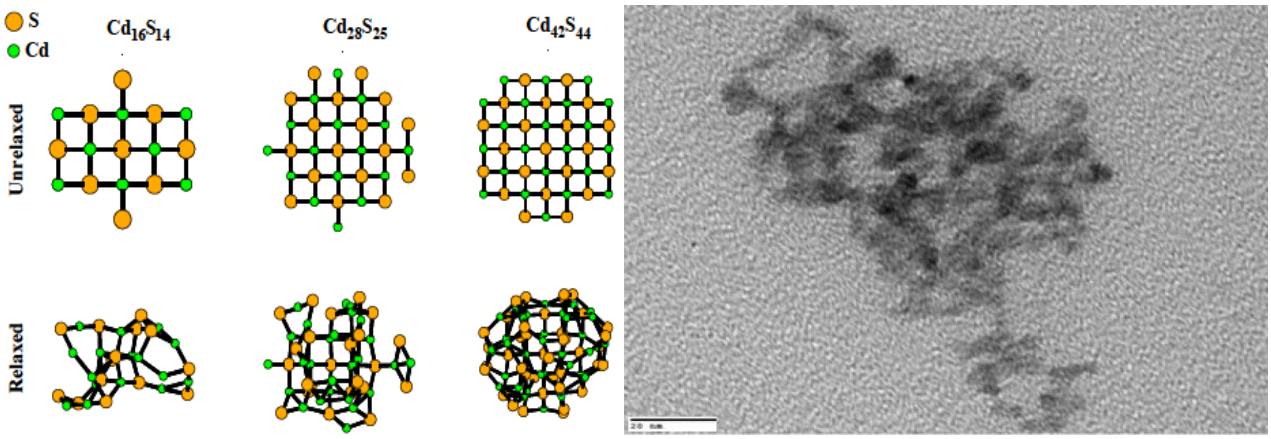

Figure 3. Representation of unrelaxed and relaxed cubic CdS nanoparticles, published on Favero *et al.*, 2006 (left); TEM image of the CdS QDs, published on Martínez-Castañón *et al.*, 2005 (right).

Aim of the project

The aim of this work was to apply a genome-wide approach to determine the toxicity and the mechanism of CdS QDs using different model species as *Arabidopsis thaliana* (L.) Heynh (accession Landsberg erecta) and *Saccharomyces cerevisie*. Mutagenized lines of these organisms were also used for an *in vivo* study to study the effects and toxicity of cadmium as a bulk material, such as in $CdSO_4$, from that of CdS QDs. At present, there is not a general consensus on the differences related to the toxicity of metal ions and their derived NMs. One of the goal was to identify detoxification pathways in *A. thaliana* relative to CdS QDs that can be informative for other plants and for higher eukaryotes in general. A genome-wide transcriptomic analysis was merged with the mutant screening and genetic characterization. Data mining and system biology approach were used to give an interpretation of the observed phenomena. To reach information concerning the preservation of the tolerance/resistance mechanisms of response to CdS QDs, a similar genomic approach was used to investigate the phenomenon using the EUROSCARF non-essential knock-out mutants collection of *S. cerevisiae*. Preservation of the response in different species could provide new information about the potential toxicity of the CdS QDs and NMs in general.

Arabidopsis thaliana

Previous studies

This part of the project is published in Marmiroli, Pagano *et al.*, 2014.

Manufactured nanoparticle: CdS QDs

Quantum dots of the type CdS were utilized throughout the experiment, with a bulk density of 4.82 g/cm3 and a diameter of 5 nm, synthesized according to Villani et al., 2012 (IMEM-CNR, Parma, Italy). The X-ray diffractometric spectrum of the QDs was used to establish the purity of the synthetic process. Cd represents the 78% of the dry weight of the nanoparticle.

MIC determination for CdS QDs and $CdSO_4$

An *in vitro* test was used for the estimation of MIC for CdS QDs for two different wild type lines of *A. thaliana* accessions, Wassilewskija (Ws-2) and Landsberg erecta (Ler-0), both for the germination and for growth. Plants were grown in 25 mL Petri dishes on nutrient medium Murashige and Skoog (Duchefa Biochemie, Haarlem, The Netherlands) containing 1% sucrose solidified with agar (0.8%) under controlled temperature (24°C), humidity (30%), and photoperiod (16h light, 8h dark; 120 µM m^{-2} s^{-1} photosynthetic photon flux). Forty seeds were treated for assess germination with increasing concentrations of CdS QDs, from 40 µg L^{-1} to 300 mg L^{-1}. For the growth test 25 seeds per dish (for four replicates) were treated for 14 d on MS medium and after then 25 plants were transferred to MS medium supplemented with CdS QDs, increasing concentrations from 40 µg L^{-1} to 300 mg L^{-1}, for other 21 d of treatment. We used, as control, in both cases different concentration of $CdSO_4$ (Sigma Aldrich, St. Louis, MO, USA) from 1 µM (0.11 mg L^{-1} of Cd^{2+}) to 210 µM, equal to 24.5 mg L^{-1} of Cd^{2+} (Howden *et al.*, 1992). For the $CdSO_4$ MIC was as reported in literature (Howden *et al.*, 1992) namely 23.3 mg L^{-1} of Cd. For the CdS QDs MIC observed was higher in total Cd, than when using $CdSO_4$. The MIC on seeds germination was higher than for growth (Fig. 5). With a concentration of 80 mg $L^{-1}$of CdS QDs, corresponding to 62.4 mg $L^{-1}$of Cd^{2+}, it was observed a complete leaves chlorosis and an inhibition of root growth (Fig. 4).

A control was made to exclude the possibility that the toxic effect observed was due to CdS QDs suspension liquid: QDs liquid suspension medium was separated by ultracentrifugation (Optima MAX-XP Ultracentrifuge, Beckman Coulter, Brea, CA, USA) at 50000 rpm for 20 m at 4°C and added to the MS medium used for germination and growth. When the nanoparticles liquid medium, avoid of CdS QDs, was added to seeds no inhibition of growth and germination was detected.

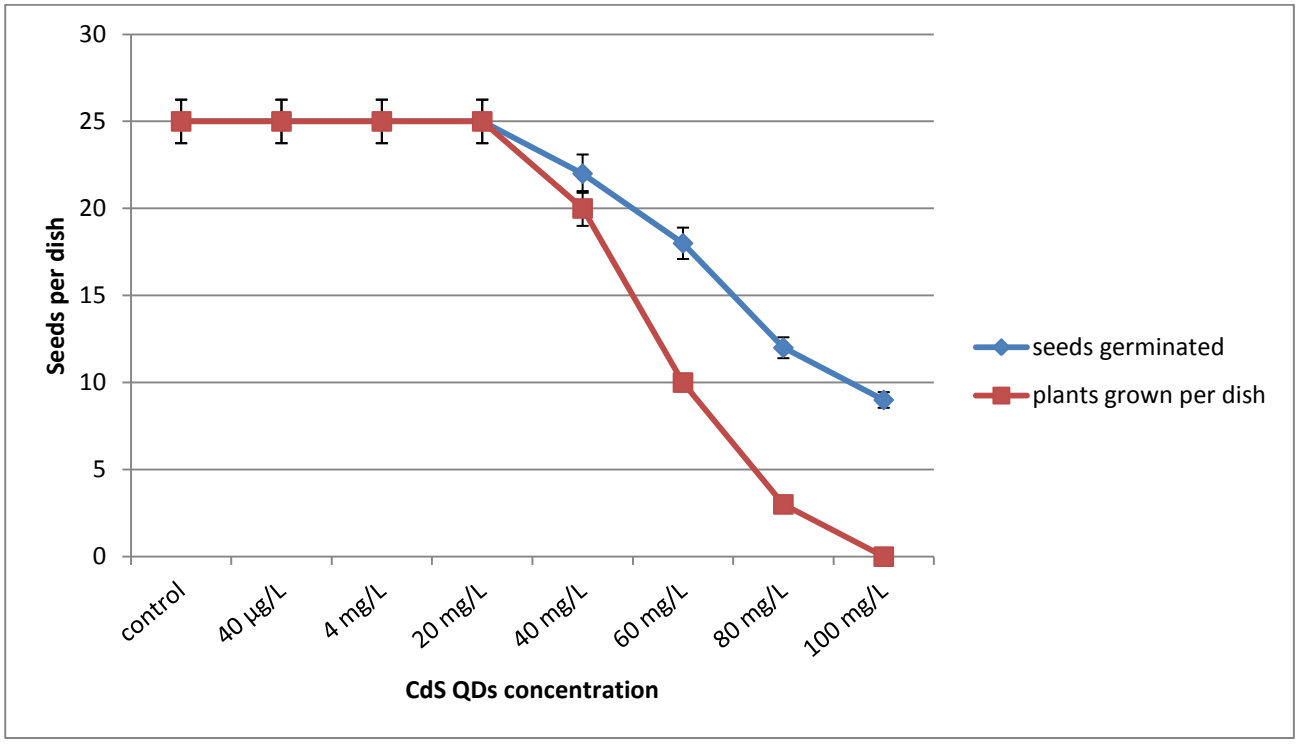

Figure 4. The effect of CdS QDs on germination and seedling growth on wild type *A. thaliana*. Measurements taken after a 21 d exposure from 0 to 100 mg L^{-1} CdS QDs.

Mutant collection screening

A collection of 398 mutants lines of *Arabidopsis thaliana* (L.) Heynh were utilized: 234 lines of Wassilewskija accession with T-DNA insertion (Feldmann, 1991) and 164 lines of Landsberg erecta accession with maize Ac/Ds transposon insertion (Soll&Johnson collection), obtained from NASC (Nottingham Arabidopsis Stock Centre, UK). These lines are the product of cross between parental lines that contain sAc-GUS transposase, Ds element and selectable marker based on antibiotic resistance (streptomycin Str^R and hygromycin Hm^R). The Ds element was obtained by substituting the central portion of Ac transposase sequence (1,77 Kb) between the restriction sites HindIII (1783) and XhoI (3557) with CaMV35S-Hm^R-ocs3', that codifies for hygromycin phosphotransferase gene (Bancroft *et al.*, 1992). Ten seeds were planted for each of the 398 mutant

lines to test both for resistance during germination (MIC = 40 mg L^{-1}) and during growth (MIC = 80 mg L^{-1}) on MS medium added with CdS QDs. The same procedure was followed with $CdSO_4$, both for germination (MIC =103 µM, 11.66 mg L^{-1} of Cd) and for growth test (MIC = 207 µM, 23.33 mg L^{-1} of Cd). The plants were treated as previously described. During these screenings 600 Petri dishes were tested amounting to 19320 seeds, including replicates. To confirm the phenotypes of the isolated mutants the identified lines of interest were checked furtherly by testing 150 seeds for each line.

Out of the 398 original mutant lines tested at CdS QDs MIC of 80 mg L^{-1} two putative tolerant/resistant mutants were isolated, which were named *atnp01* and *atnp02* (Fig. 5). Two different mutants resistant to lethal concentration of $CdSO_4$, are still under investigation.

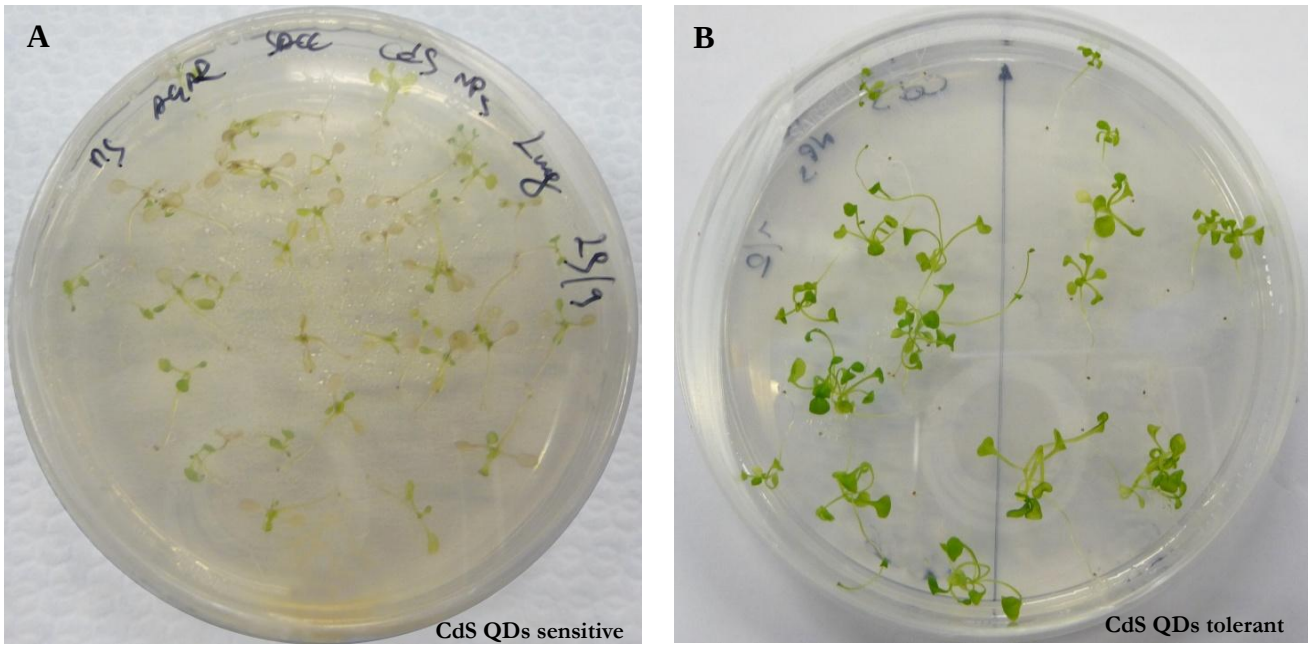

Figure 5. Lethal concentration of CdS QDs for (a) wild type Ler-0 plants and (b) the two mutant lines *atnp01* (left) and *atnp02* (right).

Molecular characterization of mutant lines

The genomic DNA (gDNA) was extracted from 0.5 g of plant material from the wild type line (Ler-0) and from the two mutant lines (*atnp01* and *atnp02*) by 2x CTAB method (Fulton *et al.*, 1995). DNA was tested for: the absence of Ac transposase, the presence and the integrity of Ds elements, the number Ds element copies and their position in each mutant line. The presence of the Ds elements inside the mutant lines was evaluated through amplification by PCR reaction of hygromycin phosphotransferase gene (Hm^R) insert in the Ds element. For the evaluation of the Ds element integrity three overlapping sequence called Ac_{1-1000} (from 1 to1000 bp), $Ac_{900-1800}$ (from 900 to 1783 bp), $Ac_{3500-4500}$ (from 3557 to 4500 bp) were amplified to cover, together with the Hm^R gene amplicon, the complete Ds element sequence (Tab.1). The amplification protocol: 95°C for 30 s (denaturation), 60°C for 20 s (annealing), 72°C for 90 s (amplification), for 40 cycles. Absence of Ac transposase was detected by amplification of the central region of transposase using the $Ac_{900-1800}$ Fwd primer with sAc Rev primer. All these amplifications were performed on the wild type DNA and the two mutant lines DNAs in three biological replicates.

Name	Sequence	Annealing T (°C)	Amplicon length (bp)
sAc Rev	TTTTGACAAGATGTCCACATATCCA	61	1500
probe Hm Fwd	GCAAGGAATCGGTCAATACACT	64	700
probe Hm Rev	TCCACTATCGGCGAGTACTTCT	64	
Hm Fwd	ATGAAAAAGCCTGAACTCACC	61	1000
Hm Rev	CTATTTCTTTGCCCTCGGAC	61	
Ac_{1-1000} Fwd	CAGGGATGAAAGTAGGATGGG	64	1000
Ac_{1-1000} Rev	TGAGGAATGGAGTCGTAGCC	64	
$Ac_{900-1800}$ Fwd	GCTCTGCAACACCTGCTGAT	62	1000
$Ac_{900-1800}$ Rev	AGGCTAACCACTTCATCGTACTT	62	
$Ac_{3500-4500}$ Fwd	GGTGCTAGACTCTGTTATTGCTG	61	1000
$Ac_{3500-4500}$ Rev	AGGGATGAAAACGGTCGGTA	61	

Table 1. Primer sequences used to amplify segments of the Ds element in the selected *A. thaliana* mutants and the probe used for Southern hybridization to assess Ds copy number.

The copy number of the Ds element was determined using a colorimetric Southern blot assay: the probe was generated by PCR amplification of the central portion of hygromycin phosphotransferase gene. The probe was purified with GE Healthcare Life Science GFX™ PCR kit (Buckinghamshire, UK) and quantified by Varian Cary 50 (Agilent Technologies). After quantification the probe was labeled by Roche DIG High Prime DNA Labeling and Detection Starter Kit I (Roche, Basel, CH). For each line 15 µg of gDNA were digested with restriction endonucleases EcoRI, HindIII and BamHI (Sigma-Aldrich, St. Louis, MO, USA) (10 U μg^{-1}) overnight at 37°C. The restricted gDNA were separated on agarose gel 1% and blotted on Amersham Hybond N+ nylon filter (GE Healthcare, Buckinghamshire, UK). The hybridization with the probe for Hm and the colorimetric detection were performed with Roche DIG High Prime DNA Labeling and Detection Starter Kit I. The position of the Ds elements for each mutant line was determined by genome walking; 0.5 µg of genomic DNA for each line were digested with restriction endonucleases EcoRI, and MseI (20 U μg^{-1}) and ligated with the adapters for 4h at 37°C. The Genome Walking protocol of Ausubel *et al.*, 1994 was followed (Tab. 2).

Name	Sequence	Annealing T (°C)
Adapter EcoRI	GTAATACGACTCACTATAGGGCACGCGTGGTTTAA	-
Adapter MseI	GTAATACGACTCACTATAGGGCACGCGTGGTAT	-
AP1	GTAATACGACTCACTATAGGGC	67
AP2	ACTATAGGGCACGCGTGGT	72
5’ GSP1	CGGTGAAACGGTCGGGAAACTAGCTCT	67
3’ GSP1	CAAAAATACCGGTTCCCGTCCGATTTC	67
5’ GSP2	TAACGGTCGGTACGGGATTTTCCCATC	72
3’ GSP2	CGACCGGATCGTATCGGTTTTCGATTA	72

Table 2. Primer sequences and adapters used in the “genome walking” protocol to amplify flanking sequences of the Ds elements inserted into the selected *A. thaliana* mutants.

The genomic library obtained was amplified in two subsequent steps to isolate the Ds element’s flanking regions. The amplicons obtained were cloned into an *Escherichia coli* plasmid (Promega pGem vector II, Promega, Medison, WI, USA) and sequenced.

Amplification of the overlapping regions of the Ds element highlighted the integrity of the transposon sequence in both mutant lines. Moreover both amplicons sizes were as expected. The

amplification of the central portion of Ac transposase did not produce any amplicon. This result suggests that the insertion of hygromycin phosphotransferase gene into the Ds element determined deletion of the Ac transposase gene and consequently its loss of function. The Southern blot analysis gave a reliable estimation of the copy number of Ds elements for each mutant line. The restriction endonuclease EcoRI and HindIII produced two hybridization bands for *atnp01* and one band for *atnp02*. These results together with the genome walking analysis, demonstrate that the two mutant lines contained three different Ds elements. The amplification fragments produced were sequenced and compared *in silico* with *Arabidopsis thaliana* genome using Basic Local Alignment Search Tool (BLAST) algorithm (blast.ncbi.nlm.nih.gov). Alignment with Arabidopsis database led to the identification of six candidate genes in the two tolerant lines. In *atnp01* three genes were putatively interested in the transposition: an unknown protein localized in the chloroplast (*At3g46880*), a calmodulin binding protein located in cytoplasm and involved in leaf development and meristem structural organization (*DLR1*), and an *ELM2* (included in the *MYB* superfamily) domain-containing protein for a DNA binding protein expressed during the growth stages (*At1g13880*). The two Ds element are inserted in the *At3g46880* coding sequence and between *DLR1* and *At1g13880*. In *atnp02* three genes identified encoded for: an O-glicosyl hydrolase located on endomembrane system (*At3g24330*), an ATP binding protein located in chloroplast (*At3g24430*) named HCF101. The protein belongs to FSC-NTPase (4F-4S) cluster, of the P-loop NTPase superfamily. Several members of this superfamily play a crucial role in Fe/S cluster. The third gene is a pseudogene encoding for a proline-rich extensin-like receptor kinase, positioned between the two foregoing genes (*At3g24400*) The Ds element is located within the *At3g24400* pseudogene.

Materials & Methods

Determination of physiological parameters for resistant lines

We measured: chlorophyll absorbance, respiratory efficiency and Cd uptake, in condition either of treatment with CdS QDs (80 mg L^{-1}) or $CdSO_4$ salts (23.33 mg L^{-1}). Total chlorophyll was extracted after grinding the plants in liquid nitrogen 0.2 g for each sample, wild type line and both mutant lines. The powder obtained was added with 1.8 ml of acetone for 10 m in an ice bath. Chlorophyll absorbance at 662 nm was analyzed with a spectrophotometer Varian Cary 50 (Varian, Inc, Agilent Technologies, Palo alto, CA, USA) (Ni *et al.*, 2009). Cellular respiration was estimated by TTC (2,3,5-triphenyltetrazolium chloride) assay (Porter *et al.*, 1994). 0.2 g of samples from the wild type and from both the mutant lines were added to 3 ml TTC buffer (TTC 0.18 M, 78% $Na_2HPO_4 \cdot H_2O$ 0.05 M, 22% KH_2PO_4 0.05 M), and incubated for 15h at 30°C. After incubation the sample was drained off and washed in distilled water. Each sample was extracted in 10 ml of ethanol 95% for 10 m at 80°C. The formazan which resulted from the TTC reduction was quantified spectrophotometrically with Varian Cary 50 (Agilent Technologies) (λ= 530 nm). Concentration of total Cd in plants was measured by FA-AAS (flame atomizer atomic absorbance spectrophotometer AA240FS, Agilent Technologies). The plants treated with CdS QDs (80 mg L^{-1}) and $CdSO_4$ (23.33 mg L^{-1}) were dried at 50°C for 24h. 0.2 g of each dry sample was digested with 20 ml of HNO_3 for 40 m at 200°C in a heating block (DK20, Velp Scientifica, Usmate, MB, Italy). The solution obtained was filtered with 0,45 µm filters (Sarstead, Nümbrecht, Germany) and analyzed by Varian FA-AAS (λ= 228.8 nm).

Cross and segregation test of the CdS QDs resistant lines

To determine stability and inheritability of the Ds element within each mutant line of interest, the backcrosses of the two mutants with wild type line was carried out. The mutant line was utilized as female (to prevent the possibility of maternal loss of the transposon) and the wild type line as pollen donor. Plants were grown for thirty days in soil until flowers production. After recovery of the pollen grains we pollinated the carpels of our mutants to obtain the F_1 progeny. The seeds of F_1, crossed with the wild type line, were grown in soil to obtain the F_2 progeny. 250 seeds of F_2 progeny, of each crossed line, were sown in vitro on hygromycin (40 µg ml^{-1}). After seven days

from the germination these plants, grown on hygromycin (Hm^R), were transferred on CdS QDs for a 14 d treatment. The F_2 plants growing on hygromycin and CdS QDs were tested further by utilizing a Genome Walking protocol, after DNA extraction, to verify the position of the Ds elements. The segregation of the character Hm^R, with resistance to CdS QDs was also determined.

Microarray experiments

Genome-wide expression footprint of *atnp01* and *atnp02* as compared to the wild type in growth media with and without CdS QDs was determined through expression microarray. Affymetrix GeneChip Arabidopsis ATH1 Genome Array (Affymetrix, Santa Clara, CA, USA) containing 22811 nuclear gene-specific tags were utilized. Seven different treatments: three for the wild type line, (exposed to 0 mg L^{-1}, 40 mg L^{-1} and 80 mg L^{-1} of CdS QDs); two for each of the mutant lines (exposed to 0 mg L^{-1}, 80 mg L^{-1} of CdS QDs). Treatments were as previously described. Total RNA was extracted from 0.1 g of plant material with Sigma Aldrich Spectrum Plant Total RNA Kit (Sigma Aldrich, St. Louis, MO, USA). After spectrophotometric quantification (Varian Cary 50), 500 ng of total RNA derived from a pool three replicates for each sample were amplified, biotin-labeled, microarray hybridized and analyzed (Biolitix AG, Witterswill, CH). Data mining and system biology analysis was carried out starting from raw data. Results are available on GEO database (accession number: GSE53989).

Real Time PCR validation

Total RNA was also in this case extracted from 0.1 g of plant material with Sigma Aldrich Spectrum Plant Total RNA Kit (Sigma Aldrich, St. Louis, MO, USA). Reverse transcription was performed on 1 μg of the total RNA using the Qiagen QuantiTect Reverse Transcription kit (Qiagen, Velno, Netherlands). Amplifications were carried out using the Applied Biosystems Power SYBR Green Master Mix (Applied Biosystems, Foster City, CA, USA) in an optical 96-well plate with the Applied Biosystems ABI PRISM 7900HT Sequence Detection System. This system allow to monitoring the incorporation of the fluorescent dye SYBR Green into PCR product in real-time and, for each reaction, highlight the threshold cycle (Ct), defined as the PCR cycle at which exponential growth of PCR product is detectable. RNA retrotranscription were performed on the same samples used for the microarray experiments: three for the wild type line, (exposed to 0 mg L^{-}

^{1}, 40 mg L^{-1} and 80 mg L^{-1} of CdS QDs); two for each of the mutant lines (exposed to 0 mg L^{-1}, 80 mg L^{-1} of CdS QDs). We designed specific primers for each gene selected from the microarray experiments (Tab. 3), using the Applied Biosystems SDS 2.3 software and the following thermal profile: 95°C for 10', 95°C for 15" and 60°C for 60" (for 40 cycles). Primers used were assessed by Real Time PCR in four serial dilutions of cDNA synthesized (1, 1:10, 1:100, 1:1000).

Name	Sequence	Annealing T (°C)
β-actin for (HK)	TCGCATGTATGTTGCCATTCA	60
β-actin rev (HK)	ATCGAGCACAATACCGGTTGT	
GAPDH for (HK)	CAGCAAAGACGCTCCATGTT	60
GAPDH rev (HK)	GCTAGCGTTGGAGACATGTCA	
256166_AT (+) for	TTCACTTATTGATGTTGCCTTATGG	60
256166_AT (+) rev	GAGCTTTGAACTGTGCCTTGATATAG	
264735_S_AT (02+) for	GGCACCTCTCTTCCAAAATCTACTA	60
264735_S_AT (02+) rev	ACTGCTGCCGCTGTAAGTAAGAC	
aspartyl protease (+) for	GGTATCAGTGTAGGCGACAAGGA	60
aspartyl protease (+) rev	CTGTGCCTGAGTCGATTATAGCA	
ATGRP19 (01-) for	GCCTCCGGTTCCTTTGGT	60
ATGRP19 (01-) rev	TCCCTCCCTGTACGTTTCTTGTA	
ATPR2 (+) for	GACACGGCCAACATCCATCT	60
ATPR2 (+) rev	GAGTACCCTGGATCGTTATCAACA	
AWPM-19 (02+) for	AGCTTCTCTACCTCATGTTGATCCAT	60
AWPM-19 (02+) rev	GTAGCATAGTCTTGGTCTCTGTATCCA	
CYP96A15 (01-) for	ATGAGACTCTACCCGCCACTTC	60
CYP96A15 (01-) rev	TTTGTGCCCGCTTGGAA	
DDBR 1B (-) for	GGTGGTTGGTGAGTATCACATAGG	60
DDBR 1B (-) rev	TCAGGCAGCTTCATGACAAGA	
ELM2 (01+) for	GCGCCACTGCAATGATCTT	60
ELM2 (01+) rev	CTGGCAGTATTGAATCACAAGGAT	
GILT (01-) for	CATGGTGAAGAGGAATGCAAAC	60
GILT (01-) rev	TTTCTGATCGGGCCAAGTTC	
Glycosyl hydrolase (-) for	CCGTCCCGCCATCCA	60
Glycosyl hydrolase (-) rev	GGATTGCACAACGATCTTCAAA	
GSH reductase (Cd) for	TGATGAGAAGAGTGATAAGGTTATTGGA	60
GSH reductase (Cd) rev	TGCAATCCCCTGCATGATC	
Hm trans-detox (-) for	GGAAGAAGTGGAAGTAGAGATGGAA	60
Hm trans-detox (-) rev	CGTACCGCTTTCAATACCTTCTTT	
ion chan inhib (02+) for	CGGCGATGTGGGTTTCA	60
ion chan inhib (02+) rev	TGTTCTTACGGCAGTTCTGATCAC	
PCS (Cd) for	CGGTGGTGACTGGAGTTGTG	60
PCS (Cd) rev	GCGTCGATGGCACTAACAGA	

PERK (02) for	AAGGAAACATATCACCATCAGATCTAAA	60
PERK (02) rev	TCCTCCAGATGAGCCATACACA	
PNP-A (01+) for	TGCATTGGTGCTACATACAACTTTG	60
PNP-A (01+) rev	CGGCAGAAATCAACTACCTTCA	
PR1 (+) for	AGCTCTTGTAGGTGCTCTTGTTCTT	60
PR1 (+) rev	CCTCGTGCCTGGTTGTGAA	
PR5(01+) for	CAGGCTGTGTCTCTGACCTCAA	60
PR5(01+) rev	AGGCCACGACATTGTTCTGAT	
Predicted PR (02+) for	TGGATGCCGAGACACTTACG	60
Predicted PR (02+) rev	CATTGACAACATCACCAGAGTTTG	
RmlC-like cupin (02+) for	GGATCCCTAGATACTTCGCGTTTT	60
RmlC-like cupin (02+) rev	TGGTGAATCCTACAAACTCGAATG	
RmlC-like fam (02+) for	CAGCGGAGGAATGGTGTTG	60
RmlC-like fam (02+) rev	TTGACCTCCTGTGACGTATAGCA	
2S albumin (02+) for	CGACGCAGCTTAGTTCATGTG	60
2S albumin (02+) rev	TTTGCCGCAACAATCTGTAGA	
Sulfotransferase1 (Cd) for	ACAGCTCCAGCAAGTTTCTCTGA	60
Sulfotransferase1 (Cd) rev	GCAGTGAGCATGAAGACGATGTA	
Sulfotransferase2 (Cd) for	GGACACCTTGCGGTTTACGT	60
Sulfotransferase2 (Cd) rev	AGCTTTTGAAAACAAGGGTGACTT	
AST68 (Cd+) for	TCATAGGTATCAGTGTAGGCGACAA	60
AST68 (Cd+) rev	CTGTGCCTGAGTCGATTATAGCA	

Table 3. Primer sequences used to amplify by Real Time PCR the target selected by microarray experiments, both for the wild type and the resistant mutant lines selected. (HK), housekeeping genes; (+), up-regulation in both mutants; (-), down-regulation in both mutants, (01+), up-regulation for *atnp01* only; (01-), down-regulation for *atnp01* only; (02+), up-regulation for *atnp02* only; (Cd), cadmium response genes; (Cd+), cadmium and CdS QDs common response.

Total proteins extraction

For the proteomic profile extrapolations, *atnp01* and *atnp02* were compared with the wild type in MS medium with and without CdS QDs. Six different treatments were performed: two for the wild type line, two for each of the mutant lines (exposed to 0 mg L^{-1}, 80 mg L^{-1} of CdS QDs). To facilitate the separation step, total proteins were extracted following the $MgSO_4$ protocol (Pirondini *et al.*, 2006). Total protein extracted were quantified by Bradford protein quantification method (Sigma Aldrich, St. Louis, MO, USA). Standard curve (λ=595 nm) was perfomed by Varian Cary 50 (Agilent Technologies).

Protein separation and characterization

Quantified proteins were analyzed through Beckman Coulter ProteomeLab PF2D (Beckman Coulter, Brea, CA, USA). ProteomeLab PF2D consist in a two-dimensional liquid chromatography system based on an high-performance chromatofocusing in the first dimension and an high-resolution reversed-phase chromatography in the second dimension. The chromatographic method can be used as a complementary approach to protein separation with 2D gel electrophoresis.

Statistical analysis

Statistics software SPSS 17.0 (http://www-01.ibm.com/software/it/analytics/spss/) was used for most of the statistics analysis. A two-sample t-test was used to evaluate possible variations between each treatment ($P < 0.05$) in case of chlorophyll extraction, respiratory efficiency (TTC assay) and cadmium uptake (FA-AAS) measured in wild type, *atnp01*, and *atnp02*. To identify deviation from mendelian distribution in case of the segregation for the characters of hygromycin resistance and CdS QDs tolerance in both mutant lines a Pearson χ^2 test ($P < 0.05$) was performed.

Concerning microarray experiments, raw data obtained were analyzed by Affymetrix Program Suite Expression Console ver. 1.1 (http://www.affymetrix.com/analysis/) . A model of gene expression was obtained from normalized CEL intensities based on a Perfect Match only model (RMA). The RMA algorithm used a robust multi-array average for background adjustment, normalization, and $\log_2$ transformation of signal values (Irizarry *et al.*, 2003). Normalization was performed using probes derived from three different housekeeping gene commonly used for the data normalization in plant *β-Actin* and *GAPDH* (glyceraldehyde-3-phosphate dehydrogenase) (Fig. 6, 7). A two-sample t-test was conducted to identify differentially expressed genes. To evaluate differential gene expression between each treatment the differences in gene expression between the wild type profiles, in condition of treatment, as standard referee (calibrator) for the mutant profiles ($P < 0.01$) were performed. Differences in gene expression within each treatment were calculated again maintaining the wild type as the calibrator. Heatmaps were performed with Eisen Software Labs Treewiev ver. 1.60 (http://rana.lbl.gov/EisenSoftware.htm, Eisen *et al.*, 1998). Pearson correlation Hierarchical Clustering was performed with MeV ver. 4.7.4 (http://www.tm4.org/; Mar *et al.*, 2011). The profiling data sets in the context of existing knowledge was performed with VirtualPlant 1.2 (http://www.virtualplant.org/; Katari *et al.*, 2011) using a p-value cut-off of 0.01, AraNET

(http://www.functionalnet.org/aranet/; Lee *et al.*, 2010) and Cytoscape 3.0.1 (http://www.cytoscape.org/; Shannon *et al.*, 2003).

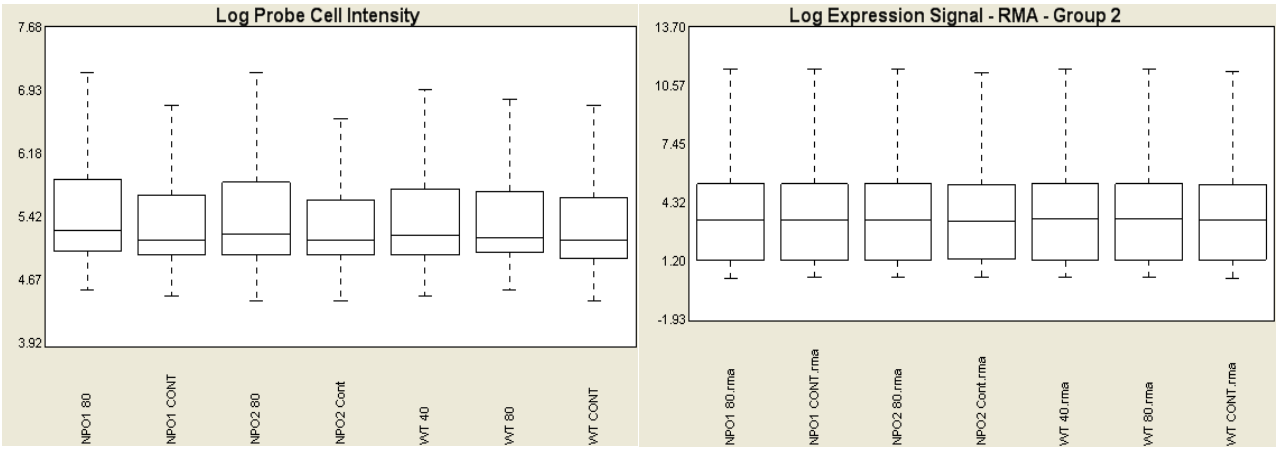

Figure 6. Log Probe cell intensity before (left) and after (right) processing with RMA algorithm.

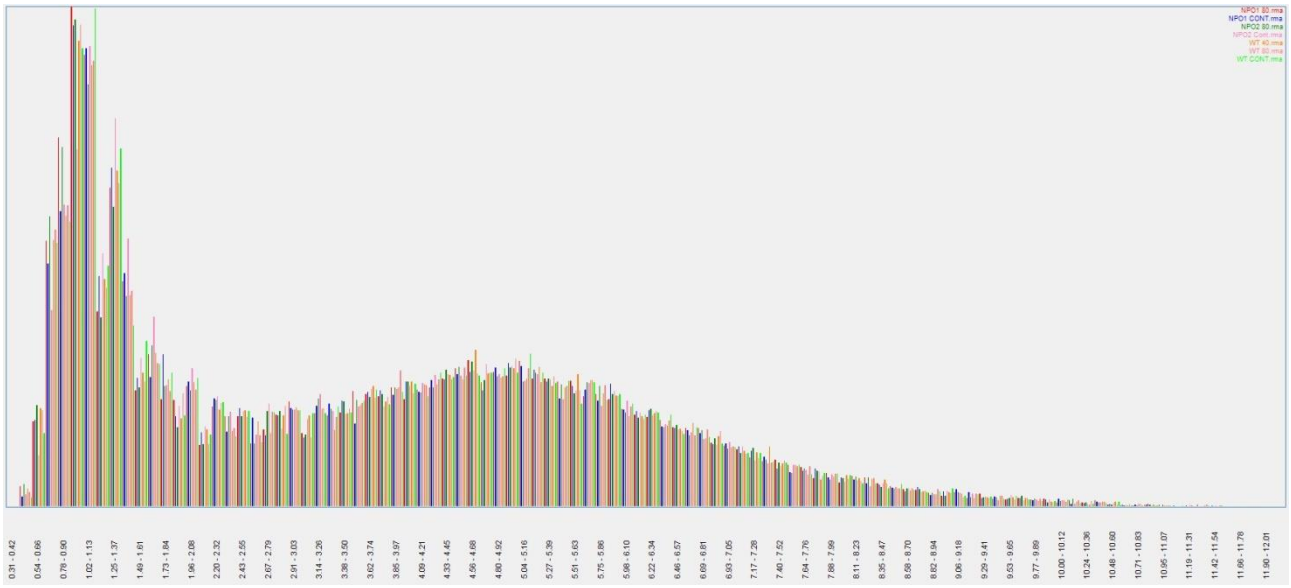

Figure 7. Density histogram of microarray raw data intensities as processed by the RMA algorithm. The y-axis denotes the frequency with which total RNA has a certain abundance as shown by the x-axis. The x-axis represent total RNA abundance in terms of the range of measured intensities.

The presence of a single amplicon in each Real Time PCR reaction was confirmed by dissociation curves. Relative expression was estimated through ΔΔCt method (Schmittgen *et al.*, 2008), with *β-actin* and *GAPDH* specific primers as housekeeping genes. The relative quantity of the transcript assayed in each RNA sample was determined by normalizing on the housekeeping genes expression level and calculated as an arithmetic mean of the three independent repeated reactions. Heatmaps concerning the wild type and the mutant lines in different conditions of treatments were performed with Eisen Software Labs Treewiev ver. 1.60. To evaluate differential gene expression between each treatment, the wild type in condition of treatment, was use as calibrator.

Results & Discussion

Physiological parameters for resistant mutants

Physiological analysis evidenced some of the features of the tolerance/resistance in the mutant lines *atnp01* and *atnp02*. The AAS analysis showed, after treatment with 80 mg L^{-1} of CdS QDs, concentrations of total Cd uptake not statistically different in all the Arabidopsis lines (t-test, $P < 0.05$). For the treatment with $CdSO_4$ and CdS QDs the internal concentrations of Cd were not statistically different ranging from 4.5 mg Kg^{-1} to 5.2 mg Kg^{-1} (Tab. 4). Respiration and chlorophyll content in wild type and mutants have similar basal levels, but with the addition of CdS QDs (80 mg L^{-1}) in the wild type there was a complete inhibition of chlorophyll productuon and a 50% reduction of the respiration. In the two mutants the treatment with CdS QDs did not affect respiration nor chlorophyll content. Treatment with $CdSO_4$ (23.3 mg L^{-1}) inhibited chlorophyll production and respiration both in wild type and mutants at the same extent (Tab. 4).

Samples	Cd conc.[a]	Test t	Chlorophyll conc.[b]	Test t	Formazan abs.[c]	Test t
wt control	0.000 ± 0.020	-	1.809 ± 0.057	-	0.824 ± 0.022	-
wt QDs	4.523 ± 0.127	-	0.017 ± 0.030	-	0.404 ± 0.009	-
wt $CdSO_4$	5.136 ± 0.256	-	0.051 ± 0.003	-	0.042 ± 0.012	-
atnp01 control	0.000 ± 0.020	1.0000	1.896 ± 0.050	0.2856	0.877 ± 0.008	0.0802
atnp01 QDs	4.503 ± 0.010	0.8248	1.862 ± 0.028	2.0211 E-05	0.902 ± 0.004	0.1650 E-04
atnp01 $CdSO_4$	4.660 ± 0.233	0.0031	0.059 ± 0.004	0.1296	0.041 ± 0.020	0.9366
atnp02 control	0.000 ± 0.020	1.0000	1.783 ± 0.024	0.2966	0.869 ± 0.003	0.0603
atnp02 QDs	5.255 ± 0.591	0.2178	1.678 ± 0.012	5.0922 E-05	1.052 ± 0.005	7.8400 E-05
atnp02 $CdSO_4$	4.903 ± 0.243	0.0055	0.038 ± 0.006	0.0417	0.067 ± 0.006	0.0323

Table 4. Physiological parameters and Cd uptake. The effect on wild type, *atnp01* and *atnp02* plants exposed to 207 µM $CdSO_4$ (23,33 mg L^{-1} of Cd^{2+}) or 80 mg L^{-1} CdS QDs. (a) Cd concentrations in plant tissue determined by FA-AAS in µg g^{-1} dry weight. (b) Chlorophyll absorbance, determined spectrophotometrically, was transformed in chlorophyll concentration through the Lambert-Beer equation (mM). (c) Cellular respiration measured by the TTC assay.

Cross and segregation of the CdS QDs resistance character

Genetic crosses and segregation of characters showed how the CdS QDs resistance and the Hm^R are tightly bound. Considering the presence of two different Ds elements inside the mutant line *atnp01* a 9:3:3:1 (93.75%) segregation of the character Hm^R was expected. For the CdS QDs tolerance character a 3:1 (75.00%) segregation was expected because only one of the two insertions was considered as responsible of the resistant character. Conversely, for the second mutant line *atnp02*, with only one Ds element insertion, both the Hm^R and the CdS QDs resistance were considered as dominant characters with an expected segregation of 3:1 (75.00%). The segregation coefficients observed were in agreement with the parameters expected, especially for CdS QDs tolerance, and were confirmed by the statistical analyses (Tab. 5). An amplification of the flanking regions performed on DNA of the resistant lines confirmed the stability of the Ds element positions inside the two mutant lines.

Line	Seeds	Seeds expected	(a) Hm germination	(a) Expected(%)	(a) Observed(%)	(b) CdS QDs growth	(b) Expected(%)	(b) Observed(%)	Pearson χ^2
Wild type	250	0	2	0.00	0.80	0	0.00	0.00	0.1572
F_2 *atnp01*	250	234	208	93.75	83.20	208	75.00	83.20	0.0685
F_2 *atnp02*	250	187	198	75.00	79.41	198	75.00	79.41	0.3595

Table 5. The table showed the results of segregation. a: percentage of germination expected considering as dominant the resistance to hygromycin (C= 40 μg mL^{-1}). b: percentage of plant growth expected considering as dominant the "CdS QDs resistance" character (C= 80 mg L^{-1}).

Mutants resistant to engineered nanomaterial, in our case, were selected on Petri dishes with 80 mg L^{-1} CdS QDs and their growth fitness as compared with the sensitive wild type was higher (Fig. 5, Tab. 4) with no possibilities of the misinterpretation of tolerant/resistant phenotype. Treatments of *A. thaliana* seeds with CdS QDs in Petri dishes showed that the effect on growth was stronger than on germination. These results suggest that the CdS QDs could have possible difficulties in penetrating through the seed coat, and that only after the germination the CdS QDs could be taken up into the plant. When supplementing the nanoparticles liquid medium, without CdS QDs, this

didn’t produce any inhibition on growth, and on germination. This result suggest that the inhibition exercised by CdS QDs was imputable only to the CdS QDs and not to any other possible byproduct generated during the nanoparticles synthesis or during nanoparticle conservation in solution. This observation does not comply with other authors suggesting that, in some metal sulfides and metal selenides, oxides are formed and are the cause of the toxicity rather than the all nanoparticle (Hochella *et al.*, 2008). The uptake of CdS QDs in mutants and wild type lines occurred at similar extent: when measuring the quantity of total Cd within the plants the results were comparable. These results demonstrated how the mutant lines and the wild type line had a similar Cd intake and excluded that tolerance/resistance was due to a mechanism of avoidance: the mutants did not exclude the CdS QDs. In condition of treatment with CdS QDs, the wild type line drastically reduced cellular respiration and photosynthetic efficiency whereas the mutant lines maintained normal levels (Tab. 4). When wild type and mutants were grown with $CdSO_4$ they all took up total Cd at similar extents. However treatment with $CdSO_4$ and CdS QDs had the same effect on chlorophyll production and respiration in wild type, but $CdSO_4$ totally inhibited the two functions both in mutants and wild type. This confirms also the suggestion that in our case the metal sulfide did not produced ion Cd in the condition of treatment with CdS QDs. The tolerance of the mutant lines to CdS QDs is a true resistance which rests on some physiological and genetic mechanisms triggered by specific genes rather than from the exclusion of the CdS QDs and of Cd in particular. In our screening we have not found any CdS QDs excluder.

Microarray experiments

Treatment with CdS QDs of the concentration of 40 mg L^{-1} for 21 d gave information on the effects in non-lethal condition for the wild type. Raw analysis showed an overexpression of 23 genes in which the main functional class involved (21.7%) was temperature stress regulators. These results could represent the earlier response to the CdS QDs exposition.

Comparison between the wild type in untreated condition with treatment at MIC (80 mg L^{-1}) showed 148 up-regulated genes and 43 down-regulated genes; 32.4% of the genes induced by treatment were genes involved in detoxification: ROS (reactive oxygen species) metabolism (peroxidase, cytochrome P450 subunits), ion transporters, heat shock proteins, temperature stress regulators (Fig. 8). There were no others significant differences in wild type line between the response to 40 mg L^{-1} treatment and 80 mg L^{-1} treatment.

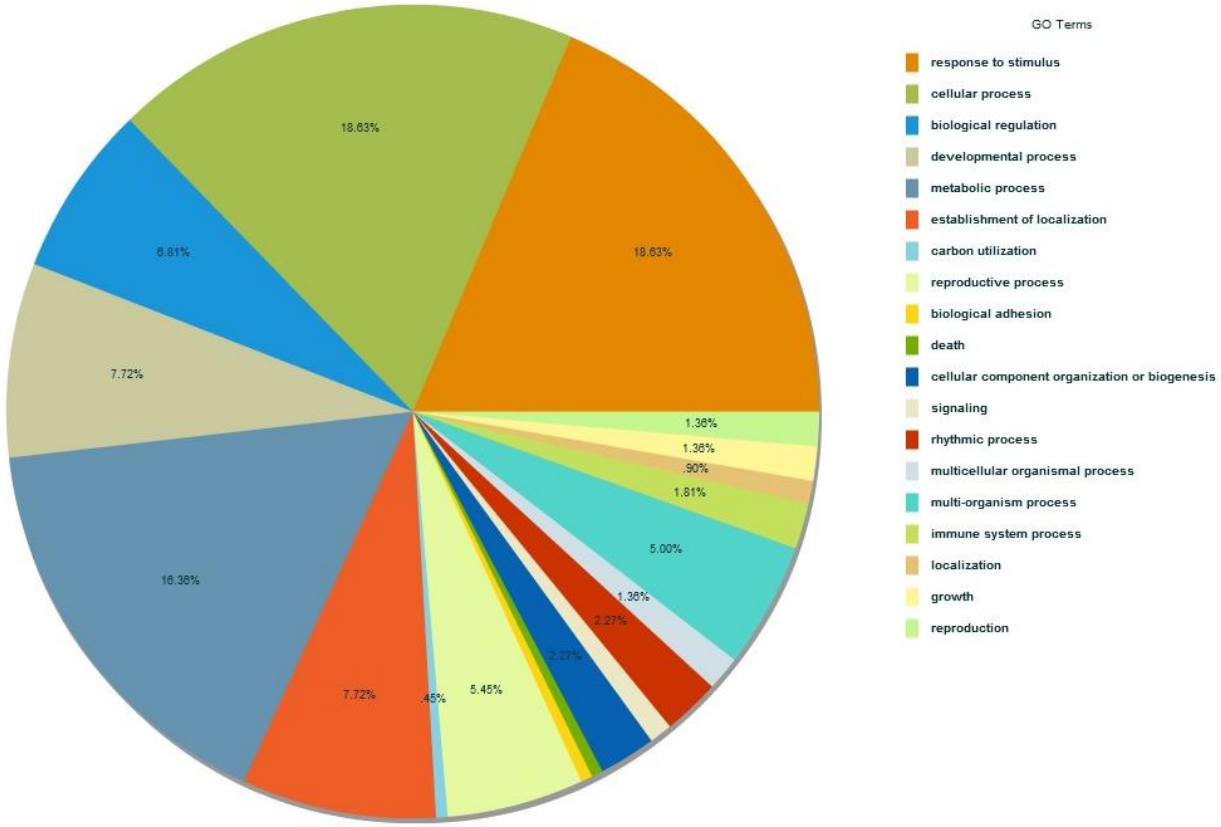

Figure 8. Biological processes pie chart of up-regulated genes using Gene Ontology (GO) terms of the software VirtualPlant in wild type exposed to CdS QDs (80 mg L^{-1}).

Comparison between the expression profile of the two mutant lines with the wild type at 80 mg L^{-1} of CdS QDs showed important transcriptomic differences. The results obtained evidenced a list of genes up-regulated and down-regulated in the two mutant lines. This list included genes involved in metabolic functions (24%), detoxification activities and stress response (22%), transporters (10%), reserve proteins (9%), protein synthesis (3%), DNA repair (1%), plant growth and development (12%), and genes with unknown function (19%). All these genes could be divided with the response to CdS QDs in three categories: common response, *atnp01* specific response, and *atnp02* specific response. Venn diagrams showed only a very partial overlap between the response of the wild type and the responses of the two mutants (Fig. 9).

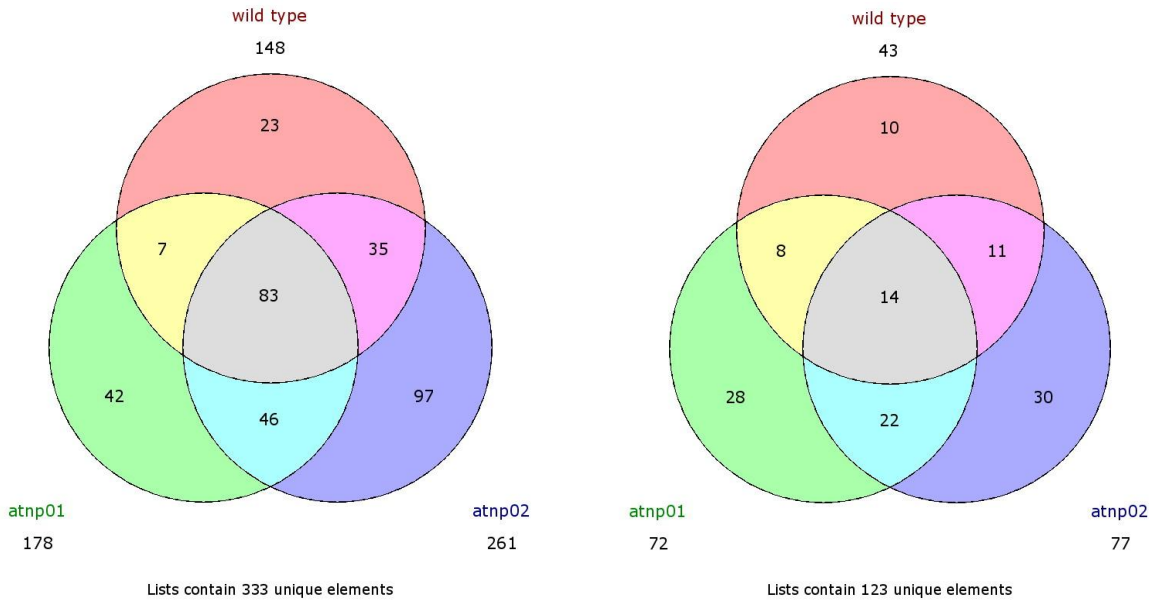

Figure 9. Up-regulated genes (left) and down-regulated genes (right): Venn diagram showing the partial overlap with the wild type response and the two mutant line responses

The common response included genes which were either up-regulated or down-regulated in both mutants. Genes showing up-regulation were: *BGL2* cellulase/glucan 1,3-beta-glucosidase/hydrolase (*At3g57260*), aspartyl protease family protein (*At5g10760*), *PR1* (*At2g14610*) involved in the defense response, and *At1g36920* that codifies for a protein with unknown function. Genes significantly down-regulated were: *DDB1B*, a damaged DNA binding/protein binding (*At4g21100*) involved in embryonic development ending in seed dormancy and which may form part of a *CUL4*-based E3 ubiquitin ligase; *At3g28970*, a copper ion transporter; *At5g27780* and *At1g29430*, genes involved in auxinic response but with unknown function.

The *atnp01* specific response included genes that in *atnp01* only showed up-regulation and down-regulation. Genes showing an up-regulation were: *PR5* (*At1g75040*), pathogen related protein, *At2g18660*, which codifies for a *EXLB3*, expansin-like B3 precursor, known also as *PNP-A* (Plant Natriuretic Peptide A). PNPs are a class of systemically mobile molecules distantly related to expansins by their true biological role remains elusive. *PNP-A* contains a signal peptide domain and is secreted into the extracellular space. Expression profiling using microarray suggest that *PNP-A* may function as a component of plant defense response and in particular SAR, which could be classified as a newly identified pathogen related proteins (*PRP*) (Morse *et al.*, 2004; Gehring *et al.*, 2003). Another important variation was in *DC-1* domain-containing protein (*At3g27473*) with function of zinc ion binding involved in signaling cascades. The fourth most overexpressed gene

was *At1g13880* (an *ELM2* domain containing protein), the same gene visited by the Ds element in the mutant *atnp01*. The mutation in this gene which leads to its overexpression might be phenotypically translated in the expression of tolerance/resistance to CdS QDs. Between the down regulated genes in *atnp01* the γ-interferon responsive lysosomal thiol reductase family protein/*GILT* family protein (*At4g12960*) with function unknown; two different glycin rich-protein, *GRP17* (*At5g07530*) and *GRP19* (*At5g07550*) with function of lipid binding and a role in lipid storage and plant defense (Mangeon *et al.*, 2010) Other genes were also identified: *At1g72260*, a gene coding for a toxin binding receptor, *Thi2.1*, involved in the response to jasmonic acid and salicylic acid, jasmonic acid which mediates signaling pathway and defense response, and *At1g65340* which codifies for *Cyp96a15*, a member of the cytocrome P450 superfamily.

The *atnp02* specific response included both up- and down-regulated genes. The up-regulated genes were mostly related to seed reserve proteins: three different genes codifying for cruciferins were identified (*At5g44120*, *At4g28520*, *At1g03880*), three different genes that encode for oleosins (*At3g27660*, *At5g40420*, *At4g25140*), two genes for cupins (*At1g03890*, *At2g28490*), four genes for seed storage albumins 2S (*At4G27160*, *At4g27140*, *At4g27170*, *At4g27150*) and two different lipid transpost proteins (*LTP*) (*At5g38160*, *At5g54740*) with function of lipid binding, nutrient storage activity, also involved in lipid transport and pollen development. But more genes were upregulated: *At2g15010* coding for a thionin, *At2g27380*, a *AtEPR1* with function of structural constituent of cell wall, involved in plant-type cell wall modification and seed germination (Debreucq *et al.*, 2000), *At1g47540*, which encodes for an ion channel involved in defense and other genes with unknown functions (*At1g04560*, *At1g62080*, *At1g62000*, *At1g62060*, *At1g62220*). As for the *atnp02* down-regulated genes, none exceeded the fixed threshold. Reserve proteins are believed to be implicated in the tolerance/resistance to CdS QDs, however, the molecular correlation with the transposition generated by Ds element is not certain in this case. Since CdS QDs seems to inhibit functions involved in protein synthesis it seems conceivable that an increase in the amount of reserve protein could reduce the toxic effect of CdS QDs.

An important consideration is related to the expression level of others genes implicated by the transposition: in *atnp01*, of the three genes interested by the Ds transposition the only gene showing a significant level of overexpression in comparison with the wild type was *At1g13880* (the *ELM2* domain-containing protein), whereas the other two genes (*At3g46880*, *At1g13870*) did not show statistically significant differences with the control. It is important to underline how the level of expression of *At1g13880* is not statistically different comparing *atnp01* in treated, using 80 mg L^{-1} of CdS QDs, and untreated conditions, which could indicate a constitutive effect on the *At1g13880*

gene expression by the Ds element. A different result was found for *atnp02*: none of the three genes implicated in the transposition by the Ds element (*At3g24330*, *At3g24430*, *At3g24400*) showed an expression level statistically different comparing mutants and wild type both in condition of treatment. Comparing the wild type and the mutants profiles in untreated conditions, there are no statistically significant differences in the expression levels, with the exception of the gene *At1g13880*.

Both mutants (*atnp01* and *atnp02*) were backcrossed with the wild type. The F_1progenies were grown and self-pollinated to obtain a significant F_2 generation of seeds. The results of segregation in these F_2 showed how the genetic determinism of resistance to the CdS QDs most probably rest on one gene in each mutant line. The segregation of resistant mutants was also consistent with dominance (Tab. 5), as for the segregation of the Hm^R character. The mutant line *atnp01* has two Ds elements inserted but three putative genes (*At3g46880, At1g13870, At1g13880*) interested by a transposition whereas the mutant line *atnp02* has one Ds element and three putative genes also interested by the transposition (*At3g24330*, *At3g24430, At3g24400*). It is conceivable that within these genes rests the expression of the resistant phenotype. To find out more about the genetic and molecular properties of these phenotype we have analyzed data emerging from a 24K Affymetrix microarray chip hybridized with aRNA (amplified RNA) from treated and untreated wild type and mutant lines. Different comparison were performed: wild type compared with 40 mg L^{-1} and 80 mg L^{-1} of CdS QDs. This first comparison was thought relevant because 40 mg L^{-1} was sublethal whereas 80 mg L^{-1} lethal but only for the wild type, all in untreated conditions and all in treated conditions with 80 mg L^{-1} of CdS QDs. The second comparison showed all in the untreated condition: small differences in the transcriptomic profiles of wild type and mutants were identified. The third comparison, between wild type and mutants in treated condition (80 mg L^{-1}) showed a treatment specific response common to all the lines and an *atnp01*- and an *atnp02*- specific one. The correlation of the responses with the gene ontology is represented in the heatmap (Fig.10). The genes up- and down-regulated common to all conditions tested in wild type and mutants are represented by Venn's diagrams (Fig. 9).

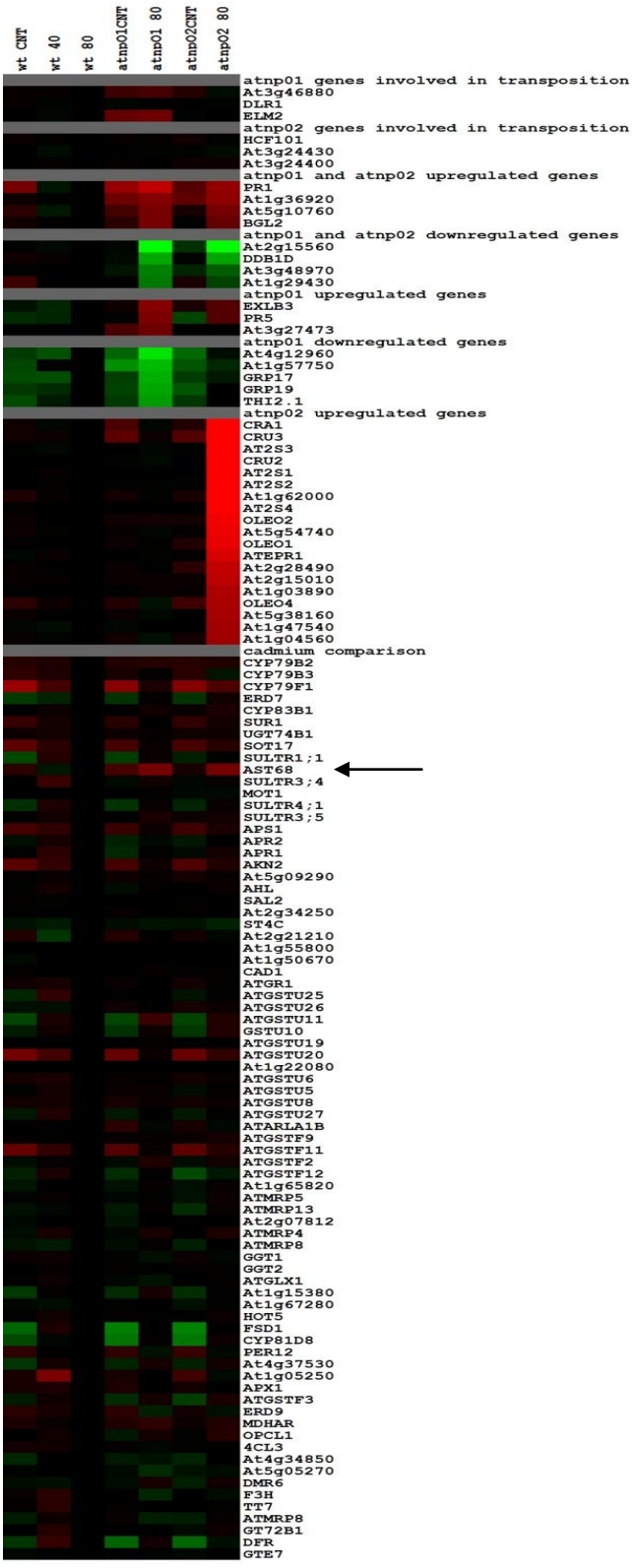

Figure 11. Heatmap illustrating the genes involved in the responses to CdS QDs (top) and $CdSO_4$ (bottom). The only gene which showed a significant difference in expression (*AST68, At5g10180*) as result of exposure to $CdSO_4$.

Metabolic pathways like starch, sucrose , and phenylpropanoids metabolism had genes which were included in the category of common response to CdS QDs, in particular *BGL2* (*At3g57260*) also named *AtPR2*. This result is interesting for the purposes of our research because considering the role of 1,3-beta-glucanase in the formation of endoplasmic reticulum bodies and their role in the response to biotic and abiotic stress (Yamada *et al.*, 2011) could explain how the plants respond to CdS QDs as to a abiotic stress. The softwares VirtualPlant, AraNET and Cytoscape allowed to make more specific considerations about the possible role of some of the genes previously enlisted after the microarray experiments, generating also a possible interaction network (Fig. 11). For *atnp01* (Fig. 10, 12), but in particular for *atnp02* (Fig. 10, 13, 14), it is possible to underline the main molecular functions involved. For *atnp02*, the implications of lipid binding proteins (p-value of 2.91e-7, 37.04%) and the nutrient reserve proteins (p-value of 1.78e-19, 45%) could be a key issue for the comprehension of the plant behavior in presence of CdS QDs. The molecular response of *atnp02* is more complex because the metabolic implications of up-regulation of genes involved in reserve proteins and lipid metabolism for the establishment of the resistant phenotype could have at least a as important as that of an O-glicosyl transferase (of the endomembranes) and of a chloroplast ATP- binding protein and certainly of the pseudogene for the putative rich-extensin like receptor, which are the three genes evidenced after the genome walking experiment in *atnp02*. There should be a network between the former and the latter genes (Fig. 11) in which one of the genes is epistatic to the function of the others, subdivided in different cluster of genes involved in CdS QDs response. The resulting pleiotropic effect is a regulatory cascade which induces morphological ultrastructural and molecular changes, essential for the resistance to CdS QDs. The overexpression of reserve proteins and lipid transport proteins could be a final step in this cascade with the effect of making cell function more independent on novel macromolecules synthesis.

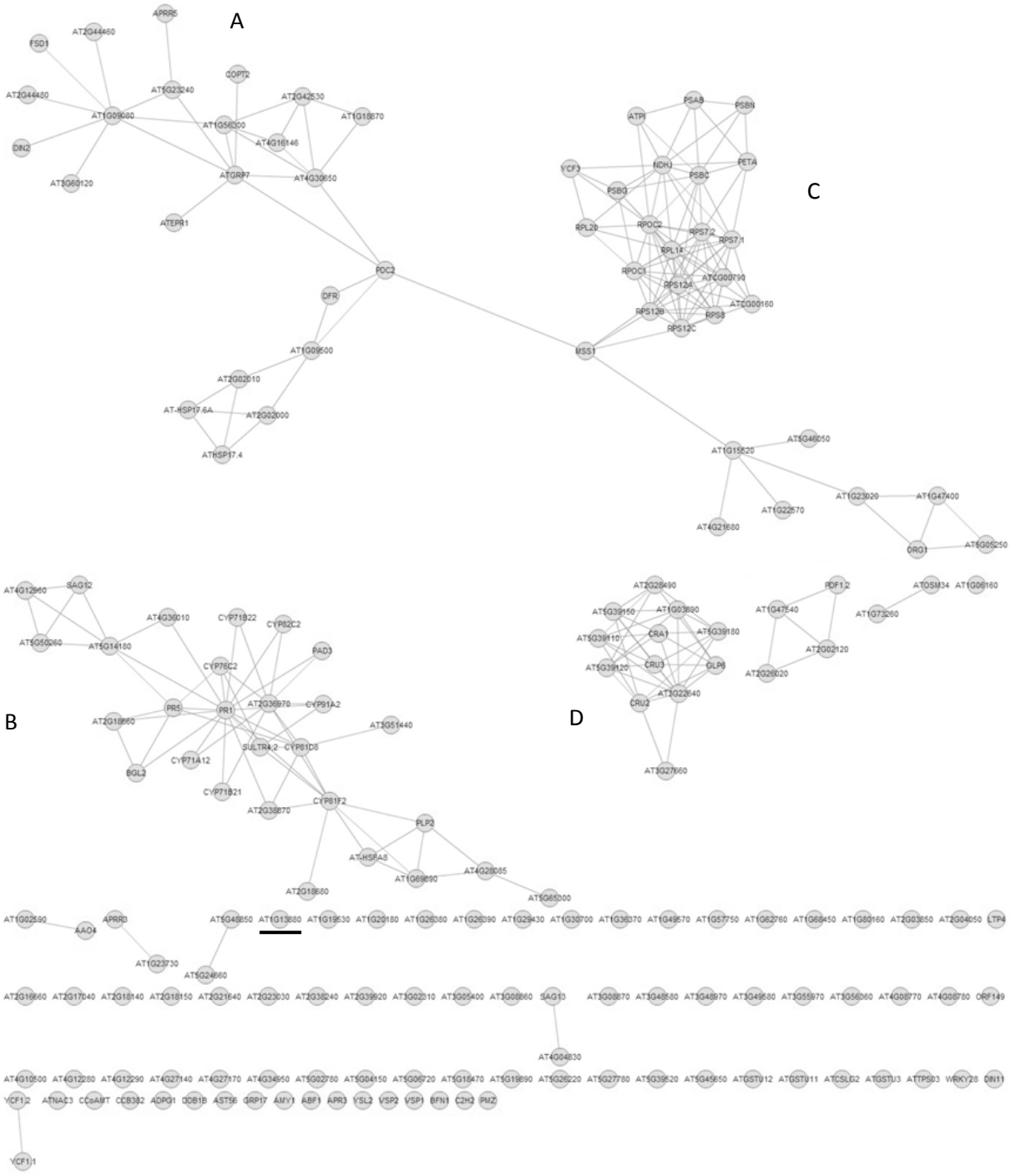

Figure 11. Interaction network of genes involved in CdS QDs response. Generated by Cytoscape. There are appreciable several cluster of genes involved in the response: A, B. genes involved in plant response to pathogen activities and oxidative stress; C. genes involved in protein synthesis; D. genes encoding for reserve protein of the seed (*atnp02* specific). *At1g13880*, underlined in black, did not show any interaction known with the other genes involved in response.

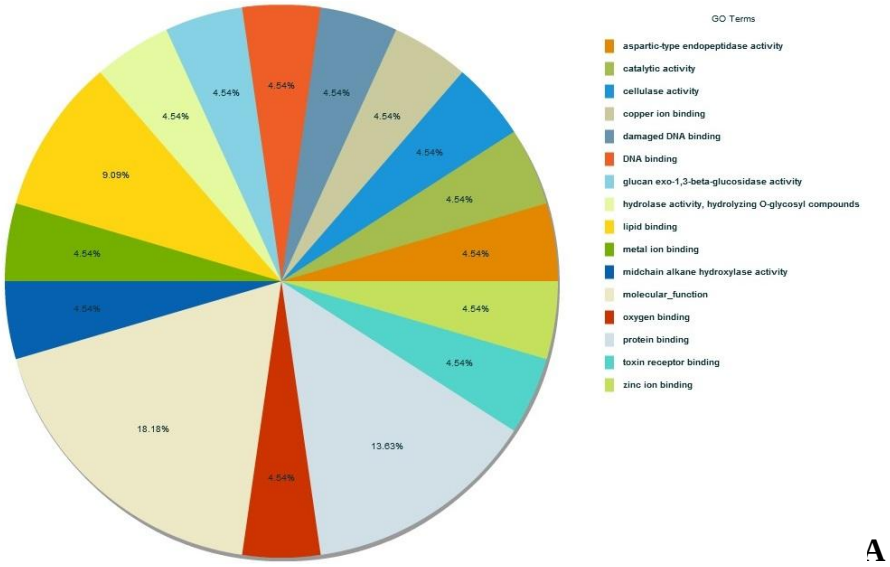

A

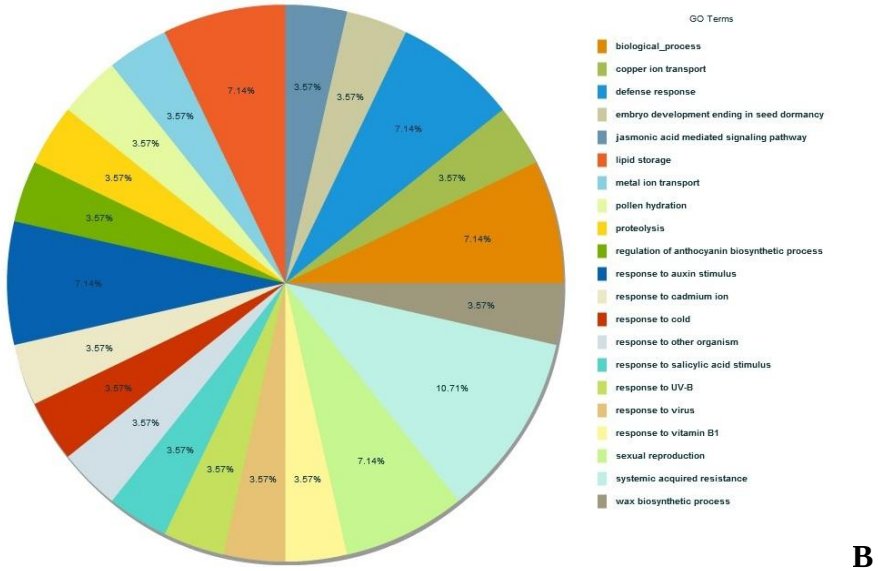

B

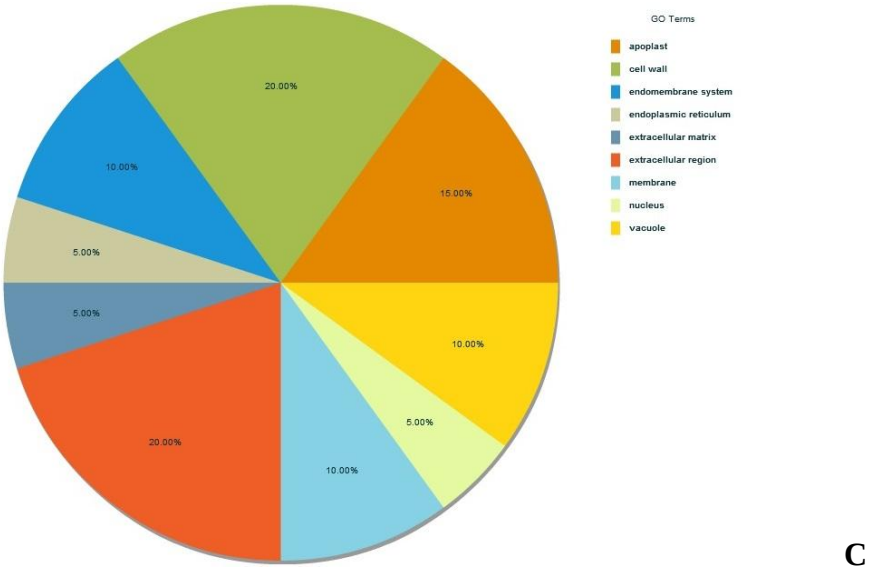

C

Figure 12. The distribution of *atnp01* upregulated genes based on Gene Ontology (GO) terms of the software VirtualPlant with respect to (A) biological processes, (B) molecular functions, (C) cellular components.

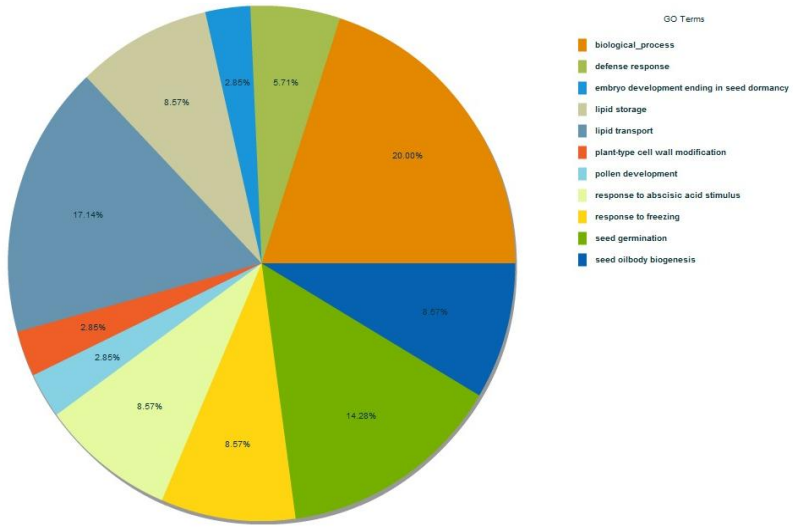

A

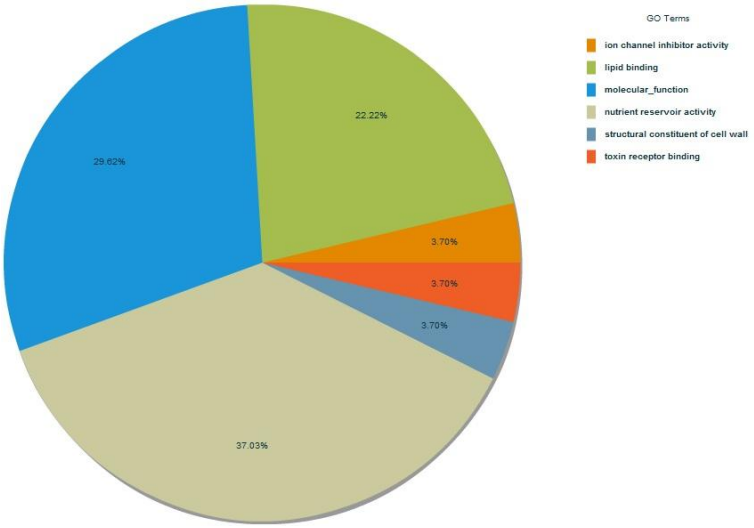

B

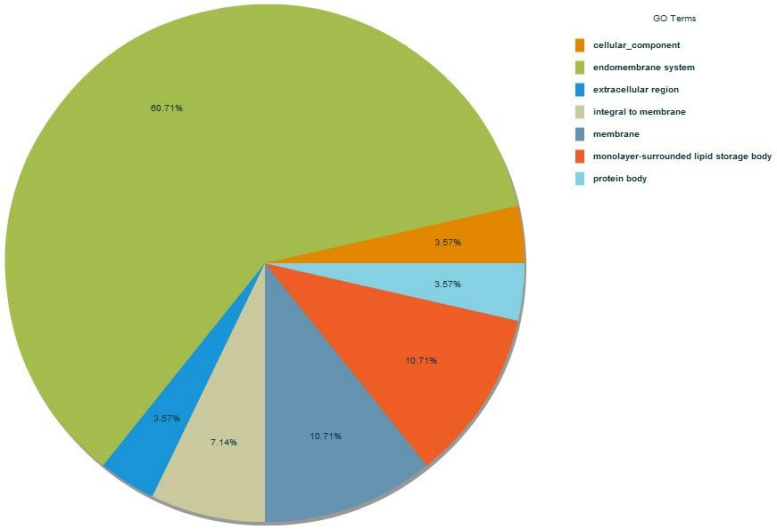

C

Figure 13. Biological processes. (A) molecular functions, (B) cellular components, (C) pie chart of *atnp02* upregulated genes using Gene Ontology (GO) terms of the software VirtualPlant. It is important to highlight, among the molecular functions (b), the involvement of seed storage proteins, in gray, in the CdS QDs response.

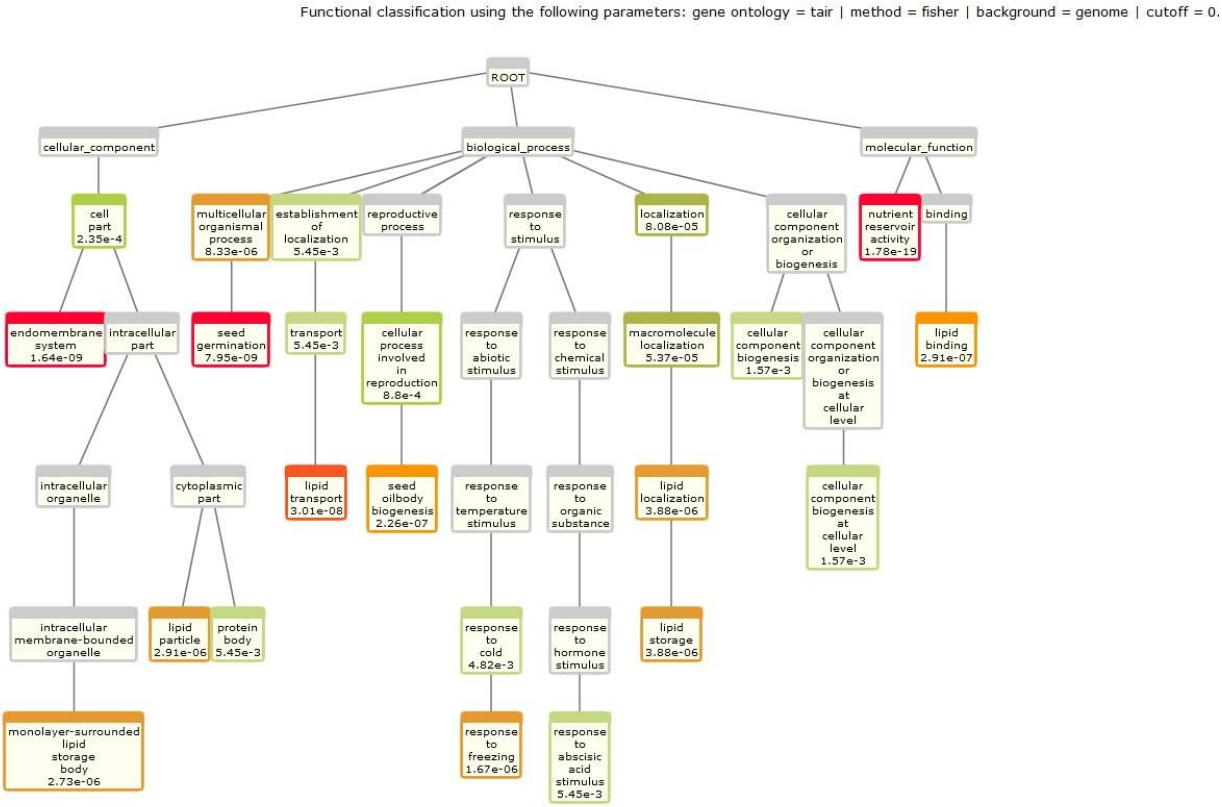

Figure 14. Flowchart of upregulated genes of *atnp02* using Gene Ontology (GO) terms of the software VirtualPlant. The significance of p-value increases from gray to red in the color of the boxes.

Another interesting aspect are the localizations of the gene product: 60.7% of the gene products was localized at the level of the endomembrane system (p-value of 1.64e-9). This result confirmed the important role of endomembrane system in condition of stress (Matsushima *et al.*, 2002). In the mutant *atnp01* it is of paramount importance *At1g13880* (*ELM2*), a putative member of the *MYB* (myeloblastosis) transcription factor superfamily, as a key factor in the regulatory networks controlling development, metabolism and responses to biotic and abiotic stresses (Dubos *et al.*, 2010). The expression levels of the *MYB*-related genes during the various treatments in wild type were generally low, most of these genes are expressed at relatively high levels during salicylic acid treatment (Yanhui *et al.*, 2006). Some members of the *MYB* family are involved in defense responses in plants, because salicylic acid has a major role in defense against plants pathogens. In condition of stress ABA signaling activates *MYB*-related genes which are significantly induced also by $CdCl_2$ and NaCl (Yanhui *et al.*, 2006). The *At1g13880* (*ELM2*) expression strongly increases the mutant *atnp01* tolerance and the segregation of this gene explain almost completely the dominance of the character CdS QDs tolerance. In this case also the up-regulation of *ELM2* was associated with a number of other genes up- and down-regulated, specifically during the treatment, inherent to this

mutant only. The hypothesis of a eQT (expression- Quantitative Trait) in which *ELM2* is the epistatic factor and some of the other genes constitute the controlled QT can be considered as hypothesis. The idea is that resistance to a stressor like CdS QDs could be controlled by a gene network with a primary gene which triggers all the cascade. The difference found between the two mutants lines suggest that different molecular patterns were involved in CdS QDs tolerance, but this does not rule out the possibility that the genetic mechanism was similar. A possible scenario is that both the mutants had an epistatic gene which triggers the first step of regulatory cascades (the overexpression of *At1g13880* in *atnp01*, the expression of reserve proteins in *atnp02*) leading to downstream effects like those observed in *atnp01* and *atnp02*.

The cadmium salt comparison

Analysis of the gene expression profiles in plant treated with Cd salts showed how the mechanisms of tolerance is completely different from tolerance to CdS QDs. In fact, a direct comparison in Arabidopsis of the genes involved in Cd response (Herbette *et al.*, 2006; Clemens, 2006) and the genes involved in the oxidative stress response (Blokhina *et al.*, 2010) showed that only one gene overexpressed in those conditions is also common to those found with our analyses (Fig. 10). This gene, *AST68* (*At5g10180*), encodes for a low-affinity sulfate transporter expressed in the root cap and central cylinder, where it is induced by sulfur starvation. *AST68* is expressed in the shoot vascular system and in these tissues is not induced by sulfur starvation (Takahashi *et al.*, 1997). In previous studies by Howden et al., 1992 *A. thaliana* Cd sensitive mutants were analyzed and showed a deficiency in synthesis of both phytochelatyn and glutathione pathways (Howden *et al.*, 1995a; Howden *et al.*, 1995b). However, no significantly differential expressions of genes related to Cd tolerance, such as phytochelatyn synthetase (*PCS*) and glutathione reductase, were found in our mutants treated with CdS QDs. These results, coupled with the sensitivity of *atnp01* and *atnp02* to Cd treatment, evidenced how the mechanisms of resistance to Cd ions and to CdS QDs are different and that the effect of treatment with CdS QDs could not merely be ascribed to the effect of Cd.

Real Time PCR validation

Real Time PCR data analysis was performed through ΔΔCt method. Data normalization was performed using the same housekeeping utilized for microarray experiments *β-actin* and *GAPDH*. Primers assessed showed a good level of amplification in all the dilution tested (Fig. 11, 12). Ct concerning the serial dilutions of cDNA analyzed (1, 1:10, 1:100, 1:1000) were not significantly different from the theoretical ratio (3,3333).

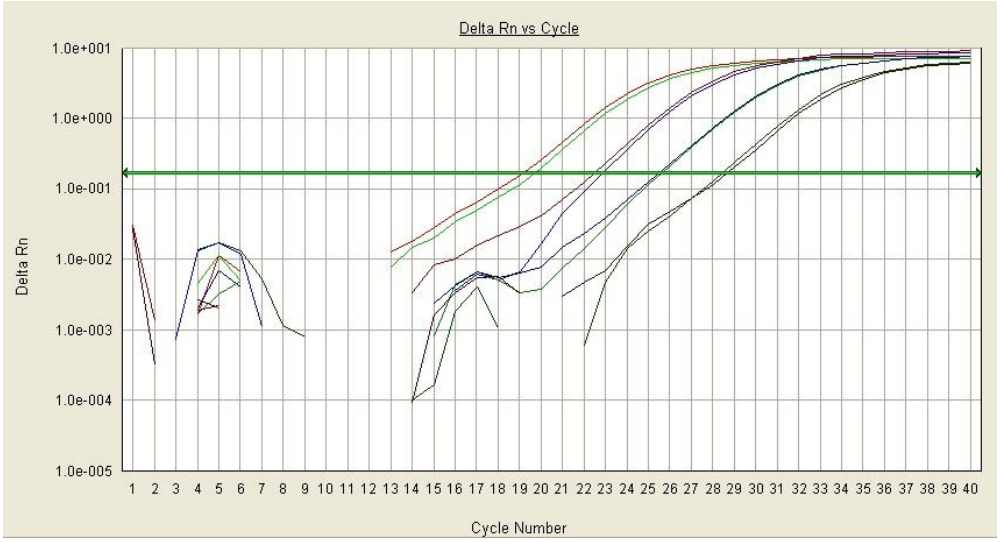

Figure 11: Real Time PCR amplification plot of *β-actin* tested in SYBR Green in serial dilution of cDNA (1, 1:10, 1:100, 1:1000). Primers were assessed on the wild type line in absence of treatment.

Figure 12: Real Time PCR amplification plot of *GAPDH* tested in SYBR in serial dilution of cDNA (1, 1:10, 1:100, 1:1000). Primers were assessed on the wild type line in absence of treatment.

Real Time PCR analyses confirmed largely the results obtained from the microarray, both in case of normalization with *β-actin* (Tab. 6, Fig. 14) and *GAPDH* (Tab. 7, Fig. 15). The wild type line in treated condition (80 mg L^{-1}) was used as calibrator. Comparison between wild type and mutants in treated condition showed, as previously seen for the microarray results, a specific response common to all the lines and an *atnp01*- and an *atnp02*- specific one. Correlation of the responses is represented in the heatmaps (Fig.14, 15).

GENE	Wild type CNT	Wild type 80	Atnp01 CNT	Atnp01 80	Atnp02 CNT	Atnp02 80
1- 256166_AT (+)	5.4732 ± 1.2626	1.0000 ± 0.7037	4.8278 ± 1.0069	16.4085 ± 1.5645	5.8764 ± 0.9801	17.4669 ± 0.2324
3- aspartyl protease (+)	2.0935 ± 1.3597	1.0000 ± 0.3310	1.0968 ± 0.1806	23.0003 ± 1.1241	0.9164 ± 0.1883	1.8036 ± 0.2258
4- ATGRP19 (01-)	0.0309 ± 0.2161	1.0000 ± 0.4716	0.8350 ± 0.0411	2.6481 ± 0.2566	0.0154 ± 0.0739	3.4223 ± 0.3285
7- CYP96A15 (01-)	0.2087 ± 0.1108	1.0000 ± 0.3004	0.2037 ± 0.1562	0.2633 ± 0.2573	0.0403 ± 0.1342	0.3698 ± 0.2691
9- ELM2 (01+)	0.4017 ± 0.8931	1.0000 ± 1.2022	1.4511 ± 0.2261	3.1537 ± 0.3123	0.3490 ± 0.4073	0.4567 ± 0.0570
10- GILT (01-)	0.0051 ± 0.8196	1.0000 ± 0.2812	0.0084 ± 0.5994	0.2842 ± 0.3190	0.0011 ± 1.0976	0.2822 ± 0.2428
17- PNA-A (01+)	0.2962 ± 1.4600	1.0000 ± 0.4213	0.4352 ± 0.1798	13.6895 ± 0.5145	0.3197 ± 0.9167	0.6574 ± 0.3772
18- PR1 (+)	1.2016 ± 0.8665	1.0000 ± 0.5863	3.4461 ± 0.4368	22.9432 ± 0.4639	1.0867 ± 0.6818	5.9175 ± 0.2330
19- PR5 (01+)	1.0460 ± 0.8763	1.0000 ± 0.1988	2.1509 ± 05658	29.9607 ± 0.1977	0.9330 ± 0.5727	10.4831 ± 0.4176
12- GSH reductase (Cd)	1.0174 ± 0.6109	1.0000 ± 0.1131	0.8207 ± 0.2148	0.9965 ± 0.4974	0.1450 ± 0.3544	0.2651 ± 0.5205
15- PCS (Cd)	0.8888 ± 0.5835	1.0000 ± 0.2167	0.6806 ± 0.0568	1.9588 ± 0.0736	0.8555 ± 0.0904	1.4691 ± 0.1670
24- Sulfotransferase1 (Cd)	1.3058 ± 0.2430	1.0000 ± 0.3807	0.6783 ± 0.1993	1.3149 ± 0.0506	0.7071 ± 0.0774	1.0754 ± 0.2398
25- Sulfotransferase2 (Cd)	0.4459 ± 0.2001	1.0000 ± 0.5371	0.1258 ± 1.2400	0.1954 ± 0.1904	0.1486 ± 0.1445	0.0698 ± 0.1650
26- Sulfur transporter (Cd+)	2.7606 ± 0.02040	1.0000 ± 0.0931	3.8771 ± 0.1172	31.5594 ± 0.0545	2.6390 ± 0.0529	5.4264 ± 0.1742

Table 6: Real Time PCR result of candidates genes analyzed using *β-actin* for the data normalization. Data shown the effects on gene expression in all the condition of treatment. Wild type in condition of treatment (80 mg L^{-1}) was used as calibrator. (+), up-regulation in both mutants; (-), down-regulation in both mutants, (01+), up-regulation for *atnp01* only; (01-), down-regulation for *atnp01* only; (02+), up-regulation for *atnp02* only; (Cd), cadmium response genes; (Cd+), cadmium and CdS QDs common response.

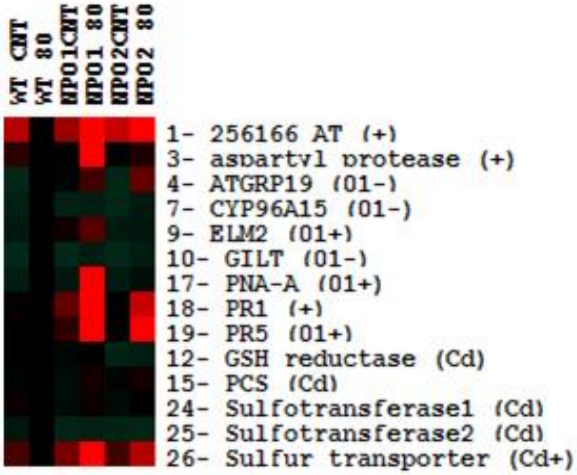

Figure 14: Heatmap representing the results of candidates genes analyzed using *β-actin* for the data normalization. Wild type in condition of treatment (80 mg L^{-1}) was used as calibrator (black). Overexpressed genes are represented different shades of red, whereas downregulated genes are represented in green.

GENE	Wild type CNT	Wild type 80	Atnp01 CNT	Atnp01 80	Atnp02 CNT	Atnp02 80
1- 256166_AT (+)	0.0256 ± 0.4144	1.0000 ± 0.1484	1.6701 ± 1.1987	11.4716 ± 0.2844	12.9062 ± 0.1376	6.4085 ± 0.0762
3- aspartyl protease (+)	1.5104 ± 0.1562	1.0000 ± 0.1637	2.2038 ± 0.4030	7.4384 ± 0.0240	1.96564 ± 0.1436	4.4382 ± 0.586
4- ATGRP19 (01-)	0.0413 ± 0.0670	1.0000 ± 0.0311	0.1154 ± 0.1062	0.1476 ± 0.2223	0.0028 ± 0.8228	0.8150 ± 0.0500
7- CYP96A15 (01-)	0.3014 ± 0.1127	1.0000 ± 0.1851	0.0850 ± 0.1742	0.1271 ± 0.1830	0.0977 ± 0.7554	0.5069 ± 0.0542
9- ELM2 (01+)	1.2226 ± 0.3061	1.0000 ± 0.0917	1.9861 ± 0.1106	5.5596 ± 0.1533	1.2354 ± 0.1749	0.6759 ± 0.2760
10- GILT (01-)	0.0010 ± 0.8196	1.0000 ± 0.2812	0.0164 ± 0.5994	0.0504 ± 0.3190	0.0064 ± 1.0976	0.9930 ± 0.2428
17 - PNA-A (01+)	0.7169 ± 0.2169	1.0000 ± 0.6183	0.7526 ± 0.2188	6.9644 ± 0.1450	1.6701 ± 0.7404	2.7415 ± 0.0977
18- PR1 (+)	4.1843 ± 0.8665	1.0000 ± 0.5863	5.8766 ± 0.4368	21.3327 ± 0.4636	3.9176 ± 0.6818	6.2549 ± 0.2330
19- PR5 (01+)	0.4553 ± 0.8763	1.0000 ± 0.1988	0.7900 ± 0.5658	5.4641 ± 0.1977	0.5105 ± 0.5727	2.7510 ± 0.4176
12- GSH reductase (Cd)	1.3899 ± 0.2422	1.0000 ± 1.1560	1.2311 ± 0.1220	2.8088 ± 0.1263	3.1711 ± 0.1849	1.8596 ± 0.2415
15- PCS (Cd)	0.5340 ± 0.2081	1.0000 ±0.0130	0.5140 ± 0.1043	1.0643 ± 0.0582	0.8467 ± 0.1477	0.6506 ± 0.2422
24- Sulfotransferase1 (Cd)	0.5285 ± 0.2081	1.0000 ± 0.0130	0.6484 ± 0.1043	1.0352 ± 0.0582	0.9965 ± 0.0147	0.6461 ± 0.0242
25- Sulfotransferase2 (Cd)	0.5605 ± 0.0300	1.0000 ± 0.4957	0.5140 ± 0.2316	1.1019 ± 0.2416	0.8766 ± 0.3674	0.6551 ± 0.4336
26- Sulfur transporter (Cd+)	1.3425 ± 0.1579	1.0000 ± 0.0264	1.5855 ± 0.0824	5.0806 ± 0.0893	1.3332 ± 0.0354	3.1166 ± 0.2602

Table 7: Real Time PCR result of candidates genes analyzed using *GAPDH* for the data normalization. Data shown the effects on gene expression in all the condition of treatment. Wild type in condition of treatment (80 mg L^{-1}) was used as calibrator. (+), up-regulation in both mutants; (-), down-regulation in both mutants, (01+), up-regulation for *atnp01* only; (01-), down-regulation for *atnp01* only; (02+), up-regulation for *atnp02* only; (Cd), cadmium response genes; (Cd+), cadmium and CdS QDs common response.

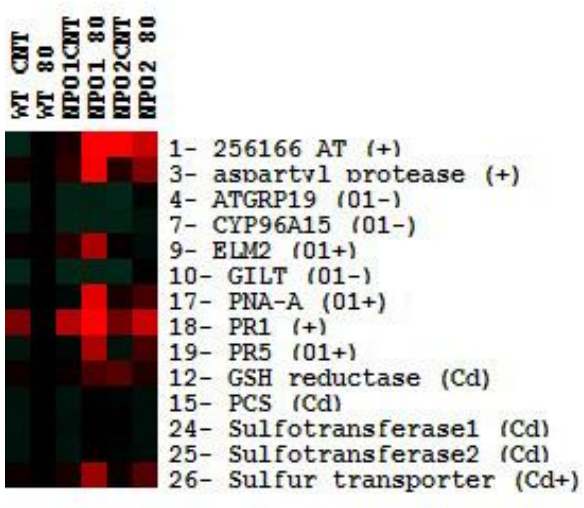

Figure 15: Heatmap representing the results of candidates genes analyzed using *GAPDH* for the data normalization. Wild type in condition of treatment (80 mg L^{-1}) was used as calibrator (black). Overexpressed genes are represented different shades of red, whereas downregulated genes are represented in green.

Real Time PCR results are comparable with the expression levels obtained from the microarray analyses. Small differences are appreciable within the comparison of the expression level of each gene in the various treatments, but the general trend remains unchanged. Considering for instance genes involved in pathogen response: *PR1*, which was induced in both the mutants treated, or *PR5*, pathogen related gene that showed overexpression only in case of CdS QDs treatment of *atnp01*, they maintained a similar expression profile in both cases also in Real Time analyses. Also considering genes involved in Cd^{2+} response, *GSH reductase* or *PCS*, used as control to evaluate the goodness of the analyses done, we observed an expression profile not statistically different from the microarray results. Only in case of *AST68*, gene common in both the response (Cd^{2+} and CdS QDs) there are no significant differences in the expression profiles. Focusing our attention on relative expression level of *At1g13880*, gene involved in Ds element insertion and putative transcriptional activator of MYB family, gene resulted to be significantly overexpressed in case of *atnp01* treated with 80 mg L^{-1} CdS QDs but not in the mutant line *atnp01* in absence of treatment (Fig. 16, 17).

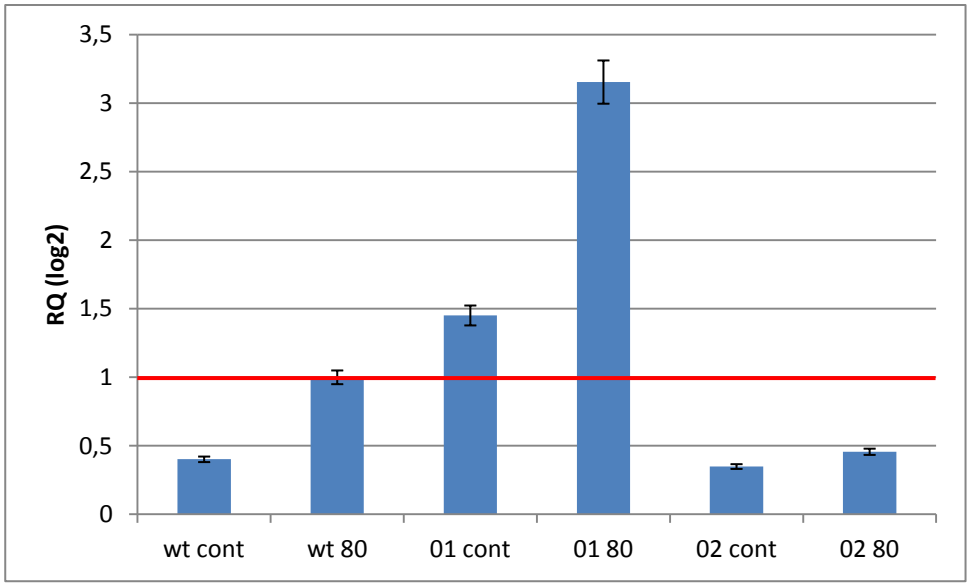

Fig. 16: Relative quantity of *At1g13880* gene, normalization performed on *β-actin*. Expression level of wild type in condition of treatment (80 mg L^{-1}) was used as calibrator.

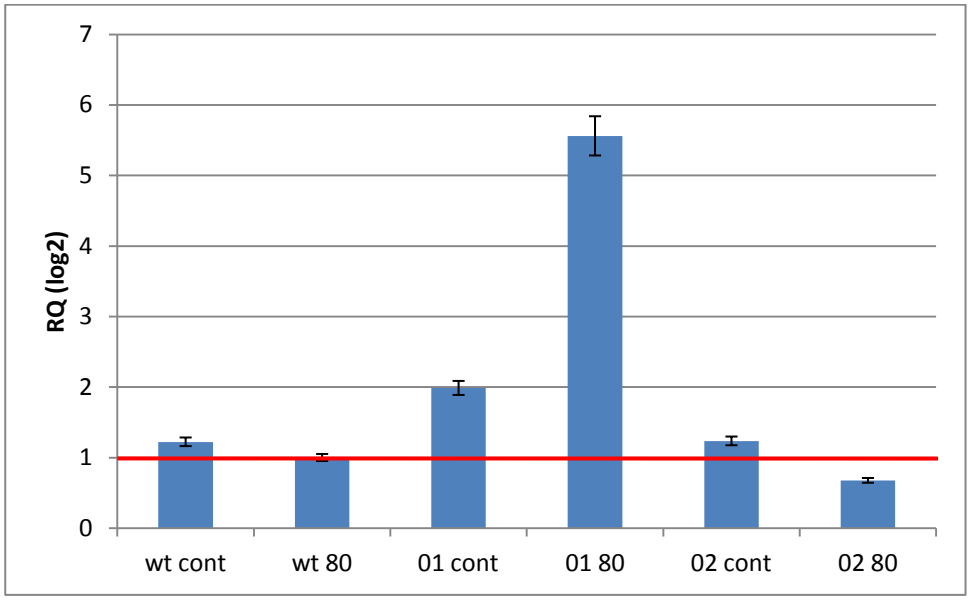

Fig. 17: Relative quantity of *At1g13880* gene, normalization performed on *GAPDH*. Expression level of wild type in condition of treatment (80 mg L^{-1}) was used as calibrator.

The *At1g13880* (*ELM2*) relative expression was strongly increased in *atnp01*. Conversely to what seen previously from microarray data, up-regulation of *ELM2* was associated specifically to the CdS QDs treatment, and not in case of absence of treatment, in which the relative expression level in considered not statistically different from the expression level of the calibrator (wild type treated). This result confirm that ELM2 gene could be an epistatic effector of the CdS QDs response which triggered a regulatory cascades leading to downstream effects, not as a constitutive effector of the response derived from the Ds element insertion but rather from the direct exposition to CdS QDs.

Saccharomyces cerevisiae

The use of yeast as model system

Saccharomyces cerevisiae is one of the most widely used model organism for biological studies at cellular and molecular level. Yeast has a significant role in the field of biotechnology: yeast exploit an haplo-diploid life cycle, and this allows to study also mutations in essential genes. It can be genetically easily manipulated and, thanks to the availability of a large set of experimental tools, it can also be exploited in genome-wide analyses. Furthermore yeast presents an high level of conservation in terms of gene functions as compared to the human genome and that of other eukaryotes. Yeast model system is the main contribution to the scientific community because it is among those organisms that allow to link genes and proteins to their function within the cell.

After the sequencing of yeast genome, the development of post-genomic technologies and the possibility to use public databases (Saccharomyces Genome Database, YEASTRACT), the number of genes encoding for proteins which have functional information has increased from 30% to 85% in few years. This percentage is much higher than any other eukaryote organism. More than thousand yeast genes are correlated with ortholog genes involved in human diseases. Among these genes, the majority of human ortholog is functional in yeast and it enables to rescue the mutant phenotypes of the corresponding yeast strain.

Most of the mechanisms correlated with cytotoxicity, adaptation and resistance to chemical and environmental stress in higher eukaryotes appear to be conserved between yeast. Changes in the levels of metabolites or proteins quantity following exposure to a toxic compound, can help to identify the cellular components and the pathways with key roles in the mechanisms of response to toxicity and stress.

Saccharomyces cerevisiae is an ideal experimental platform to explain toxicity mechanisms: transcriptomics and quantitative proteomics are used to assess changes in gene expression of genes involved in the cellular response of yeast to environmental stress; metabolomics allows to study the metabolic profiles associated with stress response, while the chemo-genomic approach allows to identify the molecular targets responsible for the cytotoxic effect. These techniques must be coupled and integrated with appropriate bioinformatics tools to shed light on the toxicological responses to general stresses.

Materials & Methods

Determination of the Minimal Inhibitory Concentration (MIC)

An *in vitro* test was used for the estimation of MIC for CdS QDs following the EUCAST protocol (EUCAST, 2000). The wild type strain used was BY4742, that contain mutation in four genes involved in aminoacid and nucleotide synthesis (his3Δ1, leu2Δ0, lys2Δ0, ura3Δ0). To determine possible implication of respiratory and metabolic pathways yeast was grown in 25 mL Petri dishes on different nutrient media (Sigma-Aldrich, St. Louis, MO): YPD agar 2% w/v (Yeast extract 1% w/v, Peptone 2% w/v, Dextrose 2% w/v), YPG agar 2% w/v (Yeast extract 1% w/v, Peptone 2% w/v, Glycerol 3% v/v) and SC (Synthetic Complete) agar 2% w/v (Yeast Nitrogen based 0,67% w/v, dextrose 2% w/v) supplemented with histidine (76 mg L^{-1}), leucine (380 mg L^{-1}), lysine (76 mg L^{-1}) and uracil (76 mg L^{-1}) under controlled temperature (30°C). Yeast was grown starting from liquid cultures pre-grown in YPD at an optical density, at 600 nm [OD600], of 1.0 and diluted 200 folds. Medium were supplemented with CdS QDs, increasing concentrations from 40 mg L^{-1} to 1000 mg L^{-1}, for 72 h. To increase the permeability of the yeast membranes and the CdS QDs intake we decided to supplement the growth media with increasing concentrations of nystatin from 0.1 mg L^{-1} to 6 mg L^{-1} (estimated in previous studies made in our laboratories).

Nystatin (represented in figure 18) is an antibiotic, isolated for the first time in 1954 from *Streptomyces noursei* and belonging to the class of polyenic macrolides, able to bind ergosterol present in the fungal cell membrane and lead to the formation of pores that alter the physical characteristics of transport and permeability of the membrane itself. Thanks to these peculiarities, the use of a sub-lethal concentration of nystatin should allow an easier intake of the nanoparticles within the yeast cell.

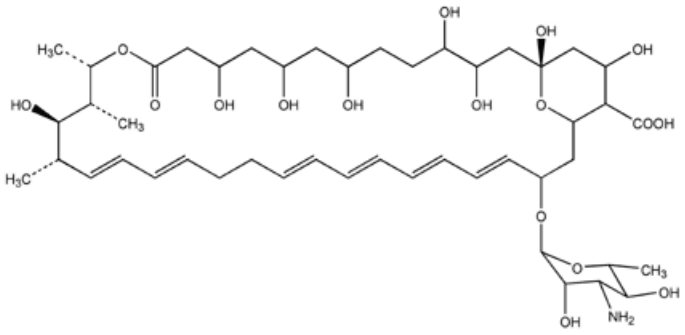

Figure 18. Structural formula of nystatin.

Screening of the knock out mutant collection

A total of 4,688 single gene deletion mutants (non essentials for the organism life), not including 90 strains that failed quality control and 48 slow-growth strains previously shown to exhibit a high false-positive rate, were utilized for genomic phenotyping. Individual plates from the deletion strain collection subdivided in 56 master plates of 96-well format (with one empty well, as contamination controls, and one wild type internal control) were inoculated into 150 μl liquid YPD (Yeast Peptone Dextrose) with 200 μg/ml gentamycin, G418 (Sigma-Aldrich, St. Louis, MO, US) using a VWR 96-pin replicator (Pbi International, Milano, IT). After 2 d at 30°C, cells were inoculated onto YPD-agar without G418, supplemented with nystatin (0,55 mg L^{-1}) and supplemented, at the same time, with nystatin and CdS QDs (200 mg L^{-1}). Replicates were performed in order to obtain a properly diluted inoculum (about 500 cells/pin). After 2 to 3 d at 30°C, plates were examined for sensitive and resistant strains according to relative colony size, followed by digital image recording. Three biological replicate of each treatment were performed.

Spot assay

To confirm the results obtained through the screening a spot assay was performed in 25 mL Petri dishes on YPD agar 2% w/v (yeast extract 1% w/v, peptone 2% w/v, dextrose 2% w/v) supplemented with CdS QDs (200 mg L^{-1}) and nystatin (0,55 mg L^{-1}) at 30°C for 2 to 3 d. Starting from cultures pre-grown in YPD at an optical density at 600 nm [OD600] of 1.0 and diluted up to 10,000 fold in ten-fold increments before spotting.

Rescue of the phenotype by complementation

To investigate of the key role of genes involved in the response of CdS QDs two different genomic libraries of the BY4742 strain were prepared. The genomic libraries were produced according to Jauert *et al.*, 2005 and inserted in a centromeric vector pRS146 (Fig. 18) and in a multicopy vector pRS426 (Fig.19). *Escherichia coli* DH5α strain was used for DNA cloning experiments. The individual libraries obtained were utilized for yeast transformation using the lithium acetate procedure (Gietz *et al*., 2003). To select putative rescued phenotypes, replicates were performed by replica plating, in 25 mL Petri dishes on agar 2% w/v (Yeast Nitrogen based 0,67% w/v) supplemented with 0,2% w/v yeast synthetic drop out without uracil. For the selection SC

(Synthetic Complete) medium was supplemented with nystatin (0,55 mg L^{-1}) and nystatin supplemented of 200 mg L^{-1} of CdS QDs. Strains were grown for 4 to 5 d at 30°C. In order to confirm the results emerging from the yeast transformation, a spot assay was performed on SC medium supplemented with nystatin (0,55 mg L^{-1}) and nystatin supplemented with CdS QDs (200 mg L^{-1}) as previously described.

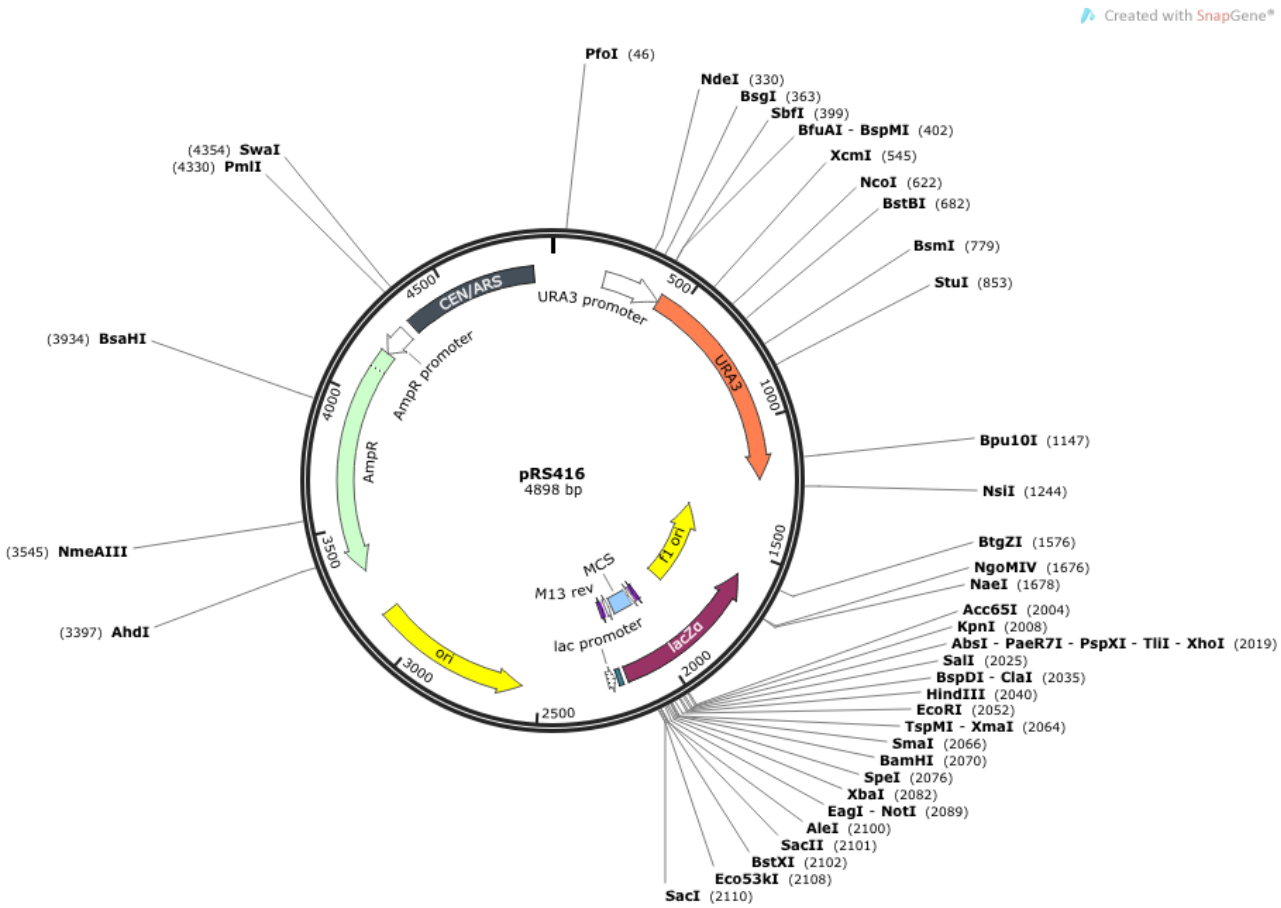

Figure 18. PRS416. Yeast centromere vector with URA3 marker and MCS derived from pBLUESCRIPT II (picture from www.snapgene.com).

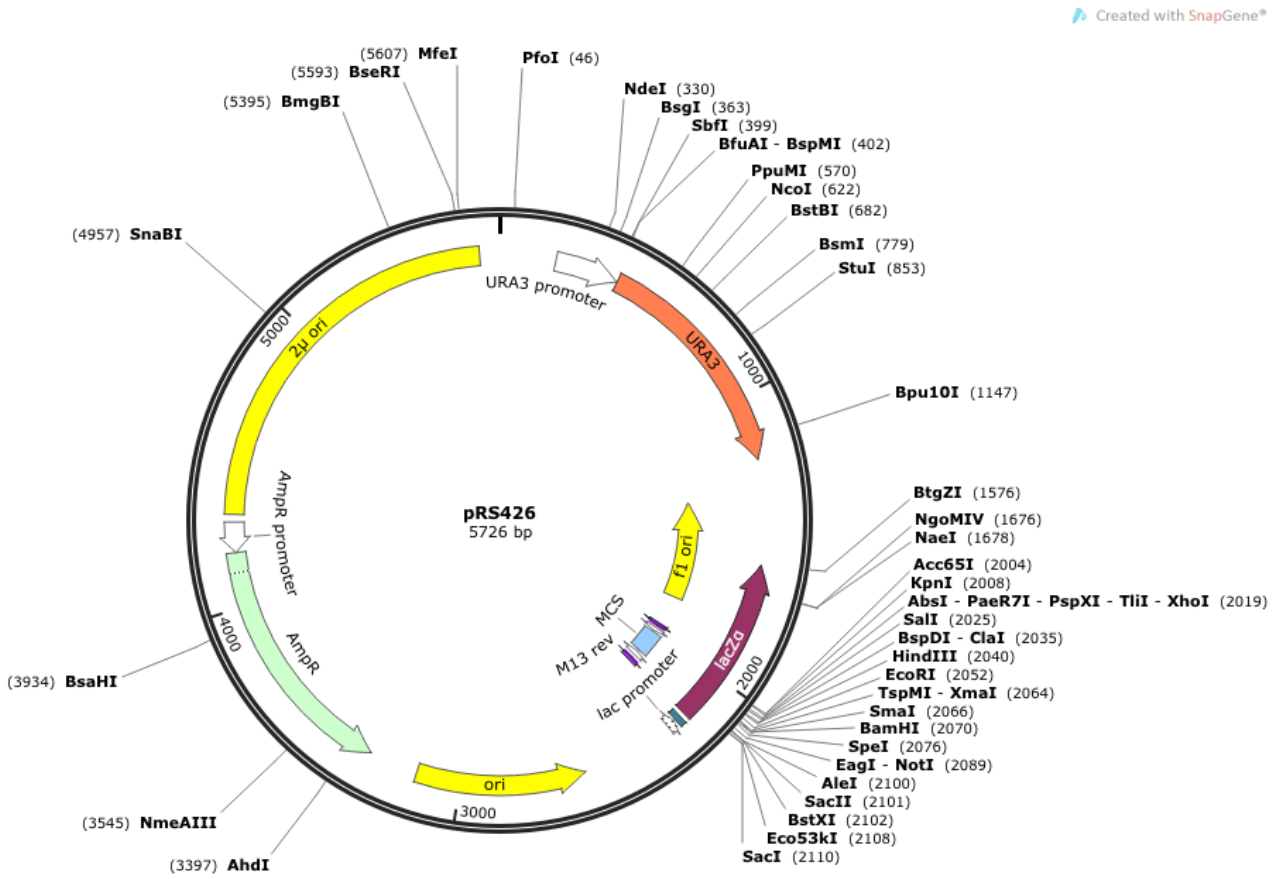

Figure 19. PRS426. Yeast episomal vector with URA3 marker and MCS derived from pBLUESCRIPT II (picture from www.snapgene.com).

From the yeast strains which showed complemented phenotype, recombinant plasmids were extracted by "Smash and Grab" DNA extraction protocol (Hoffmann *et al.*, 1987) and purified from electrophoresis gel by GE Healthcare Illustra GFX PCR DNA and Gel Band Purification kit (GE Healthcare, Buckinghamshire, UK). Five hundred ng of each purified plasmid was sequenced by BMR Genomics srl (Padova, IT). Results obtained were analyzed using BLAST algorithm and ClustalW (*www.ebi.ac.uk/Tools/msa/clustalw2*).

Environmental Scanning Electron Microscopy (ESEM) analysis

To shed light on the physical interactions and behavior of yeast cells and CdS QDs ESEM/EDX analyses were performed by environmental scanning electron microscope FEI Quanta 250FEG (FEI, Hillsboro, OR, USA). Yeast strains samples were prepared following Shen *et al.*, 2011.

Statistical analysis

Biorad Quantity One 4.2.0 software (Biorad, Hercules, CA, USA) was used to acquire and analyze each plate, both for the MIC estimation and the screening of the mutant collection. Statistics software SPSS 17.0 (http://www-01.ibm.com/software/it/analytics/spss/) was used for most of the statistics analyses. The positive results were scored when colony size in treated conditions were decreased (no growth or slow growth phenotype, in case of sensitivity) or increased (overgrowth phenotype, in case of resistance). All the results were normalized on wild type strain internal control (unaffected) and through the colony size of the corresponding strain growth on the control plate (untreated). Background correction was performed on the score of the empty well control for each plate. A two-sample t-test was used to evaluate the variations of the growth in each treatment ($P < 0.01$). Overgrowth or slow growth data corresponding to each mutant were analyzed using the Gene Ontology database (www.geneonthology.org/), DAVID Bioinformatic Database ver. 6.7 (http://david.abcc.ncifcrf.gov/; Huang *et al.*, 2008) and FunSpec software (http://funspec.med.utoronto.ca/; Robinson *et al.*, 2002). Network analyses was performed by GeneMANIA data service (www.genemania.org/; Mostafavi *et al.*, 2008).

Results & Discussion

Determination of the Minimal Inhibitory Concentration (MIC)

MIC determination was performer on YPD, YPG and SC media.

Concerning YPD, concentrations tested after 24h of incubation did not shown differences with the control untreated in cell growth before a concentration of 250 mg L^{-1} of CdS QDs. Conversely, cells grown under condition of treatment between 500 mg L^{-1} and 750 mg L^{-1} showed, compared with the control untreated, a significant reduction of the growth. Only the concentration of 1000 mg L^{-1} led to the complete inhibition of the cell growth. Concentrations tested after 72h of growth, did not shown differences with the same treatments tested after 24 h of incubation, except in case of treatment with 250 mg L^{-1}, in which the growth observed was less than the untreated control (Fig. 21). This result suggested that the cellular intake of QDs could be physically hindered by the yeast cell wall (made of 1,3 β-glucan and other tight molecules).

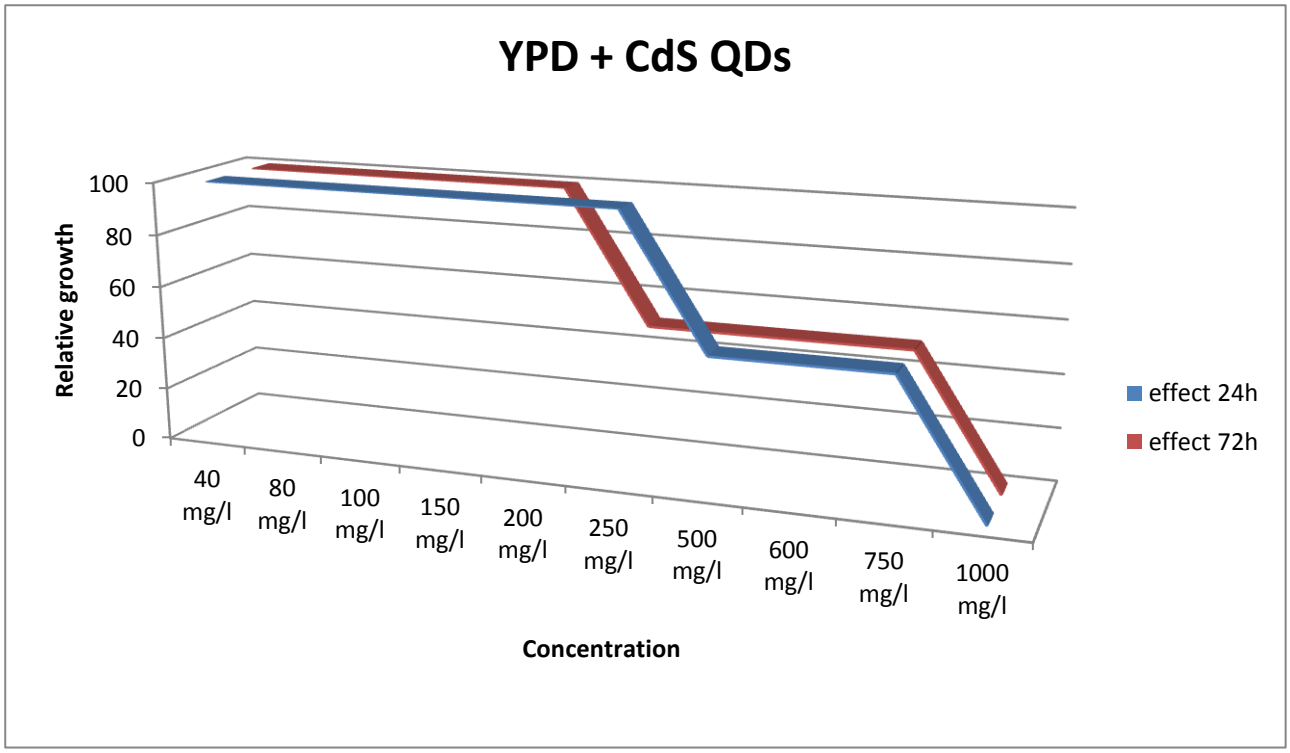

Figure 21. Plot representing growth of yeast cells on YPD medium supplemented with increasing concentration of CdS QDs, starting from 40 mg L^{-1} to 1000 mg L^{-1}, after 24h (blue) and 72h (red) of incubation. Results reported were calculated on the differences between the control untreated and the yeast grown in treated conditions.

On YPG growth medium the minimum inhibitory concentration resulted lower than on YPD growth conditions. Cells grown on CdS QDs in a range between 40 mg L^{-1} to 200 mg L^{-1} did not shown any difference with the untreated control. Increasing the concentration over 200 mg L^{-1} yeast cell growth started to decrease rapidly, in particular after 72h (Fig. 22). The significant difference between MIC estimated in YPD and in YPG medium, treated with increasing concentrations of CdS QDs, may be due to carbon source exchange, from fermentable dextrose to non-fermentable glycerol, with effect in terms of adaptive lag to the non-fermentable growth conditions. It follows that the local concentration of CdS QDs at which the yeast cells were exposed result to be higher. There are no significant differences in treated and untreated conditions after 24h growth.

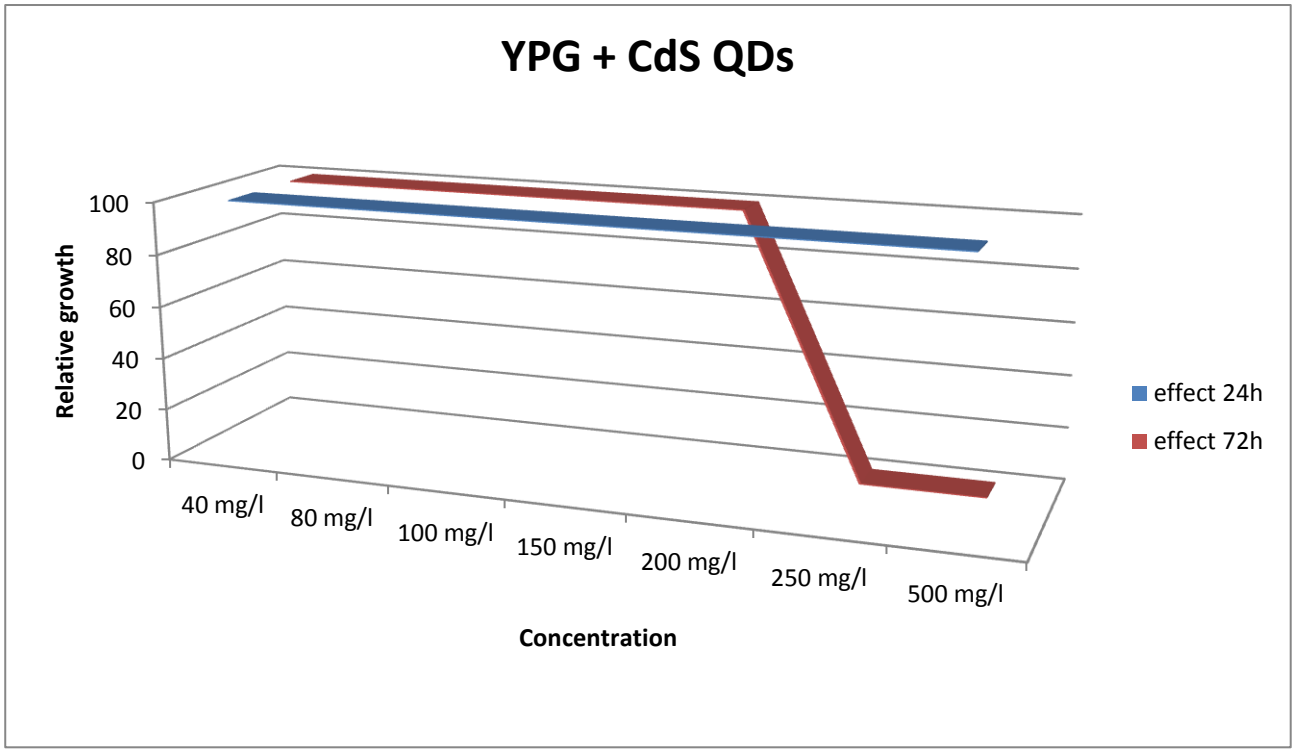

Figure 22. Plot representing growth of yeast cells on YPG medium supplemented with increasing concentration of CdS QDs, starting from 40 mg L^{-1} to 500 mg L^{-1}, after 24h (blue) and 72h (red) of incubation. Results reported were calculated on the differences between the control untreated and the yeast grown in treated conditions.

On SC medium, supplemented with histidine, leucine, lysine and uracil, the effect of "local concentration" increase was much evident (Fig. 23), and the minimal inhibitory concentration decrease in all the treatments (estimated at 250 mg L^{-1}).

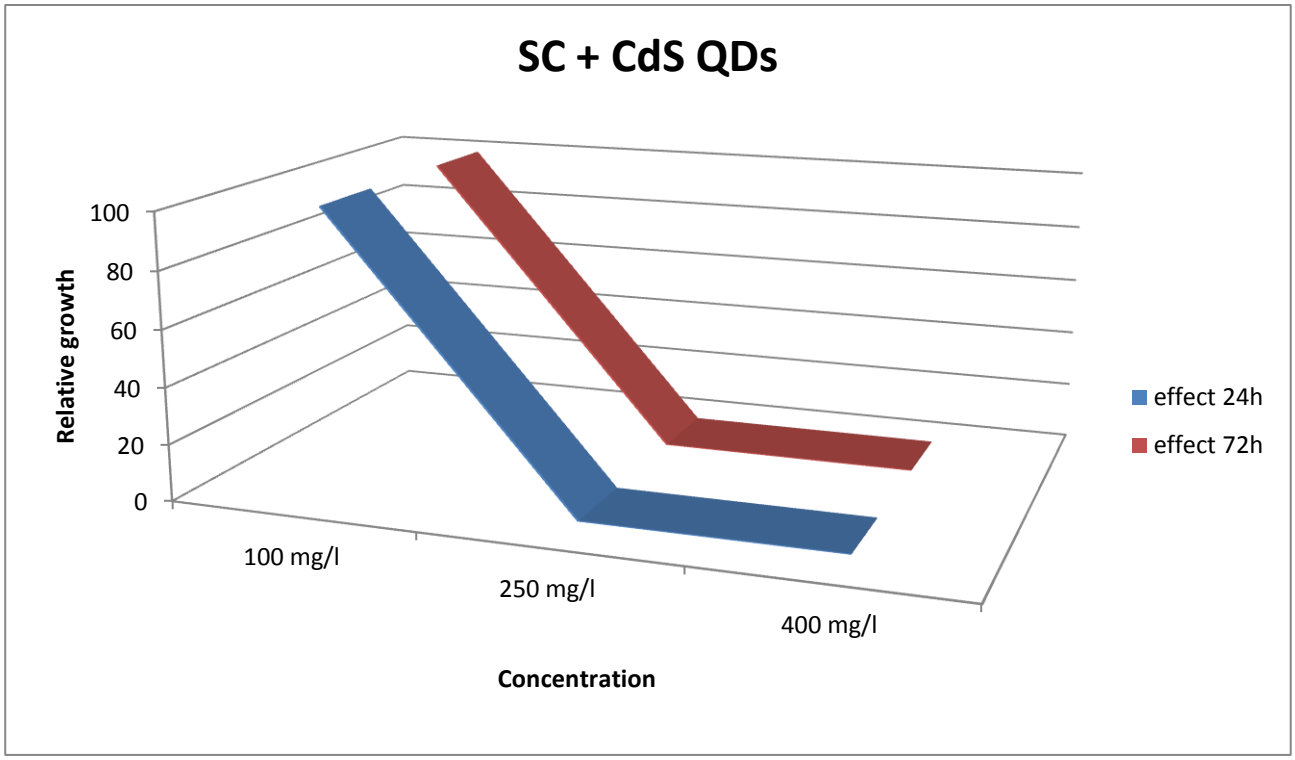

Figure 23. Plot representing growth of yeast cells on Synthetic Complete medium supplemented with His, Lys, Leu, uracil and increasing concentration of CdS QDs, starting from 100 mg L^{-1} to 400 mg L^{-1}, after 24h (blue) and 72h (red) of incubation. Results reported were calculated on the differences between the control untreated and the yeast grown in treated conditions.

Assuming that the low intake of CdS QDs from the yeast cell was caused by a low permeability of the cell wall we decided to grew yeast cells on YPD supplemented with different concentrations of nystatin to increase the cell wall permeability and, consequently, the cellular intake of the QDs to study the internal molecular mechanisms in which the QDs could be involved. Starting with 0.1 mg L^{-1} to 0.4 mg L^{-1} of nystatin, effects on the cell growth, in condition of treatment with CdS QDs, were not significantly different from the growth on YPD supplemented with QDs only. Increasing the concentration of nystatin between 1 mg L^{-1} and 3.3 mg L^{-1} (representing the minimal inhibitory concentration of nystatin in *S. cerevisiae*) the toxic effect of the drug became preponderant compared to the effect of CdS QDs (data not shown). A concentration of 0.55 mg L^{-1}, equal to 1/5 of nystatin MIC in yeast, was evaluate as the more useful to assay the effect of CdS QDs on yeast growth. Results reported in figure 24 shown the trend of growth observed increasing the concentration of CdS QDs from 50 mg L^{-1} to 500 mg L^{-1}. A minimal inhibitory concentration (MIC) of CdS QDs (200 mg L^{-1}) was estimated. This concentration was used for the screening of yeast

Knock Out mutant collection. This concentration allowed also to drastically reduce the quantity of CdS QDs used in all the following steps.

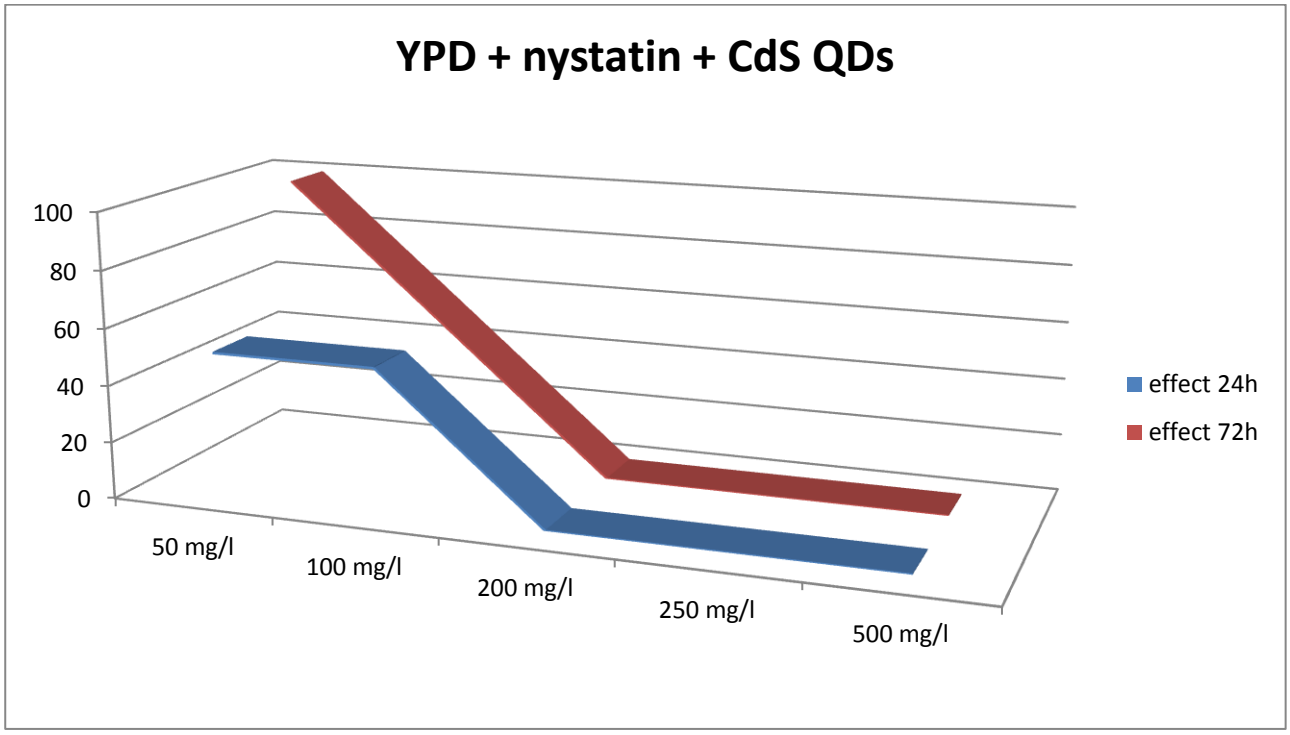

Figure 24. Plot representing growth of yeast cells on YPD medium supplemented with 0.55 mg L^{-1} and increasing concentration of CdS QDs, starting from 50 mg L^{-1} to 500 mg L^{-1}, after 24h (blue) and 72h (red) of incubation. Results reported were calculated on the differences between the control untreated and the yeast grown in treated conditions.

Screening of the knock out mutant collection

Through the acquisition of values related to the levels of growth of the yeast Knock Out mutants collection and the statistical treatment of the data 220 yeast strains that showed a growth statistically different from the controls untreated were obtained: 109 mutants in which sensitivity was observed and 113 mutants that showed a resistant phenotype.

Gene Ontology database provided, for each ORF related to the corresponding Knock Out mutant isolated, information concerning the gene encoded and the function in which the gene product was involved. Analysis provided by Funspec database (Appendix Tab.1, 2, 3, 4, 5, 6) concerning the genes corresponding to the mutant strains were subdivided in different clusters based on molecular functions and biological and cellular processes in which the genes were involved ($P > 0.05$).

Contrary to our expectations none of the genes exceeded the fixed threshold were related to ergosterol synthesis pathway. This result is probably due to the addition of nystatin that, through in sublethal concentrations for the wild-type, had on the mutants a preponderant effect compared to the CdS QDs.

Data obtained from the screening were represented through heatmap pictures (Fig 25 a,b). In each heatmap were reported the growth levels of control untreated (control), treatment with nystatin (nist) and treatment with nystatin and CdS QDs (nist+QDs). The fourth lane "delta" (Δ) represents the difference of signal obtained from the subtraction of the nystatin background signal from the overall signal derived from treatment with CdS QDs and nystatin. The results obtained were normalized using the signal of the untreated control (in black). Growth signals lower than the control were reported in green whereas the growth signal higher than the control were reported in red.

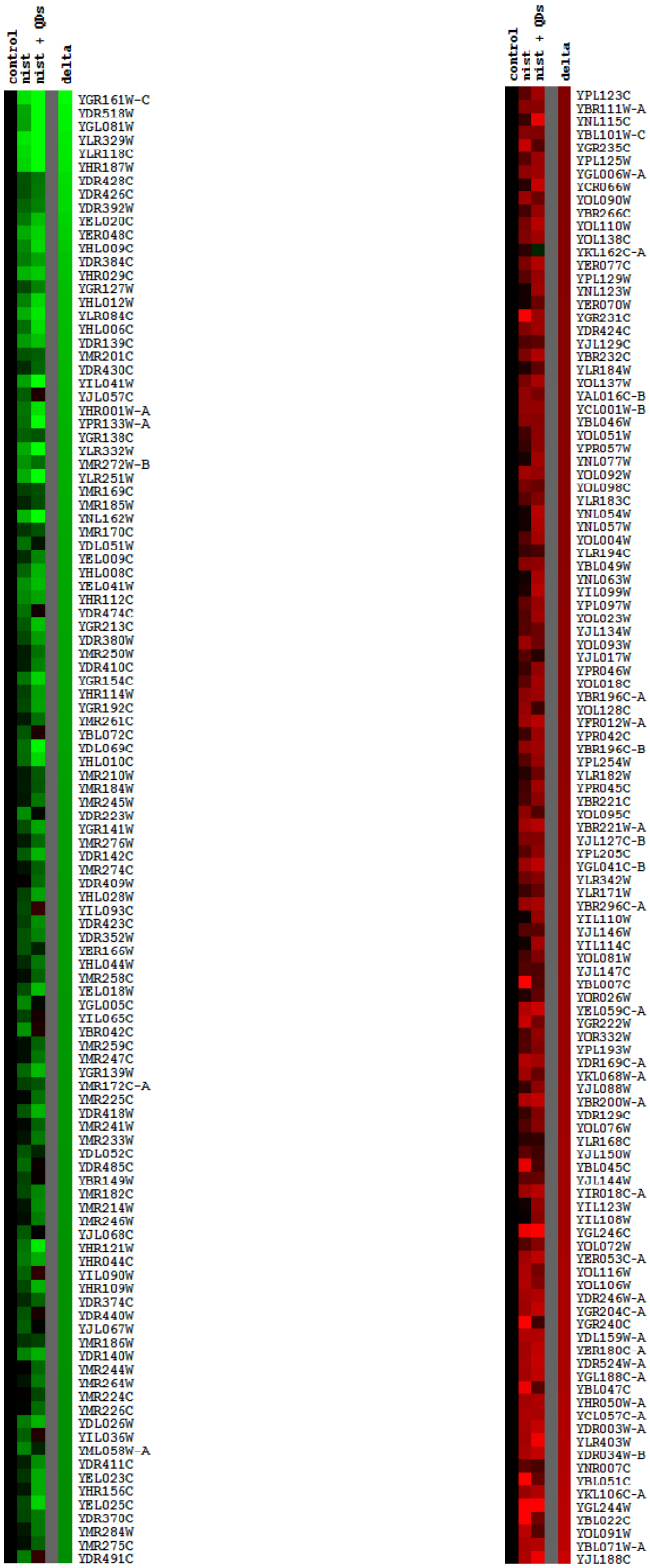

Figure 25: Heatmaps representing the growth signal of the sensitive (a) and resistant (b) deleted yeast strains.

Through the SGD Gene Ontology Slim Mapper tool, it was possible to classify the ORFs whose deletion appears to be responsible for sensitive (Fig. 26) or resistant (Fig.27) phenotypes, according to the cellular process in which were involved the corresponding gene products.

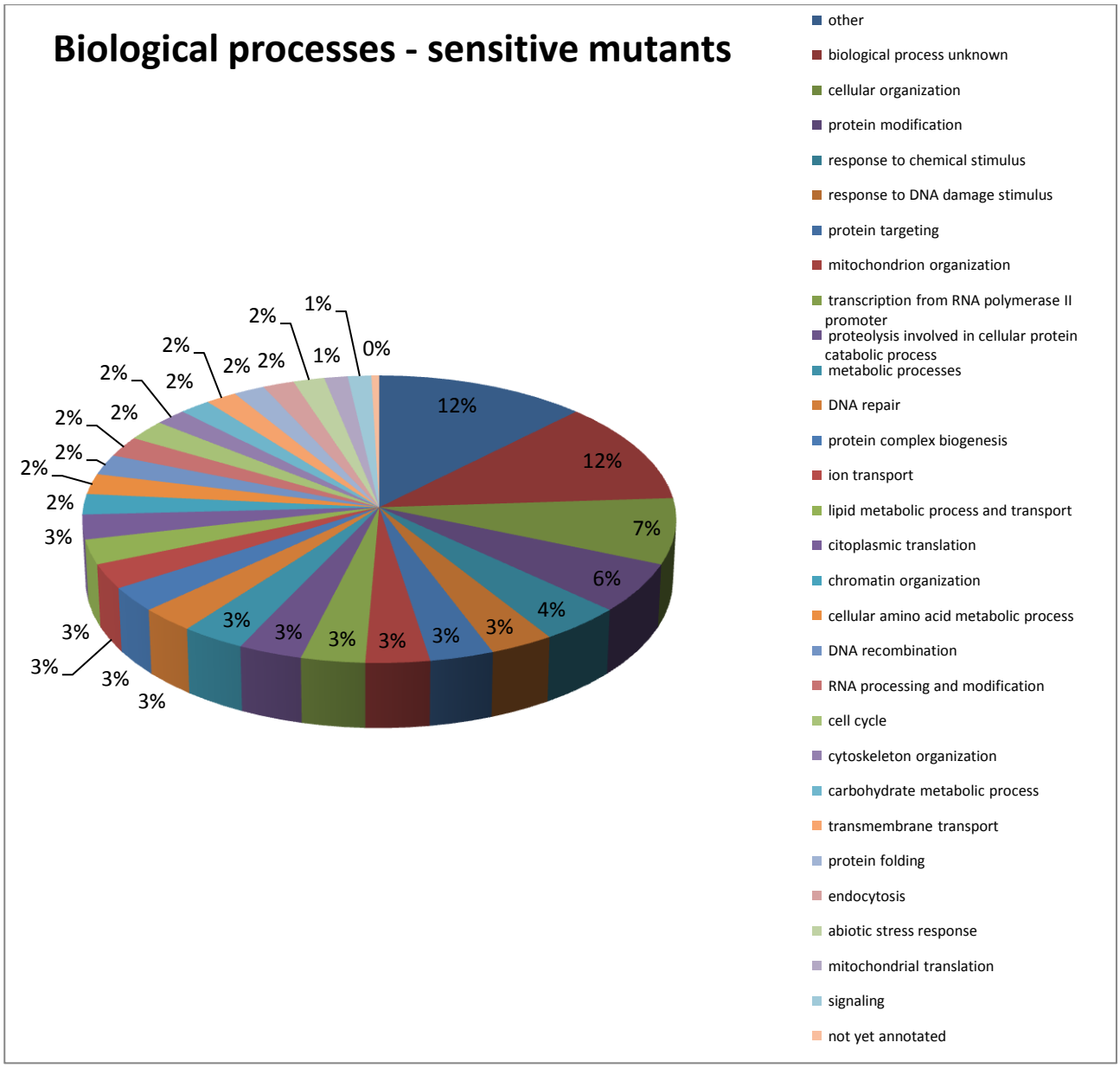

Figure 26. Pie chart of biological processes in which genes that conferring sensitive phenotype are involved. Results obtained from GO Slim Mapper tool.

Results obtained evidencing some of the genes involved in the response to stress: 4% of the genes whose deletion determined a sensitive phenotype were involved in mechanisms of abiotic stress response. Further 3% of the genes were involved in the response to DNA damage, a further 3 % in the mechanisms of DNA repair, and 2% in recombination events. Moreover 3 % of the genes are involved in ion transport, which could contribute to the detoxification by export and confinement within vesicles or organelles: one of the main detoxification mechanisms used by yeast is the internalization of xenobiotics within the vacuole, in order to decrease the cytosolic concentration below lethal values. In most cases, genes belong to generic response mechanisms, whereas some of the identified genes were already known as involved in Cd^{2+} ion specific response (*Ypr133w-a*, *Ydr423c*, *Ydr140w*, *Ymr224c*, *Yil065c*, *Yil090c*, *Ymr275c*, *Ylr332w*) (Ruotolo *et al.*, 2008; Hillenmeyer *et al.*, 2008).

A list of sensitive genes includes some functions particularly interesting for our studies: *cad1*, also known as *yap2*, encodes for a leucine zipper transcriptional activator involved in response to stress, iron metabolism and the pleiotropic drug resistance. *yap2* has a paralog called *yap1*. Although a sequence homology of 85%, the transcriptional activators encoded by the two genes are physiologically distinct. *yap1* is involved in the response to various stress signals, such as hydrogen peroxide, thiol reagents and cadmium, whereas *cad1* result not affected by these signals. However, it was observed how Cd^{2+} stimulates the transcriptional activation of *cad1* promoting its accumulation within the nucleus. Furthermore, the insertion of *cad1* gene inside a multicopy vector, allows the yeast cell to acquire cadmium resistance (Wu *et al.*, 1993). Further studies have shown that the transcriptional activation of *cad1* and *yap1* is triggered by cadmium: in normal conditions (absence of stress), the two transcriptional activators are actively transported through the nuclear membrane by *crm1* receptor. Cadmium activates the two transcriptional activators by binding of the *crm1* c-terminal cystein rich domain, that masked the nuclear export signal (Azevedo *et al.*, 2007).
gcn4, encodes for another leucine zipper transcriptional activator. The activator *gcn4* is regulated by a control system which increases its concentration within the cell in condition of lack of amino acids. *gcn4* promotes the transcription of more than thirty genes involved in the aminoacids biosynthesis (Hinnenbusch *et al.*, 2002).
yap3, as *cad1* and *gcn4*, encodes for a bZIP transcriptional activator. Unlike to the other two activators, *yap3* is not involved either in response to cadmium, or in response to hydrogen peroxide. The deletion of *yap3* gene, however, shows a decrease in the stress response (North *et al.*, 2012) .
mrpl44, encodes for a subunit of mitochondrial ribosomes; its concentration increases in response to stress in DNA replication (Graack *et al.*, 1998) .

bul1, encodes for a protein involved in ubiquitination. It is a not essential component of E3-ubiquitin ligase complex, involved in the protein vacuolar sorting. *bul1* has a functional homologue, *bul2*, with which is involved in *Gap1p* permease outbound and the activation of the *gln3* transcription factor, under nitrogen deficiency conditions. Furthermore, the deletion of *bul1* leads to a decrease in the level of resistance to cadmium chloride (Serero *et al.*, 2008). *dsk2*, encodes for another gene product involved in the ubiquitination process. It is overexpressed in response to stress in DNA replication (Dziedzic *et al.*, 2011); its deletion leads to a reduced resistance to heavy metals stress. There are also other gene products involved in ubiquitination process: *rub1*, *qcr10*, *rkr1*, *siz1* and *cue1*. Ubiquitin/proteosome system is a part of the mechanisms responsible for maintaining protein homeostasis, and is the main pathway of protein degradation in cytoplasm and nucleus of eukaryotic cells. Ubiquitin overexpression lead up to increased resistance to several biotic and abiotic stresses (Chen *et al.*, 1995), promoting the degradation of damaged proteins and protein aggregates.

mid2, which encodes for a protein localized on cell wall membrane that acts as a sensor for stress-induced remodeling of the cell wall during the growth stage. This protein is required, together with *wsc1p*, for the activation of the signaling pathway of the integrity of the wall. *mid2* deleted strain show a sensitive phenotype to treatment with cadmium chloride (Gardarin *et al.*, 2010).

Concerning metabolic functions of mitochondrial genes several were found: *tom5*, which encodes a component of the TOM (Transporter Outer Membrane) complex, involved in the import of all the proteins directed to the mitochondrion; *yhm2*, encoding an active citrate/oxoglutarate antiport carrier in mitochondria which exploit NADPH; *fis1*, which encodes for a protein involved in the fission of the mitochondrial membrane, required for localization of *dnm1p* and *mdv1p* (proteins required for the remodeling of membranes) during mitochondrial division (Karren *et al.*, 2005). Moving in this direction it is possible to conclude that mitochondria could be a possible target of CdS QDs, or in general QDs, thus influencing the redox balance of the cell (Li *et al.*, 2011).

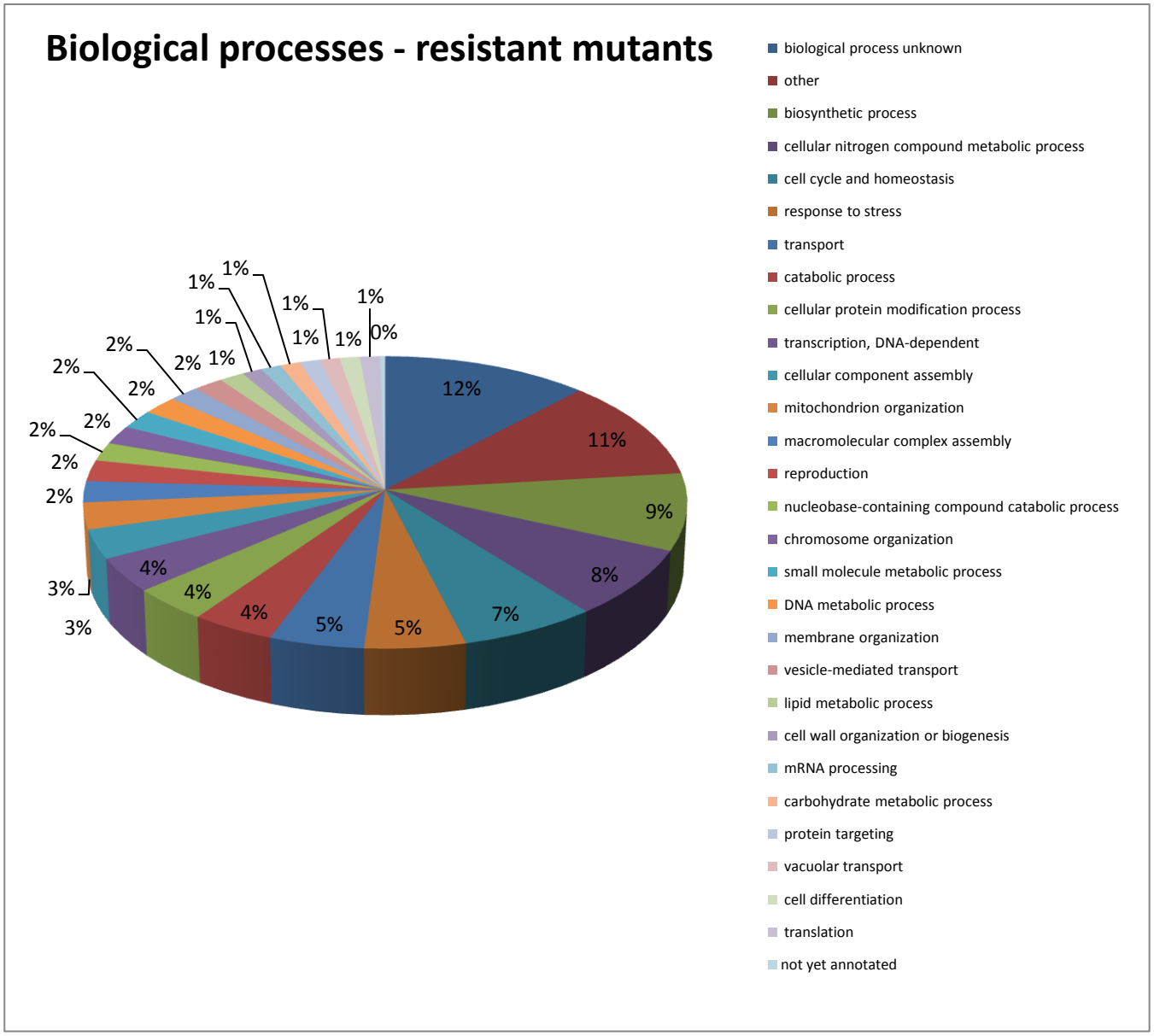

Figure 27. Pie chart of biological processes in which genes that conferring resistant phenotype are involved. Results obtained from GO Slim Mapper tool.

Among the mutants in which deleted genes produce a resistant phenotypes, genes were identified involved in general stress response and ion transports (5%), and genes involved in DNA metabolism (2%). List of resistant genes includes some functions particularly interesting for our studies: *vac7*, which encodes for a membrane protein involved in vacuolar morphology and vacuolar inheritance. The mutants deleted in *vac7* have a vacuoles size greatly increased, able to grow at high temperatures. *vac7* determine the activity of phosphatidylinositol 3-phosphate 5-kinase *Fab1* in conditions of hyperosmotic shock (Gary *et al.*, 2002).

vtc2, encodes a for subunit of the vacuolar transport chaperone complex, is involved in membrane trafficking, accumulation of polyphosphates in vacuoles and, in the non-autophagic vacuolar fusion (Uttenweiler *et al.*, 2007);

vma4, encodes for the subunit E of V1 domain of H^+-vacuolar ATPase. It is an ATP-dependent proton pump involved in the acidification of vacuolar compartments, essential for several processes including endocytosis and targeting of lysosomal enzymes synthesized. The cell concentration of this protein increases in stress response of DNA replication (Tkach *et al.*, 2012).

It is also present *yol092w* gene, which is noted as encoding a putative vacuolar transporter for cationic aminoacids.

Some of the candidate genes coincide or are closely related to those involved in mechanisms of resistance to gold nanoparticles (Smith *et al.*, 2013): for example, *trk1* is a component of the K^+ transport system Trk1p-Trk2p. Its deletion increased the phenotype of resistance to hydrogen peroxide and heavy metals. In particular it has been postulated that gold nanoparticles with a size of 0.8 nm, interact with the complex Trk1p-Trk2p allowing the leakage from the cell of cytoplasmic constituents, such as ATP and K^+.

sus1 and *hfi1* are components of the SAGA (Spt-Ada-Gcn5-Acetyltransferase) complex involved in histones acetylation. Gene Ontology analysis revealed that the majority of genes reported in Smith *et al.*, 2013 has mitochondrial localization, and their deletion lead consequently a cellular respiration deficiency.

Hierarchical clustering analysis of the data obtained through FunSpec database, highlighted the presence of genes (5%), involved in the organization of the mitochondrion whose deletion showed a resistant phenotype. These genes encode for: i) proteins of the inner membrane, ii) proteins involved in metabolic reactions, iii) proteins involved in transcription and translation processes.

mos1 and *mos2*, are essential for the organization of the inner membrane. *som1*, encodes a subunit of a peptidase required for proteins processing in the intermembrane space. *phb2*, encodes a subunit for a chaperone complex that stabilizes proteins and is also involved in the segregation of mitochondria. *hmi1*, encode for a ATP-dependent helicase necessary for the maintenance of the genome mitochondrial. *por2*, encodes a porin that is a component of a voltage-dependent anion channel. Among the genes involved in metabolic processes, is reported *pdb1*, which encodes for a subunit of the pyruvate dehydrogenase complex, *ups2* and *pim1*, that encode for proteins involved respectively in the metabolism of phospholipids and proteins.

In addition to Gene Ontology data, it was possible to identify pathways in which genes appear to be involved in the list of sensitive mutants, in particular metabolism of phenylalanine and the metabolism of xenobiotics. In both pathways has been found the presence of genes *ald2* and *ald3*,

encoding two different cytoplasmic aldehyde dehydrogenase, whose sequences showed a similarity of 92%. These genes are induced in the presence of different types of stress : in particular, *ald2* is induced by osmotic stress and low glucose levels , while *ald3* is induced by osmotic stress , heat stress, oxidative stress, chemical compounds and lack of glucose (Navarro-Aviño *et al.*, 1999). Furthermore, within the pathway of the metabolism of phenylalanine, the gene: *aro10* , coding for a phenylpyruvate decarboxylase, that catalyzes the conversion of phenylpyruvate in phenylacetaldehyde.

Concerning genes whose deletion confers a phenotype resistant to treatment, none was recognized as involved in any metabolic pathways.

The two lists of candidate genes were analyzed separately through GeneMANIA software, which uses a wide range of functional correlation data to highlight the presence of interactions between genes of interest and identifies other genes related to them. These interactions can be displayed in the form of a network of interactions, built using a heuristic algorithm derived from the Pearson correlation. Regarding the genes whose deletion determines a sensitive phenotype, were identified two main networks. The first, shown in figure 28, contains the genes involved in the mechanism of response to stress, among which we can easily identify *cad1*, involved in resistance to the ion cadmium , and other genes that have been discussed previously (*gcn4, dsk2, rub1, cue1*). One of the main interactors within our query is *hsc82* which appears to be positioned in the center of the network of interaction: it belong to the family of cytoplasmic chaperone *hsp90* , involved in the mechanisms of heat shock response and DNA stress. *hsc82p* has a paralog, *hsp82*, which functions almost identically and originated following the duplication of the entire genome. *hsc82* is constitutively expressed at levels ten times higher than the paralog, also indicated in the interaction network.

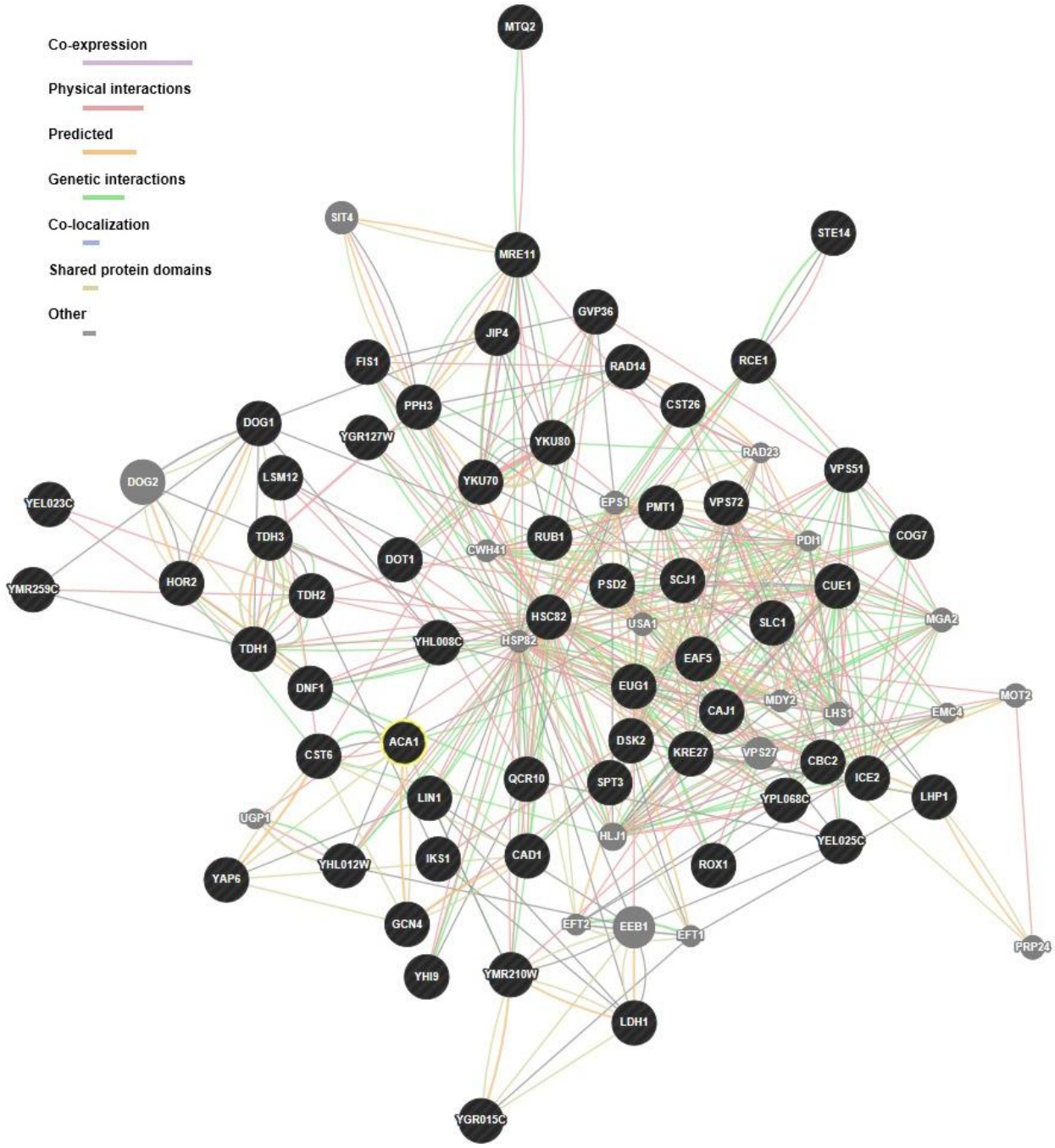

Figure 28: Network of sensitive genes which involved stress response.

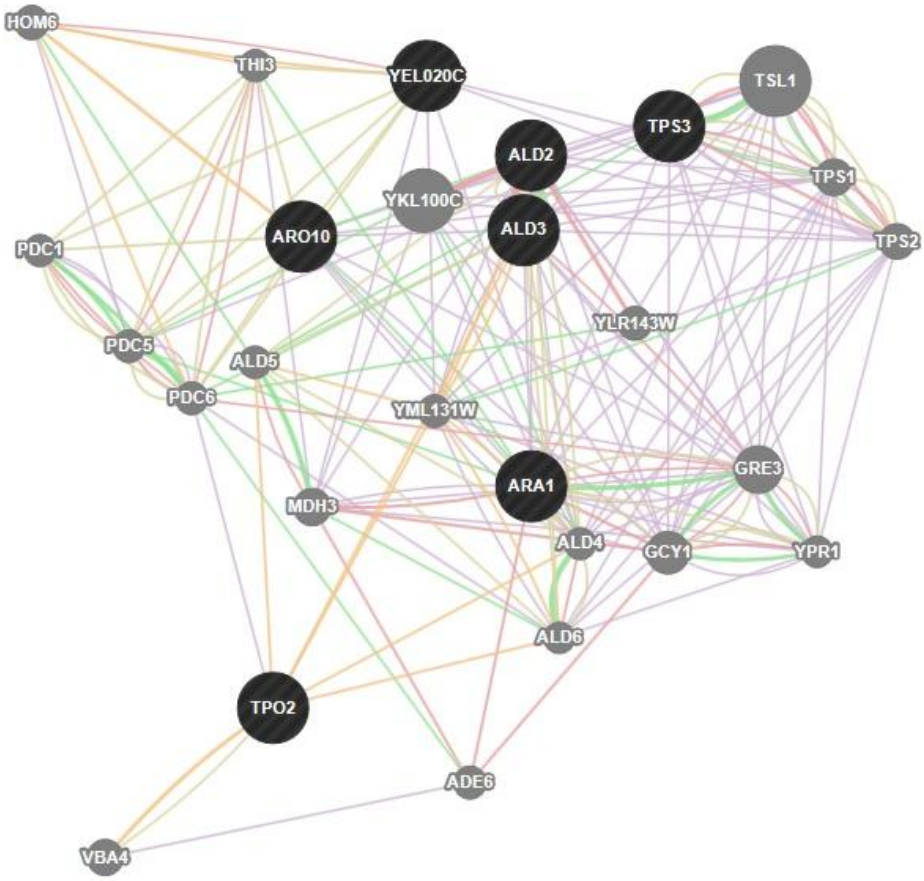

Figure 29: Network of sensitive genes which involved biosynthetic processes.

The second network contains biosynthetic genes, including *ald2*, *ald3* and *aro10* previously identified also through the analysis of gene ontology as components of the phenylalanine pathway (Fig.29).

Regarding the genes whose deletion produced a resistant phenotype, has been identified a single network (Fig. 30). In the all the network generated, it is identified the presence of genes not yet characterized. The data collected, once confirmed, could therefore help to provide information useful in defining the role of these genes in the yeast genome.

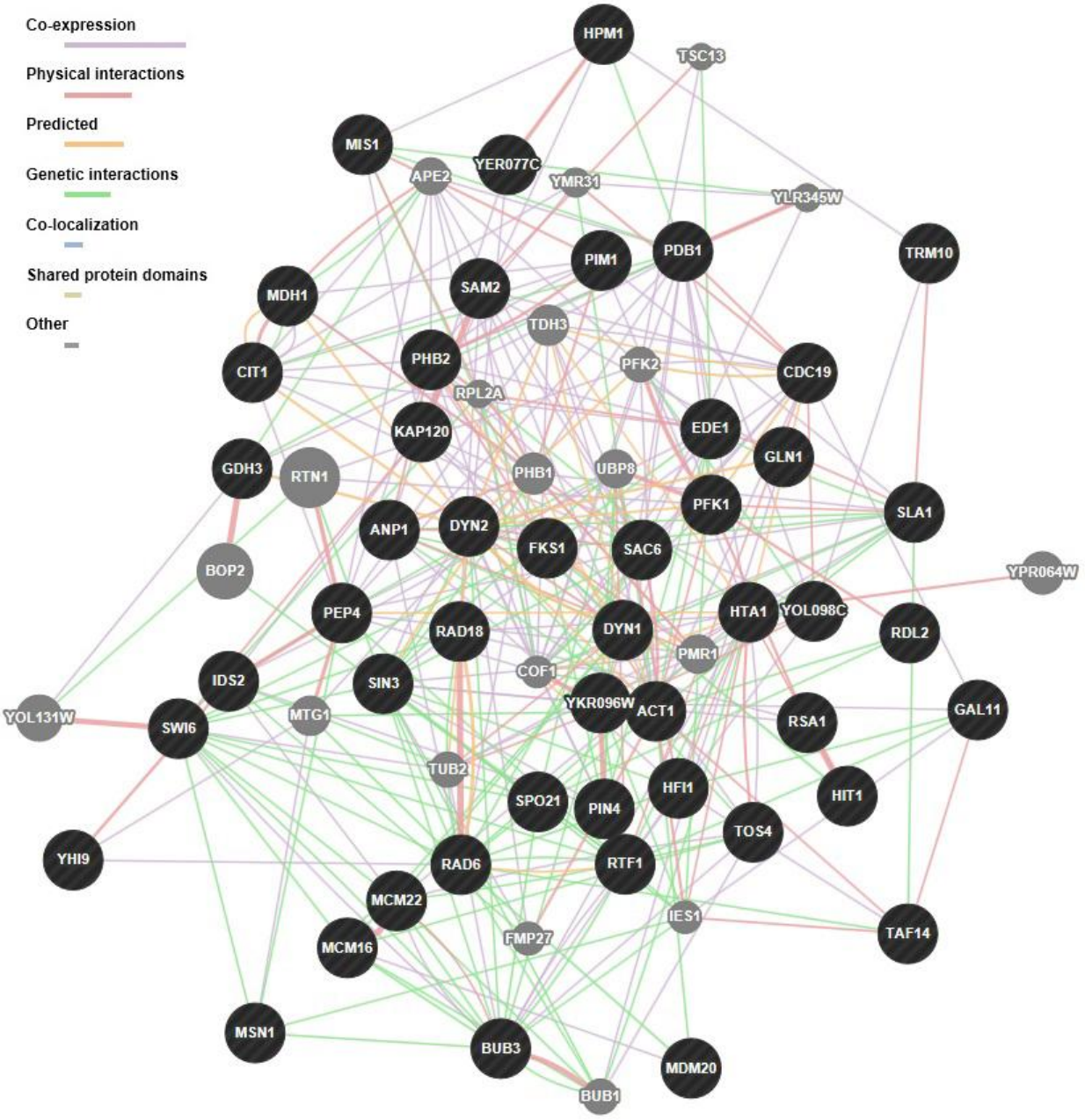

Figure 30: Network of resistant genes which involved stress response.

The cadmium salt comparison

The comparison of the results obtained with data already available becomes necessary. In fact, a direct comparison with the genes of *S. cerevisiae* involved in Cd response showed a narrow overlap with our results. Genes *ypr133w-a*, *ydr423c*, *ydr140w*, *ymr224c*, *yil065c*, *yil090c* and *ymr275c*, classified as low-sensitive and medium-sensitive to Cd ion treatment (Ruotolo *et al.*, 2008; Hillenmeyer *et al.*, 2008), are the only genes in common with our results. Also between the genes mentioned as susceptible to treatment with $CdCl_2$, appeared to be present in our list of sensitive mutants to CdS QDs, specifically *mid2* and *cad1* genes. The weak overlap between the two responses could evidence how the mechanisms of resistance to Cd ions and to CdS QDs are different and the effect of treatment with CdS QDs could not merely be ascribed to the effect of Cd. This result supports our previous hypothesis concerning the mechanisms involved in CdS QDs response in *Arabidopsis thaliana*.

Spot assay

From the list of genes whose deletion causes a sensitive phenotype to CdS QDs treatment, were selected some mutants, which were subjected to confirmation of phenotype changed by spot assay. Wild type strain BY4742 was used as positive control. This test provides a general indication of the level of sensitivity of the various mutants to treatments, based on the last dilution in which growth was observed .

After 48 hours of growth it was possible to identify sensitive phenotypes in the mutants screened and this result confirmed the screening mentioned above.

Particularly, focusing the attention on *Δcue1* and *Δcst6* mutants, they showed an higher level of sensitivity than the other mutant analyzed. Growth, for these two mutants, appears to be already inhibited at concentrations of 10^5 cells/ml (Fig. 31). For the mutants *Δrkr1*, *Δvps62*, *Δzap3*, *Δshu1* and *Δmid2*, growth is inhibited at concentrations of 10^4 cells/ml. For the mutants *Δrgm1*, *Δhsc82*, *Δdsk2*, *Δyku70*, *Δspt3*, *Δbul1* and *Δsiz1* was observed a very limited growth in concentrations of 10^4 cells/ml, at levels lower than the positive control present in each plate.

Mutants tested, along with the others present in the gene list whose mutation causes a sensitive phenotype, were validated by transformation with centromeric and multicopy plasmids containing

the deleted genes. This approach allows to obtain, through their phenotypes, information about genes with a key role in the response to CdS QDs.

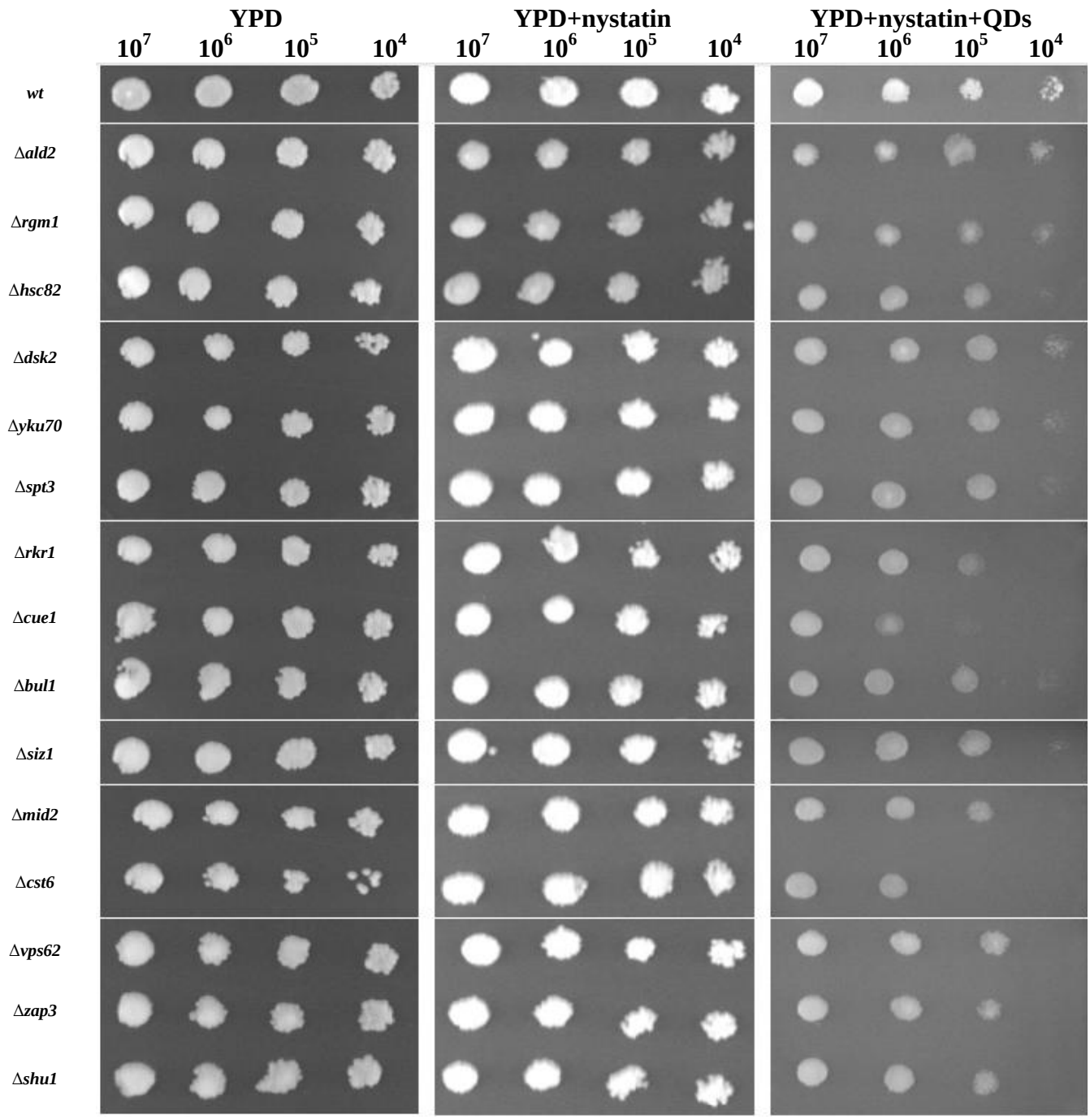

Figure 31: Spot assay of the mutants in genes whose deletions showed a sensitive phenotype to CdS QDs. In the first lane (YPD) mutants and wild type strains were grown without treatment; in the second lane (YPD+nystatin) mutants and wild type strains were grown on nystatin (0,55 mg L^{-1}); in the third lane mutants and wild type strains were grown YPD supplemented with nystatin (0,55 mg L^{-1}) and CdS QDs (200 mg L^{-1}).

Rescue of the phenotype by complementation

Through the complementation of the phenotype, using two genomic library inserted in the centromeric and multicopy vectors, some transformed colonies were observed and isolated. These colonies showed on the SC-URA supplemented medium a growth not statistically different from the control (not supplemented). To facilitate the isolation of possible revertant strains the sensitive mutants were subdivided in 12 pools. Description of the 12 pools of mutants is reported in Appendix Table 7. In the first round of screening revertant phenotypes were observed in pool 9. A second round of transformation and screening on nystatin and CdS QDs was performed only on the single strain isolated from the pool. Only for the mutant Δ*hsc82*, the revertant phenotype was evidenced. To confirm the revertant phenotype a spot assay was performed (Fig.32).

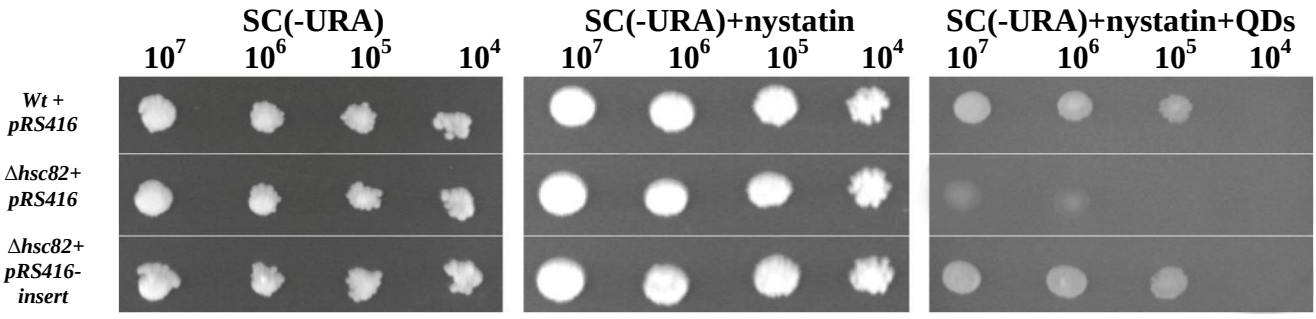

Figure 32: Spot assay of Δ*hsc82* mutant. In the first lane (SC-URA) transformed wild type and *Δhsc82* strains were grown without treatment; in the second lane (SC-URA+nystatin) transformed strains were grown on nystatin (0,55 mg L^{-1}); in the third lane transformed strains were grown on SC(-URA) supplemented with nystatin (0,55 mg L^{-1}) and CdS QDs (200 mg L^{-1}).

The analysis of the wild type+pRS416 (empty plasmid) was used as positive control for the growth of the wild type on SC-URA medium. Since the wild type strain does not carry the *ura3* gene and the non-transformed strain would not be able to grow on SC medium without uracil. Transformed mutants Δ*hsc82* with the empty plasmid was used as a negative control for growth. On medium containing nystatin it was observed, as expected, the growth of yeast strains in all dilutions because the sub-lethal concentration of nystatin used acts only to increase the permeability of the cell wall. On medium containing nystatin and CdS QDs growth of the complemented mutant was not significantly different from the growth of the wild-type. This result constitutes the proof that the fragment inserted into the centromeric vector rescued the mutation.

The sequence contained in plasmids sequenced was recognized by BLAST (E-value = 0.0, Identity = 99%) as the upstream region of the gene encoding the heat shock protein of *Saccharomyces cerevisiae hsc82*. This confirmed the complementation of the deleted mutant Δ*hsc82*.

This result highlighted the importance of this gene in the response to stress inducted by CdS QDs. The key role of *hsc82* gene at this point becomes fundamental in the response to CdS QDs and as previously seen in the network of sensitive genes (Fig. 28) the heat shock protein is recognized as one of the hub of the interaction network. It is not possible to identify this gene as the main character of the resistance but the phenotype of *hsc82* is undoubtedly epistatic in respect of the other genes. This phenomenon becomes evident when the condition of growth, due to the change of growth medium necessary for the selection of transformed yeast strains, are more restrictive and the time to develop the growing colony is higher. Certainly *hsc82* is not an arrival point, but rather a starting point on which to build future experiments.

Environmental Scanning Electron Microscopy (ESEM) analysis

For the first time we were able to analyzed the interactions between nano-aggregates of CdS QDs and yeast cells (Fig. 33). This could suggest finally how the cells physically interact with the nanomaterials.

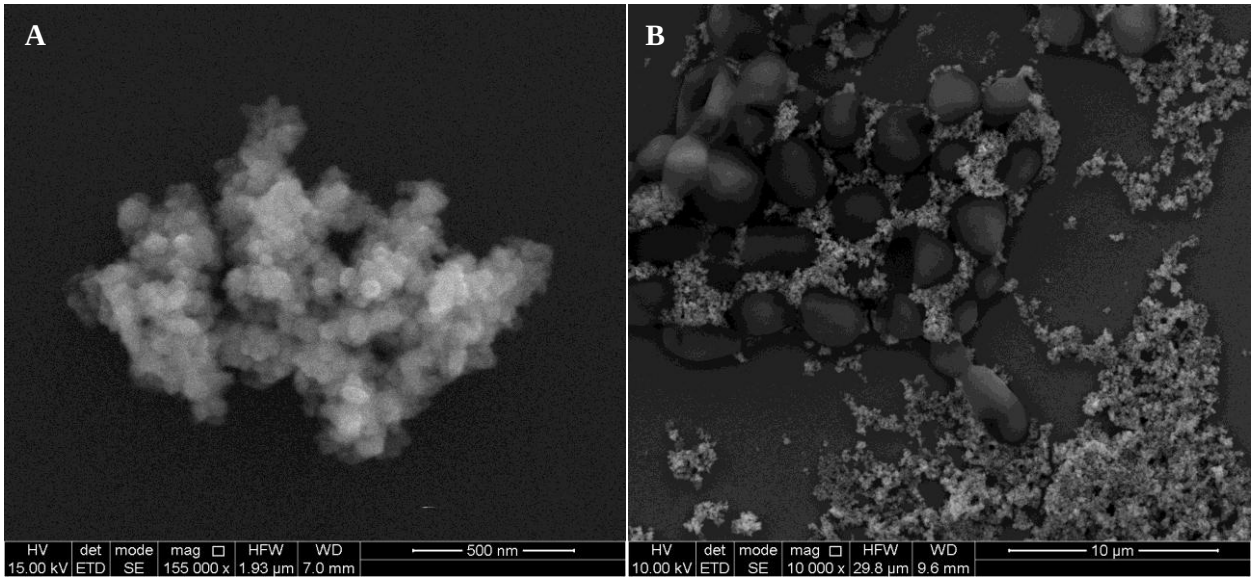

Figure 33: nanomaterials analyzed with ESEM/EDX. CdS QDs aggregates (A). Nanomaterials aggregates interactions with yeast cells (B). Scale and ESEM parameters are showed below.

The microanalysis conducted to highlight the elements (data not shown) showed the presence of only the elements cadmium (Cd) and sulfur (S) in equal proportions. The individual particles are found to be of a diameter not exceeding 20 nm. These findings certify the successful identification of the CdS QDs. Microanalysis conducted on cells has not provided yet significant results on the presence or absence of the nanoparticles within the cells since the cell wall, together with the treatment performed, do not allow to obtain the expected result.

This result do not clarify the mechanism of internalization and also which could be the physico-chemical form of CdS QDs is internalized in the cell. Further analyses will be performed to elucidate this point, both for yeast and plants.

Conclusions

Concluding, two *A. thaliana* mutants, *atnp01* e *atnp02* resistant to CdS QDs were isolated. Through the AAS analysis we found that mutants and wild type showed a same level of Cd^{2+} uptake whereas *atnp01* e *atnp02* resulted to be more tolerant than the wild type in condition of CdS QDs treatment. Physiological parameters highlighted that mutant lines are tolerant to CdS QDs, not $CdSO_4$. Genetic backcrosses clarified the stability of the mutant lines, ensured by the absence of transposition.

Microarray analyses and Real Time PCR confirmed how our mutant lines can be an instrument for the understanding of the CdS QDs tolerance/resistance mechanisms and the key genes involved. *At1g13880* (ELM2, putative MYB transcriptional activator) could offer a possible explanation of the mechanisms of stress response involved in tolerance/resistance to CdS QDs. Furthermore, the comparison with cadmium ion stress response, confirmed by Real Time PCR and physiological parameters analyzed, has shown that Cd^{2+} and CdS QDs exploit different pathways of tolerance/resistance.

Analyses performed on yeast may suggest a similar response both for plant and fungi. The combination of the results obtained in plant and in yeast could offer a possible hypothesis for the torelance/resitance mechanism in which the CdS QDs are involved. Similarly to *A. thaliana*, also in case of *S. cerevisiae*, the results found suggested how the CdS QDs and the Cd^{2+} could exploit different pathways of tolerance/resistance. It was observed a possible epistatic activity by which the up- or down-regulation of one or few genes (*At1g13880* in plant or *hsc82* in yeast) could lead to a cascade of other genes regulated during the CdS QDs response, both in yeast and plants.

Results obtained from this study could add information about the possible mechanisms exploited by CdS QDs and the potential risk attributable to the Cd-based QDs, and NMs in general. The use of model organisms, as *A. thaliana* or *S. cerevisiase*, could offer safe strategies for the risk assessment of NMs concerning environment and health. Therefore, plant-based model systems are able to provide information about plant-specific targets and could be also useful to investigate targets of more general interest in more complex organisms, such as animals, about the risks posed by the exposition and contact with NMs. Our approach, which merge the classical top-down approach (the isolation of the resistant mutants) and the bottom-up approach (transcriptomic and proteomic experiments), allows to shed light on function and functionality of our targets: from observing phenotype to knowing what lays genetically behind that phenotype.

Future Perspectives

There are many possibility and many aspects that we would study in deep. First of all, our future studies will be direct to define pathways and networks of interactions relating the CdS QDs tolerance/resistance mechanisms and understand also the conservation of CdS QDs tolerance mechanisms in other organisms, phylogenetically near and far, from human cells, many organisms along the food chain, from *Daphnia magna* to zebrafish (*Danio rerio*). Also other higher plants can become the target of this type of study.

The definition of specific target, both in yeast and plants, will open to new possibility for understanding what lays genetically behind the phenomenon of CdS QDs tolerance/resistance. Utilizing complementation on yeast by heterologous expression of *A. thaliana* genes (and vice versa), we will be able to clarify the importance of the candidates genes isolated in our studies.

Proteomic analysis on *A. thaliana* mutants are in still in progress. Total protein extracts were already separated by ProteomeLab PF2D platform. The results will be processed to highlight the differences between wild type and mutants in treated (80 mg L^{-1} of CdS QDs) and untreated conditions. Furthermore results must be implemented with the characterization of the peptides identified by MS-MS fingerprinting.

In order to find out information about localization of CdS QDs within cells and plant tissues, we will also perform analyses using environmental scanning microanalysis (ESEM/EDX).

Aknowledgements

I wish to thank Prof. Nelson Marmiroli for introducing me to this project, allowing to me to grow as well as researcher as person. Dr. Marta Marmiroli and Prof. Elena Maestri to help me during these years of work. All the colleagues of the Department of Life Sciences, in particular Dr. Maria Luisa Savo Sardaro and Dr. Davide Imperiale.

Prof. Carlo V. Bruschi and all the colleagues of the YMG group of the International Centre of Genetic Engineering and Biotechnology (ICGEB), for help and mentor me during my period of training in Trieste.

I wish to thank also Dr. Andrea Zappettini and Dr. Marco Villani of the IMEM-CNR (Parma, Italy) for providing certified CdS QDs, useful comments and suggestions on the physics of nanomaterials. The Italian Ministry of Research Grant PRIN 2008-XS9YBC_002 for financing the research activities. The EU project TRACEBACK and the COST Action FA0905.

I wish to thank my family, friends and students without whom the PhD fellowship experience would no doubt be more difficult to deal with.

References

Ausubel F. M., Brent R., Kingston R. E., Moore D. D., Seidman J. G., Smith J. A., Struhl A. 1994. *In Current Protocols in Molecular Biology.* Vol. 1, pp. Unit 16 p. 1-24. 6 vols. John Wiley & Sons, Inc., Hoboken, N.J.

Azevedo D., Nascimento L., Labarre J., Toledano M. B., Rodrigues-Pousada C. 2007. The S. cerevisiae Yap1 and Yap2 transcription factors share a common cadmium-sensing domain. *FEBS Letters* 581: 187-195.

Bancroft I., Bhatt A.M., Sjodin C., Scofield S., Jones J.D.G., Dean C. 1992. Development of an efficient two-element transposon tagging system in Arabidopsis thaliana. *Mol. Gen. Genet*. 233: 449-461.

BCC Research. 2011. Nanotechnology: A realistic market assessment, Market Report. *ReportsnReports*.

Blokhina O., Fagerstedt K. V. 2010. Oxidative metabolism, ROS and NO under oxygen deprivation. *Plant Physiology and Biochemistry*. 48: 359-373.

Chen J.L., Zhu C.Q. 2005. Functionalized cadmium sulfide quantum dots as fluorescence probe for silver ion determination. *Analytica Chimica Acta*. 546: 147-153.

Chen Y., Piper P.W. 1995. Consequences of the overexpression of ubiquitin in yeast: elevated tolerances of osmostress, ethanol and canavanine, yet reduced tolerances of cadmium, arsenite and paromomycin. *Biochim. Biophys. Acta.*1268(1): 59-64.

Clemens S. 2006. Toxic metal accumulation, responses to exposure and mechanisms of tolerance in plants. *Biochimie*. 88: 1707-1719.

Debreucq B., Berger N., Vincent E., Boisson M., Pelletier G., Caboche M., Lepiniec L. 2000. The Arabidopisis AtEPR1 extensin-like gene is specifically espresse in endosperm during seed germination. *The Plant Journal*. 23: 643-652.

Dubos C., Stracke R., Grotewold E., Weisshaar B., Martin C. Lepiniec L. 2010. MYB transcription factors in Arabidopsis. *Trends in Plant Science*. 15: 573-581.

Dziedzic S. A., Caplan A. B. 2011. Identification of autophagy genes participating in zincinduced necrotic cell death in Saccharomyces cerevisiae. *Autophagy* 7(5): 490-500.

EFSA Scientific Committee. 2011. Guidance on the risk assessment of the application of nanoscience and nanotechnologies in the food and feed chain. *EFSA Journal*. 9(5): 2140-2176.

EUCAST. 2000. Determination of minimum inhibitory concentrations (MICs) of antibacterial agents by agar dilution. *Eucast Definitive Document E.Def 3.1*. 509-515.

Eisen M. B., Spellman P. T., Brown P. O., Botstein D. 1998. Cluster analysis and display of genome-wide expression patterns. *Proc. Natl. Acad. Sci. USA.* 95: 14863-14868.

Favero P. P., de Souza-Parise M., Fernandez J. L. R., Miotto R., Ferraz A. C. 2006. Surface Properties of CdS Nanoparticles - *Brazilian Journal of Physics.* 36: 1032-1034.

Feldmann K.A. 1991. T-DNA insertion mutagenesis in Arabidopsis: mutational spectrum - *The Plant Journal.* 1: 71-82.

Fulton T. M., Chunzoongse J., Tanksley S. D. 1995. Microprep protocol for extraction of DNA from tomato and other herbaceous plants, *Plant Molecular Biology* 13: 207-209.

Gardarin A., Chédin S., Lagniel G., Aude J.C., Godat E., Catty P., Labarre J. 2010. Endoplasmic reticulum is a major target of cadmium toxicity in yeast. *Molecular Microbiology*. 76(4): 1034-1048.

Gary J. D., Sato T. K., Stefan C. J., Bonangelino C. J., Weisman L. S., Emr S. D. 2002. Regulation of Fab1 Phosphatidylinositol 3-Phosphate 5-Kinase Pathway by Vac7 Protein and Fig4, a Polyphosphoinositide Phosphatase Family Member. *Mol Biol Cell.* 13(4): 1238-1251.

Geisler-Lee J., Wang Q., Yao Y., Zhang W., Geisler M., Li K., Huang Y., Chen Y., Kolmakov A., Ma X. 2013. Phytotoxicity, accumulation and transport of silver nanoparticles by Arabidopsis thaliana. *Nanotoxicology*. 7: 323-337.

Gehring C. A., Irving H. R. 2003. Natriuretic peptides - a class of heterologous molecules in plants. *The International Journal of Biochemistry & Cell Biology*. 35: 1318-1322.

Gietz R.D., Woods R.A. 2002. Transformation of yeast by lithium acetate/single-stranded carrier DNA/polyethylene glycol method. *Methods Enzymol.* 350: 87-96.

Gill S. K., Hope-Weeks L. J. 2009. Monolithic aerogels of silver modified cadmium sulfide colloids. *Chem. Commun*. 4384-4386.

Graack H., Wittmann-Liebold B. 1998. Mitochondrial ribosomal proteins (MRPs) of yeast. *Biochem. J.* 329: 433-448.

Hawthorne J., Musante C., Sinha S. K., White J.C. 2012. Accumulation and phytotoxicity of engineered nanoparticles to Cucurbita pepo. *Int J Phytoremediation*. 14: 429-442.

Herbette S., Taconnat L., Hugouvieux V., Piette L., Magniette M.-L.M., Cuine S., Auroy P., Richaud P., Forestier C., Bourguignon J., Renou J.-P.,Vavasseur A., Leonhardt N. 2006. Genome-wide transcriptome profiling of the early cadmium response of Arabidopsis roots and shoots. *Biochimie*. 88: 1751-1765.

Hernandez-Viezcas J.A, Castillo-Michel H.,Andrews J. C., Cotte M., Rico C., Peralta-Videa J. R., Ge Y., Priester J.H., Holden P. A., Gardea-Torresdey J. L. 2013. In Situ Synchrotron X-ray Fluorescence Mapping and Speciation of CeO2 and ZnO Nanoparticles in Soil Cultivated Soybean (Glycine max). *ACS Nano* 7, 2: 1415-1423.

Hillenmeyer M.E., Fung E.,Wildenhain J., Pierce S.E., Hoon S., Lee W., Proctor M.,St.Onge R.P., Tyers M., Koller D., Altman R.B., Davis R.W., Nislow C., Giaever G. 2008. The Chemical Genomic Portrait of Yeast: Uncovering a Phenotype for All Genes. *Science*. 320: 362-365.

Hinnenbusch A. G., Natarajan K. 2002. Gcn4p, a Master Regulator of Gene Expression, Is Controlled at Multiple Levels by Diverse Signals of Starvation and Stress. *Eukaryotic Cell.* 1(1): 22-32.

Hochella M. F., Lower S. K., Maurice P. A., Penn R. L., Sahai N., Sparks D. L.; Twining B. S. 2008. Nanominerals, mineral nanoparticles, and earth systems. *Science*, 319: 1631-1635.

Hoffman C.S., Winston F. 1987. A ten-minute DNA preparation from yeast efficiently releases autonomous plasmids for transformation of Escherichia coli. *Gene* 57 (2): 267-272.

Howden R., Cobbett C. S. 1992. Cadmium-Sensitive mutants of Arabidopsis thaliana, *Plant Physiol.* 99: 100-107.

Howden R., Coldsbrough P. B., Andersen C. R. , Cobbett C. S. 1995. Cadmium-sensitive, *cad1* mutants of *Arabidopsis thaliana* are phytochelatin deficient. *Plant Physiol.* 107: 1059-1066.

Howden R., Coldsbrough P. B., Andersen C. R., Cobbett C. S. 1995. A cadmium-sensitive, glutathione-deficient mutant of *Arabidopsis thaliana*. *Plant Physiol.* 107: 1067-1073.

Huang D. W., Sherman B. T., Lempicki R. A. 2008. Systematic and integrative analysis of large gene lists using DAVID bioinformatics resources. *Nature Protocols.* 4: 44-57.

Huang D., Geng F., Liu Y., Wang X., Jiao J., Yu L. 2011. Biomimetic interactions of proteins with functionalized cadmium sulfide quantum dots. *Colloids and Surfaces A: Physicochem. Eng. Aspects.* 392: 191- 197.

Irizarry R. A., Hobbs B., Collin F., Beazer-Barclay Y. D., Antonellis K. J., Scherf U., Speed T. P. 2003. Exploration, normalization, and summaries of high density oligonucleotide array probe level data. *Biostatistics*. 4(2): 249-264.

Jauert P.A., Jensen L.E., Kirkpatrick D.T. 2005. A novel yeast genomic DNA library on a geneticin-resistance vector. *Yeast.* 22: 653-657.

Ju-Nam Y., Lead J. R. 2008. Manufactured nanoparticles: an overview of their chemistry, interactions and potential environmental implications. *Sci. Total. Environ*. 400: 396-414.

Kahru A., Dubourguier H. C. 2010. From ecotoxicology to nanoecotoxicology. *Toxicology*. 269: 105-119.

Karren M.A., Coonrod E.M., Anderson T.K. , Shaw J.M. 2005. The role of Fis1p–Mdv1p interactions in mitochondrial fission complex assembly. *Journal of Cell Biology*. 171(2): 291-301.

Katari M. S., Nowicki S. D., Aceituno F. F., Nero D., Kelfer J., Thompson L. P., Cabello J. M., Davidson R. S., Goldberg A. P., Shasha D. E., Coruzzi G. M., Gutierrez R. A. 2010. VirtualPlant: a software platform to support systems. *Plant Physiol*. 152: 500-515.

Kasemets K., Ivask A., Dubourguier H.C., Kahru A. 2009. Toxicity of nanoparticles of ZnO, CuO and TiO2 to yeast Saccharomyces cerevisiae. *Toxicology in vitro*. 23: 1116-1122.

Kasemets K., Suppi S., Kunnis-Beres K., Kahru A. 2012. Toxicity of CuO Nanoparticles to Yeast Saccharomyces cerevisiae BY4741 Wild-Type and Its Nine Isogenic Single-Gene Deletion Mutants. *Chem. Res. Toxicol.* 26(3): 356-367.

Kaveh R., Li Y.S., Ranjbar S., Tehrani R., Brueck C. L., Van Aken B. 2013. Changes in arabidopsis thaliana gene expression in response to silver nanoparticles and silver ions. *Environ. Sci. Technol.* 47: 10637-10644.

Lee I., Ambaru B., Thakkar P., Marcotte E.M., Rhee S. Y. 2010. Rational association of genes with traits using a genome-scale gene network for *Arabidopsis thaliana*. *Nature Biotechnology*. 28: 149-156.

Li J., Zhang Y., Xiao Q., Tian F., Liu X., Li R., Zhao G., Jiang F., Liu Y. 2011. Mitochondria as target of Quantum dots toxicity. *Journal of Hazardous Materials*. 19: 440-444.

Lin D., Xing B. 2007. Phytotoxicity of nanoparticles: Inhibition of seed germination and root growth. *Environmental Pollution.* 150: 243-250.

Lin D., Xing B. 2008. Root uptake and phytotoxicity of ZnO nanoparticles. *Environ. Sci. Technol.* 42: 5580-5585.

Lopez-Moreno M. L. , De La Rosa G., Hernandez-Viezcas J. A., Castillo-Michel H., Botez C. E., Peralta-Videa J. R., Gardea-Torresdey J. L. 2010. Evidence of the differential biotransformation and genotoxicity of ZnO and CeO2 nanoparticles on soybean (*Glycine max*) Plants. *Environ. Sci. Technol.* 44: 7315-7320.

Lowry G. V., Gregory K. B., Apte S. C., Lead J. R. 2012. Transformations of Nanomaterials in the Environment. *Environ. Sci. Technol.* 46: 6893-6899.

Mangeon A., Magrani Junqueira R., Sachetto-Martins G. 2010. Functional diversity of the plant glycine-rich proteins superfamily. *Plant Signaling & Behavior*. 5: 99-104.

Mar J.C., Wells C.A., Quackenbush J. 2011. Defining an informativeness metric for clustering gene expression data. *Bioinformatics.* 27: 1094-100.

Marmiroli M., Pagano L., Savo Sardaro M.L., Marmiroli N. 2014. Genome-wide approach in *Arabidopsis thaliana* to assess the toxicity of cadmium sulfide quantum dots. *Environmental Science & Technologies*. In press.

Martinez-Castanon G.A., Sanchez-Loredo M.G., Martinez-Mendoza J.R. and Ruiz F. 2005. Synthesis of CdS nanoparticles: a simple method in aqueous media. *Advances in Technology of Materials and Materials Processing.* 7(2): 171-174.

Matsushima R., Hayashi Y., Kondo M., Shimada T., Nishimura M., Hara-Nishimura I. 2002. An endoplasmic reticulum-derived structure that is induced under stress conditions in Arabidopsis. *Plant Physiology*. 130: 1807-1814.

Menard A., Drobne D., Jeme A. 2011. Ecotoxicity of nanosized TiO2. Review of in vivo data. *Environmental Pollution*. 159: 677-684.

Morse M., Pironcheva G., Gehring C. 2004. AtPNP-A is a systemically mobile natriuretic peptide immunoanalogue with a role in Arabidopsis thaliana cell volume regulation. *FEBS Letters*. 556: 99-103.

Mostafavi S., Ray D., Warde-Farley D., Grouios C., Morris Q. 2008. GeneMANIA: a real-time multiple association network integration algorithm for predicting gene function. *Genome Biology* 9 (S4): 1-15.

Musante C., White J.C. 2010. Toxicity of silver and copper to Cucurbita pepo: differential effects of nano and bulk-size particles. *Environ Toxicol.* 27: 510-517.

Navarro-Aviño J. P., Prasad R., Miralle V. J., Benito R. M., Serrano R. 1999. A proposal for nomenclature of aldehyde dehydrogenase in Saccharomyces cerevisiae and characterization of the stress inducible ALD2 and ALD3 genes. *Yeast* 15: 829-842.

Ni Z., Kim E.D., Chen Z.J. 2009. Chlorophyll and starch assays .*Protocol Exchange.* doi:10.1038/nprot.2009.12.

North M., Steffen J., Loguinov A.V.E., Zimmerman G.R., Vulpe C.D., Eide D. J. 2012. Genome-Wide Functional Profiling Identifies Genes and Processes Important for Zinc-Limited Growth of Saccharomyces cerevisiae. *PLoS Genetics* 8(6). doi: 10.1371/journal.pgen.1002699.

NRC. 2012. A Research Strategy for Environmental, Health, and Safety Aspects of Engineered Nanomaterials. *The National Academic Press*.

Porter D.R., Nguyen H.T., Burke J.J. 1994. Quantifying acquired thermal tolerance in winter wheat. *Crop Science*. 34: 1686-1689.

Pirondini A., Visioli G., Malcevschi A., Marmiroli N. 2006. *J Chromatogr B Analyt Technol Biomed Life Sci***.** 833(1): 91-100.

Rico C. R, Majumdar S., Duarte-Gardea M., Peralta-Videa J.R. Gardea-Torresdey J. L. 2011. Interaction of nanoparticles with edible plants and their possible implications in the food chain. *J. Agric. Food Chem.* 59: 3485-3498.

Robinson M.D., Grigull J., Mohammad N., Hughes T.R. 2002. FunSpec: a web-based cluster interpreter for yeast. *BMC Bioinformatics.* 3: 35-39.

Ruotolo R., Marchini G., Ottonello S. 2008. Membrane transporters and protein traffic networks differentially affecting metal tolerance: a genomic phenotyping study in yeast. *Genome Biology* 9(4): R67.

Servin A. D., Castillo-Michel H., Hernandez-Viezcas J. A., Corral Diaz B., Peralta-Videa J. R., Gardea-Torresdey J. L. 2012. Synchrotron micro-XRF and micro-XANES confirmation of the uptake and translocation of TiO2 nanoparticles in cucumber (Cucumis sativus) plants. *Environ. Sci. Technol*. 46: 7637-7643.

Shannon P., Markiel A., Ozier O., Baliga N. S., Wang J. T., Ramage D., Amin N., Benno Schwikowski B., Ideker T. 2003. Cytoscape: a software environment for integrated models of biomolecular interaction networks. *Genome Research*. 13: 2498-2504.

Serero A., Lopes J., Nicolas A., Boiteux S. 2008. Yeast genes involved in cadmium tolerance: identification of DNA replication as a target of cadmium toxicity. *DNA repair* 7(8):1262-1275.

Shen Y., Nakajima M., Ahmad M.R., Kojima S., Homma M., Fukuda T. 2011. Effect of ambient humidity on the strength of the adhesion force of single yeast cell inside environmental-SEM. *Ultramicroscopy* 111: 1176-1183.

Schmittgen T. D., Livak K. J. 2008. Analyzing real-time PCR data by the comparative C_t method. *Nature Protocols.* 3: 1101-1108.

Smith M.R., Boenzli M.G., Hindagolla V., Ding J., Miller J.M., Hutchison J.E., Greenwood J.A., Abeliovich H., Bakalinsky A.T. 2013. Identification of gold nanoparticle-resistant mutants of *Saccharomyces cerevisiae* suggests a role for respiratory metabolism in mediating toxicity. *Appl. Environ. Microbiol.* 2013, 79(2): 728-733.

Stampoulis D., Sinha S. K., White J.C. 2009. Assay-dependent phytotoxicity of nanoparticles to plants. *Environ. Sci. Technol.* 43: 9473-9479.

Takahashi H., Yamazaki M., Sasakura N., Watanabe A., Leustek T., De Almeida Engler J., Engler G., Van Montagu M., Saito K. 1997. Regulation of sulfur assimilation in higher plants: a sulfate transporter induced in sulfate-starved roots plays a central role in *Arabidopsis Thaliana. Proc. Natl. Acad. Sci. USA.* 94: 11102-11107.

Tkach J. M., Yimit A., Lee A. Y., Rifle M., Costanzo M., Jaschob D., Hendry J.A., Ou J., Moffat J., Boone C., Davis T.N., Nislow C., Brown G.W. 2012. Dissecting DNA damage response pathways by analyzing protein localization and abundance changes during DNA replication stress. *Nature Cell Biology*. 14: 966-976.

Tsuji J.S., Maynard A.D., Howard P.C., James J.T., Lam C., Warheit D.B., Santamaria A.B. 2006. Research strategies for safety evaluation of nanomaterials, part IV: risk assessment of nanoparticles *Toxicological Sciences.* 89(1): 42-50.

Uttenweiler A., Schwarz H., Neumann H., Mayer A. 2007. The vacuolar transporter chaperone (VTC) compex is required for microautophagy. *Mol. Biol. Cell.* 18(1): 166-175.

Villani M., Calestani D., Lazzarini L., Zanotti L., Mosca R., Zappettini A. 2012. Extended functionality of ZnO nanotetrapods by solution-based coupling with CdS nanoparticles. *J. Mater. Chem.* 22: 5694-5699.

Yamada K. Hara-Nishimura I., Nishimura M. 2011. Unique defense strategy by the endoplasmic reticulum body in plants. *Plant Cell Physiol*. 52: 2039-2049.

Yanhui C., Xiaoyuan Y., Kun H., Meihua L., Jigang L., Zhaofeng G., Zhiqiang L., Yunfei Z., Xiaoxiao W., Xiaoming Q., Yunping S., Li Z., Xiaohui D., Jingchu L., Xing-Wang D., Zhangliang C., Hongya G., Li-Jia Q. 2006. The MYB transcription factor superfamily of Arabidopsis: expression analysis and phylogenetic comparison with the rice MYB family. *Plant Molecular Biology*. 60: 107-124.

Weir A., Westerhoff P., Fabricius L., Hristovski K., von Goetz N. 2012. Titanium dioxide nanoparticles in food and personal care products. *Environ. Sci. Technol*. 46: 2242-2250.

Wu A., Wemmie J. A., Eddington N. P, Goebl M., Guevara J. L., Moye-Rowley W. S. 1993. Yeast bZip proteins mediate pleiotropic drug and metal resistance. *J. Biol. Chem.* 268(25): 18850-8.

Zhai T., Fang X., Li L., Bando Y., Golberg D. 2010. One-dimensional CdS nanostructures: synthesis, properties, and applications. *Nanoscale*. 2: 168-187.

Appendix

Table 1: GO Molecular Function - sensitive mutants

Category	p-value	In Category from Cluster	Number of genes observed in category	Number of genes in category
protein dimerization activity [GO:0046983]	0.0002978	CAD1 GCN4 YAP3 CST6	4	20
carboxylesterase activity [GO:0004091]	0.0009108	YJL068C YLR118C YMR210W	3	12
aldehyde dehydrogenase (NAD) activity [GO:0004029]	0.00271	ALD3 ALD2	2	5
transmembrane receptor activity [GO:0004888]	0.00271	WSC4 MID2	2	5
carboxy-lyase activity [GO:0016831]	0.003139	ARO10 YEL020C GAD1	3	18
aldehyde dehydrogenase [NAD(P)+] activity [GO:0004030]	0.00402	ALD3 ALD2	2	6
oxidoreductase activity, acting on the aldehyde or oxo group of donors, NAD or NADP as acceptor [GO:0016620]	0.005566	TDH3 YMR226C	2	7
thiamine pyrophosphate binding [GO:0030976]	0.00734	ARO10 YEL020C	2	8
RNA polymerase II transcription factor activity [GO:0003702]	0.008124	SPT3 CAD1 RGM1	3	25
phenylpyruvate decarboxylase activity [GO:0050177]	0.01681	ARO10	1	1
protein C-terminal S-isoprenylcysteine carboxyl O-methyltransferase activity [GO:0004671]	0.01681	STE14	1	1
glutamate decarboxylase activity [GO:0004351]	0.01681	GAD1	1	1
histone methyltransferase activity (H3-K79 specific) [GO:0031151]	0.01681	DOT1	1	1
ubiquitin-protein ligase activator activity [GO:0097027]	0.01681	CUE1	1	1

Category	p-value	In Category from Cluster	Number of genes observed in category	Number of genes in category
palmitoyl-(protein) hydrolase activity [GO:0008474]	0.01681	YLR118C	1	1
peroxisome matrix targeting signal-2 binding [GO:0005053]	0.01681	PEX7	1	1
S-formylglutathione hydrolase activity [GO:0018738]	0.01681	YJL068C	1	1
[cytochrome c]-lysine N-methyltransferase activity [GO:0000277]	0.01681	CTM1	1	1
mRNA 3'-UTR binding [GO:0003730]	0.01681	PUF6	1	1
methyltransferase activity [GO:0008168]	0.03108	MTQ2 STE14 DOT1 CTM1	4	71
translation repressor activity, nucleic acid binding [GO:0000900]	0.03334	PUF6	1	2
tricarboxylate secondary active transmembrane transporter activity [GO:0005371]	0.03334	YHM2	1	2
arylformamidase activity [GO:0004061]	0.03334	BNA7	1	2
D-arabinose 1-dehydrogenase [NAD(P)+] activity [GO:0045290]	0.03334	ARA1	1	2
2-deoxyglucose-6-phosphatase activity [GO:0003850]	0.03334	DOG1	1	2
nucleosomal histone binding [GO:0031493]	0.03334	DOT1	1	2
GTPase inhibitor activity [GO:0005095]	0.03334	ROY1	1	2
UTP:glucose-1-phosphate uridylyltransferase activity [GO:0003983]	0.03334	YHL012W	1	2
chaperone binding [GO:0051087]	0.03976	CAJ1 SCJ1	2	19
lyase activity [GO:0016829]	0.04345	ARO10 YEL020C YHR112C GAD1	4	79
damaged DNA binding [GO:0003684]	0.0437	RAD14 YKU70	2	20
metalloendopeptidase activity [GO:0004222]	0.04778	CYM1 RCE1	2	21

Category	p-value	In Category from Cluster	Number of genes observed in category	Number of genes in category
glyceraldehyde-3-phosphate dehydrogenase activity [GO:0008943]	0.0496	TDH3	1	3
glyceraldehyde-3-phosphate dehydrogenase (NAD+) (phosphorylating) activity [GO:0004365]	0.0496	TDH3	1	3
cystathionine beta-lyase activity [GO:0004121]	0.0496	YHR112C	1	3
NAD+ kinase activity [GO:0003951]	0.0496	YEF1	1	3
NADH kinase activity [GO:0042736]	0.0496	YEF1	1	3
histone-lysine N-methyltransferase activity [GO:0018024]	0.0496	DOT1	1	3
G-quadruplex DNA binding [GO:0051880]	0.0496	MRE11	1	3
ATPase activity, coupled [GO:0042623]	0.0496	HSC82	1	3
double-stranded telomeric DNA binding [GO:0003691]	0.0496	MRE11	1	3
trehalose-phosphatase activity [GO:0004805]	0.0496	TPS3	1	3
1-acylglycerol-3-phosphate O-acyltransferase activity [GO:0003841]	0.0496	SLC1	1	3
alpha,alpha-trehalose-phosphate synthase (UDP-forming) activity [GO:0003825]	0.0496	TPS3	1	3
nuclear localization sequence binding [GO:0008139]	0.0496	ETP1	1	3

Table 2: GO Biological Process - sensitive mutants

Category	p-value	In Category from Cluster	Number of genes observed in category	Number of genes in category
beta-alanine biosynthetic process [GO:0019483]	0.0002801	ALD3 ALD2	2	2
polyamine catabolic process [GO:0006598]	0.000831	ALD3 ALD2	2	3
ER-associated protein catabolic process [GO:0030433]	0.001181	DFM1 ADD37 SCJ1 CUE1 DSK2	5	48
tryptophan catabolic process [GO:0006569]	0.005566	ARO10 BNA7	2	7
peptide pheromone maturation [GO:0007323]	0.00734	STE14 RCE1	2	8
meiotic DNA double-strand break formation [GO:0042138]	0.01154	REC102 MRE11	2	10
recombinational repair [GO:0000725]	0.01154	DOT1 SHU1	2	10
negative regulation of GTPase activity [GO:0034260]	0.01681	ROY1	1	1
glutamate catabolic process [GO:0006538]	0.01681	GAD1	1	1
methionine catabolic process to 3-methylthiopropanol [GO:0000951]	0.01681	ARO10	1	1
protein deacylation [GO:0035601]	0.01681	YLR118C	1	1
establishment of protein localization in endoplasmic reticulum membrane [GO:0097051]	0.01681	CUE1	1	1
glutamate metabolic process [GO:0006536]	0.01681	GAD1	1	1
cellular response to oleic acid [GO:0071400]	0.01681	CST6	1	1
peptidyl-lysine methylation [GO:0018022]	0.01681	CTM1	1	1
alpha-ketoglutarate transport [GO:0015742]	0.01681	YHM2	1	1
tricarboxylic acid transport [GO:0006842]	0.01681	YHM2	1	1
regulation of transcription during meiosis [GO:0051037]	0.01681	MRE11	1	1
DNA metabolic process [GO:0006259]	0.01936	CST6 MRE11	2	13

Category	p-value	In Category from Cluster	Number of genes observed in category	Number of genes in category
endoplasmic reticulum unfolded protein response [GO:0030968]	0.01936	DFM1 YHI9	2	13
methylation [GO:0032259]	0.03108	MTQ2 STE14 DOT1 CTM1	4	71
tyrosine catabolic process [GO:0006572]	0.03334	ARO10	1	2
negative regulation of ribosomal protein gene transcription from RNA polymerase II promoter [GO:0010688]	0.03334	CRF1	1	2
C-terminal protein methylation [GO:0006481]	0.03334	STE14	1	2
long-chain fatty-acyl-CoA metabolic process [GO:0035336]	0.03334	FAA4	1	2
positive regulation of transcription initiation from RNA polymerase II promoter [GO:0060261]	0.03334	GCN4	1	2
peptidyl-glutamine methylation [GO:0018364]	0.03334	MTQ2	1	2
chloride transport [GO:0006821]	0.03334	YHL008C	1	2
monocarboxylic acid transport [GO:0015718]	0.03334	YHL008C	1	2
response to ethanol [GO:0045471]	0.03334	ETP1	1	2
cell morphogenesis involved in conjugation [GO:0000767]	0.03334	MID2	1	2
formaldehyde catabolic process [GO:0046294]	0.03334	YJL068C	1	2
CAAX-box protein processing [GO:0071586]	0.03334	RCE1	1	2
branched chain family amino acid catabolic process to alcohol via Ehrlich pathway [GO:0000950]	0.03334	ARO10	1	2
glycerophospholipid biosynthetic process [GO:0046474]	0.03334	SLC1	1	2
mitochondrial citrate transport [GO:0006843]	0.03334	YHM2	1	2
response to stress [GO:0006950]	0.04238	DFM1 RTA1 WSC4 MID2 HSC82 TPS3	6	152

Category	p-value	In Category from Cluster	Number of genes observed in category	Number of genes in category
chromatin modification [GO:0016568]	0.04249	SPT3 DOT1 VPS72 EAF5 RKR1	5	114
endocytosis [GO:0006897]	0.04871	DNF1 BZZ1 GVP36 ROY1	4	82
NADP biosynthetic process [GO:0006741]	0.0496	YEF1	1	3
histone lysine methylation [GO:0034968]	0.0496	DOT1	1	3
leucine catabolic process [GO:0006552]	0.0496	ARO10	1	3
medium-chain fatty acid biosynthetic process [GO:0051792]	0.0496	YMR210W	1	3
global genome nucleotide-excision repair [GO:0070911]	0.0496	DOT1	1	3
cell cycle arrest [GO:0007050]	0.0496	HUG1	1	3

Table 3: GO Cellular Component - sensitive mutants

Category	p-value	In Category from Cluster	Number of genes observed in category	Number of genes in category
lipid particle [GO:0005811]	0.003955	CST26 SLC1 TDH3 FAA4	4	39
Doa10p ubiquitin ligase complex [GO:0000837]	0.00402	DFM1 CUE1	2	6
nuclear inner membrane [GO:0005637]	0.01395	STE14 HEH2	2	11
DNA-dependent protein kinase-DNA ligase 4 complex [GO:0005958]	0.01681	YKU70	1	1
endoplasmic reticulum lumen [GO:0005788]	0.02234	EUG1 SCJ1	2	14
peroxisome [GO:0005777]	0.02456	PEX7 PEX29 GTO1 FIS1	4	66
integral to endoplasmic reticulum membrane [GO:0030176]	0.02726	ICE2 CUE1 RCE1	3	39
integral to nuclear inner membrane [GO:0005639]	0.03334	HEH2	1	2
cellular bud scar [GO:0005621]	0.03334	RAX2	1	2
Ku70:Ku80 complex [GO:0043564]	0.03334	YKU70	1	2
eRF1 methyltransferase complex [GO:0035657]	0.03334	MTQ2	1	2
nucleotide-excision repair factor 1 complex [GO:0000110]	0.0496	RAD14	1	3
Mre11 complex [GO:0030870]	0.0496	MRE11	1	3

Table 4: GO Molecular Function - resistant mutants

Category	p-value	In Category from Cluster	Number of genes observed in category	Number of genes in category
transcription coactivator activity [GO:0003713]	0.004172	SWI6 SIN3 HFI1	3	20
molecular_function [GO:0003674]	0.008453	MOH1 PIN4 YBR196C-A YBR196C-B YBR200W-A YBR221W-A YBR296C-A YCL001W-B YCL057C-A YDL159W-A YDR003W-A YDR034W-B YDR169C-A YDR246W-A DYN2 YER053C-A YER077C VTC2 YFR012W-A YGL006W-A YGL041C-B YGL188C-A YGR204C-A PHB2 YGR235C YHR050W-A YIL108W SIM1 YIR018C-A YJL127C-B YJL144W IDS2 YJL147C YKL068W-A YKL106C-A UPS2 VAC7 YNL115C YOL092W YOL098C BSC6 RTC1 RSA1 THP3 MCM16	45	1973
serine-type endopeptidase activity [GO:0004252]	0.01134	PIM1 NMA111	2	10
ribonuclease T2 activity [GO:0033897]	0.01666	RNY1	1	1
ornithine carbamoyltransferase activity [GO:0004585]	0.01666	ARG3	1	1
glucan 1,4-alpha-glucosidase activity [GO:0004339]	0.01666	SGA1	1	1
serine-type peptidase activity [GO:0008236]	0.01903	PIM1 NMA111	2	13
ubiquitin binding [GO:0043130]	0.02318	SLA1 EDE1 BUB3	3	37
pyruvate dehydrogenase (acetyl-transferring) activity [GO:0004739]	0.03304	PDB1	1	2
double-strand/single-strand DNA junction binding [GO:0000406]	0.03304	MSH2	1	2

Category	p-value	In Category from Cluster	Number of genes observed in category	Number of genes in category
sphingosine-1-phosphate phosphatase activity [GO:0042392]	0.03304	LCB3	1	2
single base insertion or deletion binding [GO:0032138]	0.03304	MSH2	1	2
potassium ion transmembrane transporter activity [GO:0015079]	0.03304	TRK1	1	2
carboxyl- or carbamoyltransferase activity [GO:0016743]	0.03304	ARG3	1	2
tyrosine-tRNA ligase activity [GO:0004831]	0.03304	MSY1	1	2
6-phosphofructokinase activity [GO:0003872]	0.03304	PFK1	1	2
tRNA (guanine-N1-)-methyltransferase activity [GO:0009019]	0.03304	TRM10	1	2
protein phosphatase regulator activity [GO:0019888]	0.03304	PSY4	1	2
ATP-dependent peptidase activity [GO:0004176]	0.03304	PIM1	1	2
metalloendopeptidase activity [GO:0004222]	0.04701	COR1 YOL098C	2	21
voltage-gated anion channel activity [GO:0008308]	0.04916	POR2	1	3
porin activity [GO:0015288]	0.04916	POR2	1	3
1,3-beta-D-glucan synthase activity [GO:0003843]	0.04916	FKS1	1	3
guanine/thymine mispair binding [GO:0032137]	0.04916	MSH2	1	3
tRNA (guanine) methyltransferase activity [GO:0016423]	0.04916	TRM10	1	3
Y-form DNA binding [GO:0000403]	0.04916	MSH2	1	3

Table 5: GO Biological Process - resistant mutants

Category	p-value	In Category from Cluster	Number of genes observed in category	Number of genes in category
biological_process [GO:0008150]	0.0008038	MOH1 YBR196C-A YBR196C-B YBR200W-A YBR221W-A YBR296C-A YCL001W-B YCL057C-A YDL159W-A YDR003W-A YDR034W-B YDR169C-A YDR246W-A YER053C-A YER077C YFR012W-A YGL006W-A YGL041C-B YGL188C-A YGR204C-A YGR235C YHR050W-A YIL108W YIR018C-A YJL127C-B YJL147C YKL068W-A YKL106C-A APJ1 YNL115C YOL092W YOL098C BSC6 RTC1	34	1203
proteolysis [GO:0006508]	0.001377	PIM1 COR1 SOM1 NMA111 YOL098C YGK3	6	74
cellular chaperone-mediated protein complex assembly [GO:0034619]	0.01666	PIM1	1	1
mitochondrial tyrosyl-tRNA aminoacylation [GO:0070184]	0.01666	MSY1	1	1
mitochondrial DNA metabolic process [GO:0032042]	0.01666	HMI1	1	1
histone modification [GO:0016570]	0.01666	RTF1	1	1
phosphatidylethanolamine metabolic process [GO:0046337]	0.01666	UPS2	1	1
translational readthrough [GO:0006451]	0.01666	MTQ1	1	1
polysaccharide metabolic process [GO:0005976]	0.01666	SGA1	1	1
error-free postreplication DNA repair [GO:0042275]	0.03304	RAD18	1	2
positive regulation of kinase activity [GO:0033674]	0.03304	VAC7	1	2

Category	p-value	In Category from Cluster	Number of genes observed in category	Number of genes in category
negative regulation of cAMP biosynthetic process [GO:0030818]	0.03304	IRA2	1	2
ornithine metabolic process [GO:0006591]	0.03304	ARG3	1	2
negative regulation of transcription during meiosis [GO:0051038]	0.03304	SIN3	1	2
negative regulation of proteolysis [GO:0045861]	0.03304	PHB2	1	2
DNA transport [GO:0051027]	0.03304	POR2	1	2
tyrosyl-tRNA aminoacylation [GO:0006437]	0.03304	MSY1	1	2
transcription from RNA polymerase II promoter [GO:0006366]	0.03444	RTF1 GAL11 TAF14 HFI1	4	74
endocytosis [GO:0006897]	0.04738	SLA1 EDE1 SAC6 TLG2	4	82
regulation of anion transport [GO:0044070]	0.04916	POR2	1	3
glycogen catabolic process [GO:0005980]	0.04916	SGA1	1	3
N-terminal peptidyl-methionine acetylation [GO:0017196]	0.04916	MDM20	1	3
regulation of transcription involved in G2/M-phase of mitotic cell cycle [GO:0000117]	0.04916	SIN3	1	3
meiotic gene conversion [GO:0006311]	0.04916	MSH2	1	3
actin filament-based process [GO:0030029]	0.04916	DYN2	1	3
mannosyl-inositol phosphorylceramide metabolic process [GO:0006675]	0.04916	TLG2	1	3
negative regulation of chromatin silencing at silent mating-type cassette [GO:0061186]	0.04916	SIN3	1	3
negative regulation of chromatin silencing at rDNA [GO:0061188]	0.04916	SIN3	1	3
histone monoubiquitination [GO:0010390]	0.04916	RTF1	1	3
positive regulation of Ras GTPase activity [GO:0032320]	0.04916	IRA2	1	3

Category	p-value	In Category from Cluster	Number of genes observed in category	Number of genes in category
protein methylation [GO:0006479]	0.04916	MTQ1	1	3
positive regulation of phosphatidylinositol biosynthetic process [GO:0010513]	0.04916	VAC7	1	3
negative regulation of DNA damage checkpoint [GO:2000002]	0.04916	PSY4	1	3

Table 6: GO Cellular Component – resistant mutants

Category	p-value	In Category from Cluster	Number of genes observed in category	Number of genes in category
cellular_component [GO:0005575]	0.001088	MOH1 YBR196C-A YBR196C-B YBR200W-A YBR221W-A YBR296C-A YCL001W-B YDL159W-A YDR003W-A YDR034W-B YDR169C-A YDR246W-A YFR012W-A YGL006W-A YGL041C-B YGL188C-A YGR204C-A YHR050W-A YIR018C-A YJL127C-B YKL068W-A YKL106C-A YGK3	23	704
transcription export complex 2 [GO:0070390]	0.001614	SUS1 THP1	2	4
actin cortical patch [GO:0030479]	0.01464	SLA1 EDE1 SAC6 FKS1	4	57
nuclear pore [GO:0005643]	0.01552	SUS1 DYN2 THP1 KAP120	4	58
integral to endosome membrane [GO:0031303]	0.01666	TLG2	1	1
ornithine carbamoyltransferase complex [GO:0009348]	0.01666	ARG3	1	1
microtubule associated complex [GO:0005875]	0.01666	DYN2	1	1
vacuole [GO:0005773]	0.01812	VTC2 VAC7 YNL115C YOL092W RTC1 VMA4 RNY1	7	162

Category	p-value	In Category from Cluster	Number of genes observed in category	Number of genes in category
NatB complex [GO:0031416]	0.03304	MDM20	1	2
MutSbeta complex [GO:0032302]	0.03304	MSH2	1	2
6-phosphofructokinase complex [GO:0005945]	0.03304	PFK1	1	2
endoplasmic reticulum palmitoyltransferase complex [GO:0031211]	0.03304	SHR5	1	2
transcriptionally active chromatin [GO:0035327]	0.03304	THP3	1	2
mitochondrial matrix [GO:0005759]	0.03731	PIM1 PDB1 PET54 HMI1 MSY1	5	111
extrinsic to mitochondrial inner membrane [GO:0031314]	0.03911	PET54 UPS2	2	19
Rpd3L-Expanded complex [GO:0070210]	0.03911	TOS4 SIN3	2	19
nucleoplasm [GO:0005654]	0.0407	SUS1 RTF1 RSA1	3	46
SAGA complex [GO:0000124]	0.04299	SUS1 HFI1	2	20
transcription factor TFIIF complex [GO:0005674]	0.04916	TAF14	1	3
pore complex [GO:0046930]	0.04916	POR2	1	3
small nuclear ribonucleoprotein complex [GO:0030532]	0.04916	BRR1	1	3
SBF transcription complex [GO:0033309]	0.04916	SWI6	1	3

Category	p-value	In Category from Cluster	Number of genes observed in category	Number of genes in category
mitochondrial inner membrane peptidase complex [GO:0042720]	0.04916	SOM1	1	3
MutSalpha complex [GO:0032301]	0.04916	MSH2	1	3
MBF transcription complex [GO:0030907]	0.04916	SWI6	1	3
vacuolar lumen [GO:0005775]	0.04916	RNY1	1	3

Table 7: Pools composition – sensitive mutants

pool (GO terms)	deleted gene
Pool 1: molecular function unknown 1	YDL026W, YDR370C, YDR426C, HEH2, EAF5, YEL020C, YEL023C, YHL044W
Pool 2: molecular function unknown 2	YHL012W, YEL025C, YGL081W, YGR127W, YGR139W, VPS62, YGR161W-C, YGR213C, YHL006C
Pool 3: molecular function unknown 3	ADD37, YMR185W, TRI1, YMR244W, YMR245W, YMR258C, YMR259C, YDR352W
Pool 4: molecular function unknown 4	YHI9, BZZ1, GVP36, FIS1, ICE2, RAX2, SYM1, REC102, YMR172C-A
Pool 5: DNA binding	CAD1, GCN4, YAP3, RGM1, RAD14, MRE11, YHM2, YKU70, CST6
Pool 6: oxidoreductase activity	ARA1, EUG1, TDH3, ALD3, ALD2, YMR226C
Pool 7: membrane transposters	ATO3, TPO2, QCR10, TOM5, RPS8A, RPL12B, MRPL44, RLP42A
Pool 8: methyltransferase / ligase	MTQ2, STE14, CTM1, SIZ1, FAA4, RKR1, BUL1
Pool 9: ATPase / phophatase / signal transduction	IKI1, HSC82, DOG1, TPS3, WSC4, MID2
Pool 10: peptidase / liase	CYM1, RCE1, ARO10, YHR112C, GAD1
Pool 11: others 1	CBS1, RUB1, PEX7, CAJ1, YHL008C, LIN1, YLR118C, SCJ1, DFM1
Pool 12. others 2	LSM12, YMR210W, CUE1, YEF1, STP3, GTO1, ETP1, DSK2, BNA7